Project Report
ATC-7

Concept Formulation Studies of the Surveillance Aspects of the Fourth Generation Air Traffic Control System

I.G. Stiglitz
J.U. Beusch
A. Eckberg
K.S. Schneider

21 September 1971

Lincoln Laboratory
MASSACHUSETTS INSTITUTE OF TECHNOLOGY
LEXINGTON, MASSACHUSETTS

Prepared for the Transportation Systems Center
of the Department of Transportation.

75

MASSACHUSETTS INSTITUTE OF TECHNOLOGY

LINCOLN LABORATORY

CONCEPT FORMULATION STUDIES OF THE SURVEILLANCE ASPECTS OF THE FOURTH GENERATION AIR TRAFFIC CONTROL SYSTEM

I. G. STIGLITZ
J. U. BEUSCH
A. ECKBERG
K. S. SCHNEIDER

Group 41

PROJECT REPORT ATC-7
(Air Traffic Control)

21 SEPTEMBER 1971

LEXINGTON MASSACHUSETTS

The work reported in this document was performed at Lincoln Laboratory, a center for research operated by Massachusetts Institute of Technology. The work was sponsored by the Transportation Systems Center of the Department of Transportation under Contract DOT/TSC-241.

ERRATA SHEET

for

Project Report ATC-7

The authors have detected errors in Project Report ATC-7 (I. G. Stiglitz, J. U. Beusch, A. Eckberg and K. S. Schneider, "Concept Formulation Studies of the Surveillance Aspects of the Fourth Generation Air Traffic Control System [U]," 21 September 1971). Please insert these pages into your copy of that report.

Page 20 — The phrase "$\overline{N}_f^u$ is an upper bound to $\overline{N}_f^u$" should read "$\overline{N}_f^u$ is an upper bound to $\overline{N}_f$."

Page 43 — Table 4.2 should be replaced by the following:

TABLE 4.2

MINIMUM AIRCRAFT ALTITUDE RESULTING IN LESS THAN 6 db MULTIPATH FADING LOSS FOR THREE ALTERNATIVE VERTICAL APERTURE

Vertical Aperture (feet)	Minimum Permitted Elevation Angle	Minimum Altitude at 100 miles (feet)	Minimum Altitude at 200 miles (feet)
9	2^{o}	23,000	52,000
20	0.8^{o}	12,000	32,000
35	0.5^{o}	10,000	27,000

Pages 214 – 217 — Replace with the enclosed four figures.

Publications
M.I.T., Lincoln Laboratory
P.O. Box 73
Lexington, Massachusetts 02173

18 November 1971

CONTENTS

LIST OF TABLES

FIGURES

SECTION 1

INTRODUCTION AND SUMMARY OF CONCLUSIONS

In this report we present a first order feasibility study of four particular candidate surveillance systems for the Fourth Generation Air Traffic Control System. No attempt has been made to compare these systems, rather we have chosen to examine in detail only the most crucial aspects of each. This analysis has brought to light many of the weak points of these systems; these must be addressed in future studies. We have also identified many of the critical assumptions underlying the analysis. These should also receive future consideration. It would be premature to compare the four systems at this time. Such a comparison will be best performed after the critical areas mentioned above have been dealt with in greater detail.

For expediency, it was necessary to make certain simplifying assumptions and to idealize the problem by excluding certain issues from consideration. In particular, it was necessary to make assumptions about the traffic model, the desired performance characteristics, the desired complexity constraints, the environmental effects, and the technological constraints. These are all considered in detail in Appendix A. We have explicitly excluded any issues of compatibility with the upgraded third generation system. Also, we have ignored interaction between the surveillance function and other aspects of the fourth generation system, (i. e. communications, navigation, and control). Our effort has only addressed the over CONtinental United States (CONUS) surveillance problem. Some of the fundamental assumptions, our most significant conclusions and recommended research and development are summarized below.

I. Fundamental Assumptions

A. Full time surveillance of all airborne aircraft with position measurement updates every few seconds and accuracies of a few hundred feet is required. A system capable of growth to 10^5 aircraft (peak load) is desired.

B. It is especially important to maintain surveillance on aircraft during typical maneuvers.

C. Because 97% of the users are projected to be general aviation aircraft it is essential that the avionics costs be kept to a minimum.

D. The system is required to operate at L-band.

II. Air-to-Satellite-to-Ground Surveillance Systems

A. Each aircraft autonomously transmits a signature, with a duration of about one msec, which consists of a few PSK pulses each of which contains a few hundred 100 nsec chips. The signature is repeated every few seconds. Two particular candidate systems are analyzed: a Fixed Signature Repetition Rate (FSRR) system in which unique identification is determined by the inter pulse time and the PSK modulation, and a Variable Signature Repetition Rate (VSRR) system in which unique identification is determined by the inter signature and inter pulse times and the PSK modulation.

B. These systems are demonstrated to be extremely sensitive to intentional interference. In particular, under optimistic assumptions each satellite can be disabled by a 42dbw ERP terminal. At the assumed L-band frequency this could be achieved with 100w of rf power and a 3.5 foot antenna (13^o half power beamwidth). This should take less prime power than a toaster, be easily transportable in a car or small boat and be within the reach of many hostile political groups, at a cost of under two thousand dollars.

C. An avionics antenna system with a sufficiently uniform pattern down to very low elevation angles is costly and complex. To avoid using costly antennas, the system is configured so that at least four satellites in the constellation are always above 15^{o} elevation angle (in a coordinate system attached to the aircraft).

D. To ensure continous coverage by four particular satellites during aircraft maneuvers with banking angles of up to 30^{o}, the four satellites must be within a cone with a 45^{o} half angle. One reasonable candidate satellite constellation employs 12 satellites, this imposes a geometric dilution penalty factor of 20.

E. From a first order performance analysis which takes into account the non-ideal link characteristics but makes no allowance for link margin, we have concluded that neither the FSRR nor VSRR systems achieves an acceptable level of performance.

1. For the FSRR system to achieve less than 10^{4} false alarms each signature period (2. 5 sec), the resultant detection probability is less than 2/3,

2. For the VSRR system analyzed the detection probability does not exceed 0. 7.

F. We have not demonstrated that air-to-satellite-to-ground systems will not work. Our first order analysis merely demonstrates unacceptably low performance levels for the two particular systems analyzed.

III. Satellite-to-Air-to-Ground Surveillance System

A. Every second each satellite transmits one 200 bit PSK modulated pulse with a 100 nsec chip direction. The intervals during which successive satellites transmit are separated by 8 msec to avoid pulse overlap over CONUS. Matched filter detection is employed on the aircraft.

B. A line of sight data communications link in which aircraft are polled by the ground terminal is used to provide the required surveillance data to the ground processing center. For a surveillance-only capability, aircraft identity and time differences between pulse arrivals are transmitted to the ground. This communication link can be used for other functions, e.g. IPC.

C. A direct navigation capability could be realized by adding satellite down-link ephemeris transmissions and an avionics position calculator. Calculator procurement costs are estimated to be less than $2,000 in quantity at today's prices; significantly lower costs are projected for 20 years hence. For this system, position and identification parameters are transmitted to the ground.

D. Since multiple access noise is not a problem with this system, satellite orbit constraints are not as severe as they are in air-to-satellite-to-ground systems. Four satellites within a 55^{o} half angle cone should be sufficient to permit bank angles up to 30^{o}.

E. The required air-ground capability is not grossly different from the current estimates for the Discrete Address Beacon System (DABS).

F. Intentional interference from ground based or airborne terminals is limited in effectiveness to line of sight areas.

G. RMS position errors less than 700 feet should be achievable using frequency standards accurate to 2 parts in 10^{6}. A factor of 3.5 improvement in accuracy should be achievable with a local oscillator stability of 5 parts in 10^{7}.

IV. Air-to-Ground Surveillance System

A. Once every few seconds each aircraft transmits a signature consisting of fourteen 10μsec PSK modulated pulses. Each pulse is selected from one of eight and thus a total of 42 bits is transmitted. These could include both identity and barometrically determined altitude. Reception by three ground stations permits position determination by multilateration techniques.

B. Intentional interference is limited in effectiveness to line of sight areas.

C. Performance estimates in the terminal and en route areas yield different results because of differences in 1) traffic density, 2) signature repetition rate and 3) maximum range. Although the resultant signal to noise ratios differ by only 2db, this difference is sufficient to provide satisfactory performance en route and unsatisfactory performance in the terminal area.

D. Because of the high sensitivity of performance to signal to noise ratio and hence to small changes in the assumptions, we cannot draw any definitive conclusions regarding the feasibility of this system.

E. In order to properly assess system performance the more tenuous assumptions underlying the analysis must be addressed in more detail. These are summarized in part C of the next section.

V. Recommendations for Future R and D

A. Air-to-Satellite-to-Ground Surveillance System

1. The extreme susceptability to intentional interference of the two specific systems analyzed raises a serious question as to the viability of any air-to-satellite system requiring low cost avionics equipment. Specifically we observe that the general topic of jamming

susceptability deserves careful consideration.

2. We have demonstrated serious weaknesses in the performance of both systems even in the absence of interference. A redesign of these systems may result in one with an acceptable level of performance. A closer approximation to a maximum likelihood tracking algorithm may be an attractive approach. The dominant question is to assess the feasibility of this class of system.

3. Since the pattern of the airborne antennas can have a significant effect on system performance it is essential to obtain more realistic antenna patterns. A currently ongoing effort at the Transportation Systems Center should be extremely helpful in this regard.

4. A second order design and analysis of satellite orbits should be conducted. Of particular interest is the possibility of dynamic, real time switching between satellites. Further investigation of alternative constellations and the resulting geometric dilution is also desirable.

5. Variations in aircraft ERP have a significant effect on system performance and deserve effort. Of particular concern are variations between aircraft and variations over time; included are antenna and power amplifier degradations.

6. Since others have addressed the hardware realization, we have not considered this area in detail. Hardware considerations should be included during the next effort in the study.

7. An improved model of the degradation due to multiple access noise is needed. A complement to this effort is a careful study of candidate codes.

8. In spite of small signal suppression, the analyzed systems assume a bandpass limiting satellite repeater. This avoids dynamic range problems inherent in a linear repeater. A more detailed study of these competing repeater designs is warranted.

9. Reflection multipath at low satellite elevation angles may serve to (1) increase the "multiple access" noise and (2) affect the design of multipath resistant modulation and demodulation equipment. A directed experimental program may be required to investigate these effects.

10. A noise measurement program to determine the level of RFI and industrial noise background at L-band could help to resolve some of the uncertainty in the system performance estimates and design.

B. Satellite-to-Air-to-Ground Surveillance System

1. Initial feasibility of the system has been demonstrated. A careful redesign is required to realize a more nearly optimized design.

2. The satellites have been assumed to operate in a pulsed mode. Alternative modes should be investigated.

3. The issue of providing onboard navigation should be reevaluated. After the first order investigation this remains a promising option. This problem must be addressed in the broader context of evaluating the required avionics hardware.

4. Because of the requirement for several hundred ground stations, it is essential to carefully study the cost and complexity of these stations.

5. The required air-to-ground communication link has been shown to be feasible both in its performance and hardware complexity. A second order design is required. This effort should take account of the upgraded third generation ATC system and the data-link requirements. Use of simple coding techniques on this link should be considered because it can result in lower power requirements and higher reliability and have the potential for higher data rates.

6. In air-to-ground communications, reflection multipath can have severe effects on system performance. Ground based antennas must be designed and sited properly to amelioriate these effects. Further investigations should include refinement of the existing computer models and design of suitable carefully directed experiments to refine the antenna designs and obtain better multipath models. The effect of reflection multipath in the satellite-to-aircraft link must also be determined.

7. Although the selection of satellite orbits is not as critical for this system as for the previous system, it deserves consideration here also. The same comments also apply to the variations in aircraft antenna patterns and background noise.

8. Temporal and spacial variations in atmospheric refraction can degrade performance by creating shadow zones, raising interference levels (through ducting) and causing position errors. Investigations are warranted.

C. Air-to-Ground Surveillance System

1. Acceptable performance has not been demonstrated for this system. Required for the next iteration is a careful redesign of the system and detailed investigation of several of the critical assumptions. The dominant problem is to assess the feasibility of this class of systems.

2. A second order model of the degradation due to multiple access noise is essential to a good performance estimate. Emphasis should be on understanding the effect due to the dynamic variation in the number of users as well as on the variation in power due to distance from the receiver.

3. Further studies of this system must address the hardware realization, particularly the cost and complexity of the several hundred required sites.

4. Reflection multipath degrades performance of this system in the same way as the air-to-ground link of the previous s system. A better understanding of this degradation must be developed.

5. Variations in antenna pattern and aircraft ERP affect performance. The size of these variations must be determined.

6. Coding should be explored as a means of improving performance.

7. Atmospheric refraction effects should be assessed.

SECTION 2

AIR-TO-SATELLITE-TO-GROUND SURVEILLANCE SYSTEMS

2.1 Introduction

In this section we consider two different air-to-satellite-to-ground surveillance systems. The fixed signature repetition rate system (FSRR) operates by having all aircraft transmit their signatures at the same fixed repetition rate. The variable signature repetition rate system (VSRR) allows different aircraft to transmit their signatures at different repetition rates. In both cases each aircraft asynchronously transmits a unique waveform consisting of a sequence of PSK modulated pulses at low duty cycle (less than 0.01 percent). The transmission is received by a constellation of at least four satellites and relayed to a ground processing station. At this station matched filtering is performed to detect each unique waveform corresponding to each aircraft.

After detecting an aircraft with at least four satellites, time of arrival differences are estimated. These can be used to compute the aircraft's position by calculating the position of the intersection of hyperbolic surfaces.

As a prelude to evaluation of the performance of the two systems, it is necessary to evaluate the received signal to noise ratio. High gain ground terminal antennas can be utilized in the satellite downlink; hence, this link can be assumed to be noiseless. Thus, only the uplink performance need be investigated in detail.

2.2 Satellite Uplink Calculation

Table 2.1 summarizes the air-to-satellite power budget. A pulse enery of 0.03 Joules is assumed. This is comparable to that achieved in

TABLE 2.1

AIR-TO-SATELLITE POWER BUDGET

Transmitted Energy	-15 dbJ	See Appendix A
Aircraft antenna gain	2.5 db	See Appendix A
Miscellaneous losses	-2 db	Feed and atmosphere losses
Path loss	-192 db	1.6 GHz, Synchronous elliptic orbit. See Appendix D.
Satellite Antenna gain	24 db	10^{o} beamwidth
Received Signal Energy	-182.5 dbJ	
Receiver noise power density	-201 dbw/Hz	RFI, thermal and front end noise of 600^{o} K
Number of users	50 db	Peak loading of 10^{5} users
Pulse repetition rate	3 db/sec	FSRR 5 pulses in 2.5 sec. VSRR 4 pulses in 2 sec.
Receiver bandwidth	73 db Hz	
Effective multiple access noise power density	-202.5 dbw/Hz	
Effective noise power density	-199 dbw/Hz	Receiver plus effective multiple access noise.
Limiter loss	-1 db	Bandpass limiter
Aircraft antenna disadvantaging	-3.5 db	See Appendix A
Aircraft power amplifier disadvantage	-1 db	See Appendix A
Decorrelation loss	-1 db	See Appendix A
Excess atmospheric absorbtion	-1 db	Oxygen absorbtion
Effective signal energy to noise power density	9 db	

the laboratory with solid state power amplifiers today. However, it is easily achievable with tube technology.

The path loss used in the power budget represents a worst case assumption for the candidate inclined sychronous elliptical satellite orbits described in Appendix D. The satellite antenna is assumed to be a reflecting dish shaped to provide a relatively uniform nominal 24 db antenna gain over CONUS. The allowance for a peak loading of 10^5 users is intended to allow for a factor of two growth from the peak aircraft loading projected for 1995. For both of the systems which were analyzed, each aircraft averages one pulse sequence in 0.5 sec. Each pulse is assumed to be phase modulated with a chip duration of 100 nsec. This implies an effective bandspreading of approximately 20 MHz.

To compute the degradation in performance due to the multiple users of the system we assume that the degradation of any particular user's performance caused by the signal of any other user is the same as it would be if this signal consisted of an equal power of white gaussian noise in the band. This should be viewed as a first order assumption. A more exact model would account for the variation in simultaneous loading.

It has been assumed that a bandpass limiting satellite repeater is employed. This avoids the problems of large dynamic range inherent in a linear repeater. Since a small signal inbedded in additive Gaussian noise suffers a loss of 1 db when passed through a bandpass limiter, a 1 db limiter loss has been assumed.

In order to compute the multiple access noise it was necessary to assume average aircraft parameters. However, to achieve the desired goal of keeping track of virtually all aircraft it is necessary to design the system, not for the average aircraft, but for a highly disadvantaged aircraft. When an aircraft banks it is especially important to retain surveillance in spite of the fact that one or more of the four satellites may be at a low elevation angle (in a coordinate system that is stationary with respect to the aircraft antenna). It is clear from the discussions in Appendix A that as this elevation angle approaches zero, the aircraft antenna gain and hence the aircraft ERP in the direction of the satellite is significantly reduced. In order to keep the resulting loss within reason the following strategy was adopted.

1. The goal was set of maintaining surveillance of all aircraft banking at angles of 30^{o} or less.

2. Satellite orbits were selected which insure that from every point over CONUS there will be at least four satellites within a cone of 45^{o} half angle centered at the Zenith position.

From examining the representative antenna patterns of Appendix A it can be observed that the resultant minimum antenna gain at 15^{o}, i.e., 45^{o} minus 30^{o}, is -1 db; hence, the minimum included aircraft antenna gain is 3.5 db lower than the nominal 2.5 db antenna gain. Requiring four satellites within a 45^{o} half angle cone imposes a geometric dilution penalty. The first order analysis of Appendix D indicates that the position errors are a factor of twenty larger than the errors in estimating time differences. (See Tables D. 1 and D. 2).

The actual rf power transmitted will vary from aircraft to aircraft. We have optimistically assumed that the minimum rf power is only 1 db below the average power. In Appendix A we have estimated a loss of 1 db due to frequency offset between the receiver frequency standard and the received waveform. This offset is caused by local oscillator instability, aircraft motion, and satellite motion.

These rather optimistic estimates lead to an estimated signal energy to noise power density at the satellite receiver of $\frac{E}{No} = 9$ db. This will form the basis of the performance analysis of the two candidate systems described in the next two sections. The link calculation which arrives at this value of signal energy to noise power density is shown in Table 2. 1.

2.3 The FSRR System

In this subsection the signal waveforms which the FSRR system utilizes are briefly described and the FSRR system performance summarized. The FSRR system is extensively described and analyzed in Appendix B.

The FSRR system operates with each aircraft transmitting a signature consisting of 5 pulses. A typical signature is shown in Figure 2.1. Pulse A is an initial synchronization pulse. The pair of pulses, B and C, are positioned symmetrically with respect to a center axis which is placed at a fixed distance from pulse A. This pair of pulses can occupy one of 317 possible pair positions. Similarly, pulses D and E are symmetric with respect to a center axis which lies at a larger fixed distance from pulse A. Pulse pair D-E also can occupy one of 317 possible pair positions around its center line..

Each of the five pulses which constitute the signature of any particular aircraft is composed of the same pseudo random sequence; other aircraft may use different sequences. The system uses ten different pseudo random sequences to construct the aircraft signatures. Hence, there are 10^6 [i.e., $10(317)^2$] possible signatures. Thus, the FSRR system can accommodate 10^6 aircraft. Each aircraft transmits its signature once every 2.5 seconds. The total time duration of the signature is at most 1 msec. Each signature pulse consists of 200 chips of 100 nsec duration. Position updates can thus be accomplished once every 2.5 sec. Small changes in the update rate have little beneficial effect on system performance. Increasing the update rate to once a second increases the multiple access noise; it can easily be shown to decrease the signal to noise ratio from 9 db to 7.5 db. On the other hand, decreasing the update rate at most increases the signal to noise ratio by 2 db.

Two parameters $\overline{N_f}$ and P_D, are used to indicate the performance of the FSRR system. The first of these parameters, $\overline{N_f}$, is the average number of false alarms generated by the system in a 2.5 second period. The

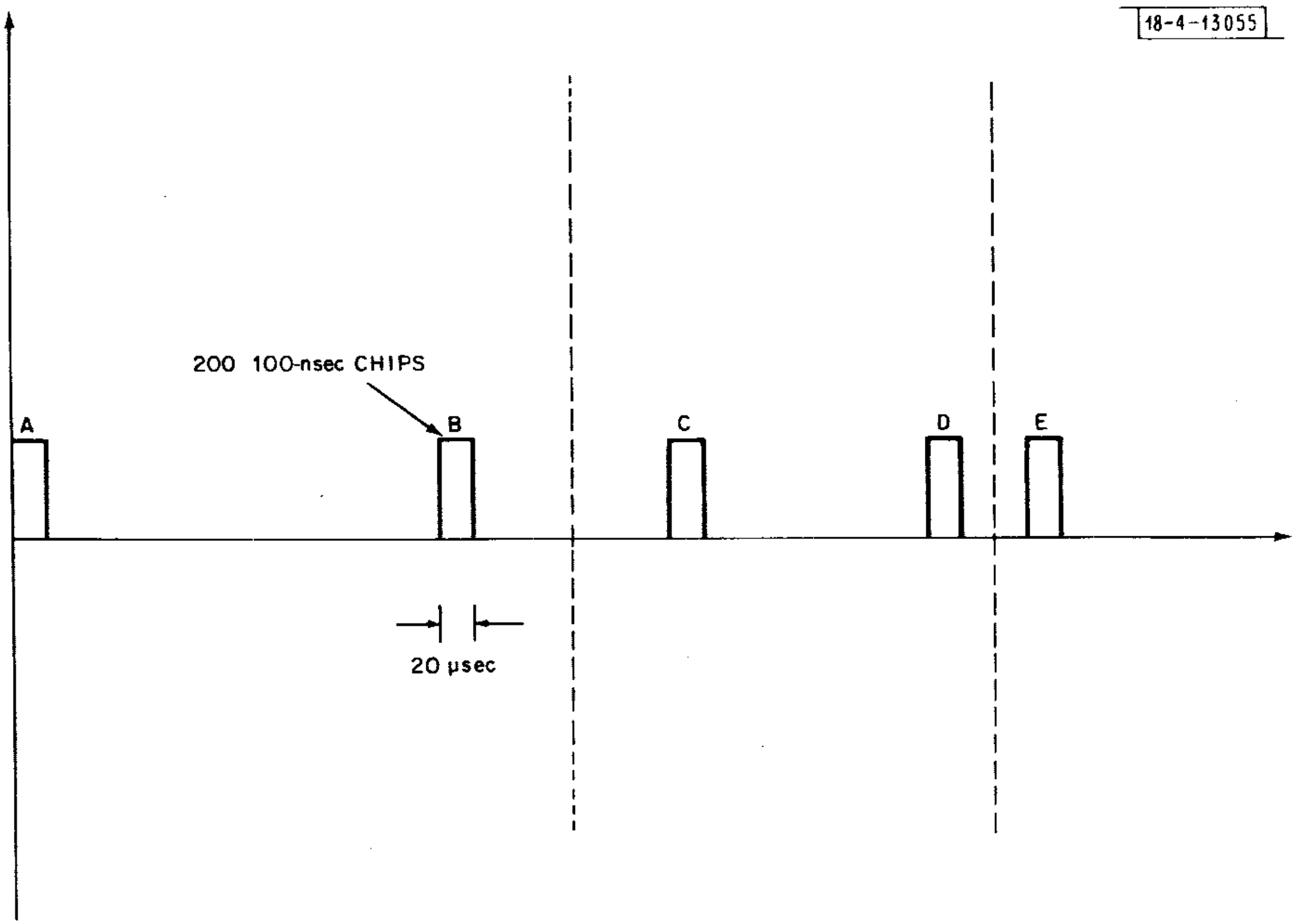

Fig. 2.1. A typical FSRR signature.

system will generate a false alarm if at a specific time it declares that an aircraft is in the airspace at a certain position and either the aircraft is not in the position given or not in the airspace at all.

The second parameter, P_D, is the probability that the ground station declares any particular aircraft to be present at its correct position at a particular time.

Table 2.2 gives the false alarm and detection performance of the FSRR system for various values of received signal to noise ratio. E/N_o · $\overline{N_f}^L$ is a lower bound to $\overline{N_f}$ and P_D^u is an upper bound to P_D. Hence, the Table represents the best possible FSRR performance. The parameter P_d is the probability that a signature pulse received at the filter to which it is matched will in fact be detected. P_f is the probability that the same filter will be excited by noise and declare a matched pulse present at its input when, in fact, none is present. In the table each (P_f, P_d) pair can be realized at the value of E/N_o given.

TABLE 2.2

FSRR SYSTEM PERFORMANCE

E/N_o	P_d	P_f	$\overline{N_f}^L$	P_D^u
9 db	0.98	0.1	1.038×10^4	0.667
9 db	0.99	0.2	3.62×10^4	0.82
9db	0.997	0.3	6.54×10^4	0.94
13.5 db	0.9998	.01	1.126	0.99
6 db	0.82	0.1	790	.0188
6 db	0.92	0.2	1.23×10^4	.188
6 db	0.94	0.3	2.64×10^4	0.29

It is evident from Table 2. 2 that for an E/N_o = 9 db (which is the link value computed in Table 2. 1) the FSRR system will not perform effectively because the average number of false alarms that the system would generate in a 2. 5 sec. period is of the order of 10^4. This represents an intolerable additional computational load that the system could be forced to accommodate. Furthermore, the system detection probability is at best equal to 0. 94 which is an unacceptably low figure.

The fact that the effective signal to noise ratio computed in Table 2. 1 is so small, i.e., 9 db,is due in large part to the aircraft antenna disadvantage. It could be argued by some that this 9 db value will only apply to one air-to-satellite link and that the other air-to-satellite links will have higher signal to noise ratios; hence, system performance should be better than that illustrated by Table 2. 2. Unfortunately, this view is fallacious. The bounds shown in Table 2. 2 (for the entries corresponding to E_o/H_o= 9 db) depend upon only one air-to-satellite channel having the deteriorated signal to noise ratio of 9 db. Even if three of the air-to-satellite channels are operating with an infinite signal to noise ratio, but one is operating with a 9 db signal to noise ratio, the performance of the FSRR system will be the degenerated performance given for 9 db in Table 2. 2.

The aircraft antenna disadvantage is due to the fact that the aircraft banks at an angle of 30 degrees potentially causing the lowest gain portion of the antenna pattern to point toward one of the satellites. Thus, the power received from this aircraft is less than the average power received from the other aircraft. Since only a fraction of the aircraft will be disadvantaged at the same time, one might conclude that the system performance is much better than that illustrated by Table 2. 2. Unfortunately, this view is also fallacious. The figures of Table 2. 2 are determined by the thresholds set at the ground station matched filters. The philosophy of an air traffic control surveillance system must be to detect the weakest aircraft in the airspace. This forces the matched filter thresholds to be designed for the disadvantaged E/N_o equal to 9 db. Hence, the actual system performance will not be any better, in terms of false alarms, than the bound given by Table 2.2. The detection performance will only be better by a negligible amount.

It should be noted that the required computational load in the FSRR surveillance system is not overly complex. Aircraft signatures are received and stored sequentially with respect to time at each of the four ground station memories. A processor moves through the memory of one of the satellite ground stations. If it locates the signature of aircraft "i" stored at an address corresponding to reception at time t_1, it notes this. The processor then interrogates the other ground station memories with an inquiry as to whether or not each of them received aircraft "i's" signature within ± 24 msec. of t_1. If they all answer in the affirmative, aircraft "i" is declared present at time t_1 and its position is computed. All of the operations just described are very simple computational procedures. This is an attractive feature of the FSRR system.

Another feature of the FSRR system concerns its performance in the event of a total system failure. The FSRR system operates with absolutely no memory from signature repetition period to signature repetition period. Each consecutive 2.5 second interval the system acquires (or attempts to acquire) all the aircraft in the airspace. Thus, a system failure will cause no extra drain on the computational power needed at the ground station. After the cause of failure is corrected the FSRR system merely proceeds operating normally. It will automatically reacquire all aircraft, (provided they are detected), within 2.5 seconds.

2.4 The VSRR System

The other air-to-satellite-to-ground surveillance system which has been considered requires that each aircraft transmit a signature at a fixed repetition rate. However, the repetition rate can vary from aircraft to aircraft. Specifically, it can be one of 100 possible rates. We call this system the Variable Signature Repetition Rate (VSRR) system. It is described in detail and analyzed in Appendix C. In this subsection the signal waveforms which this system employs are described and its performance is summarized.

The VSRR system operates with each aircraft transmitting a specific codeword every x seconds, with x being one of the 100 possible numbers in the set (2. 000, . . , 2. 099). The utilization of different codeword repetition rates is a central feature of this system. The aircraft codeword consists of 4 pulses. Each pulse is itself, a 511 chip long pseudo random sequence. A chip is 100 n sec long and carries one bit of information by PSK modulation. A typical aircraft codeword is illustrated in Figure 2. 2. The pulses are labelled A, B, C, and D. Each of these pulses is chosen from a different set of 12 pseudo random sequences, with all sets being disjoint. This implies that these are $(12)^4$ possible codewords. Since x can take on one of 100 possible values, there are 100 $(12)^4$ possible aircraft signatures. Assuming an aircraft population of 10^6 the VSRR system can then supply each aircraft with a unique signature.

The parameters used to measure the performance of the VSRR system are similar to those chosen for performance measurement of the FSRR system. One of the parameters is $\overline{N_f}$, which is the average number of false alarms generated by the system during a tracker cycle. A tracker cycle corresponds to approximately 2. 1 seconds (i. e., one codeword repetition period). The definition of a false alarm generated by the VSRR system is similar to that of the FSRR system. A false alarm is the event of the VSRR system deciding, at a central surveillance station, that a particular aircraft is at a particular position at a particular time, when in fact this is not true.

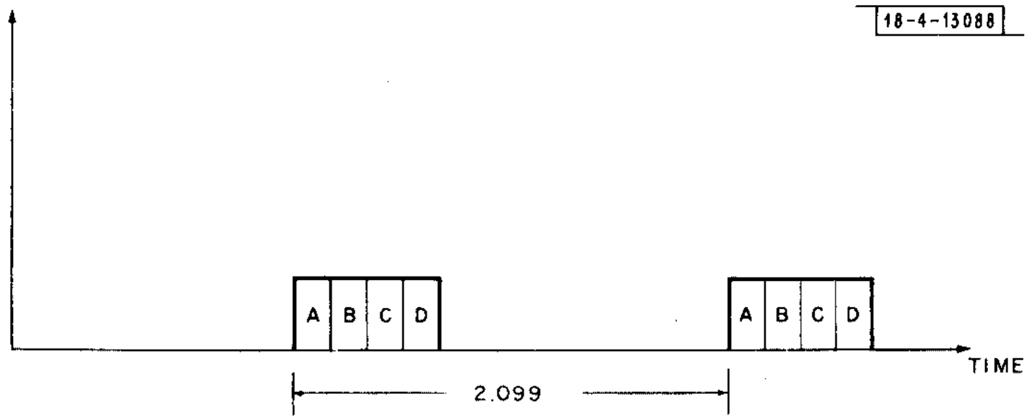

Fig. 2.2. A typical VSRR signature.

The other performance parameters used in analyzing the VSRR system measure how well this system correctly detects an aircraft. On a given tracker cycle an aircraft is said to be detected correctly if during this cycle the central surveillance station records the aircraft's position at a certain time and in fact the aircraft is at this position at this time.

Because the operation of the VSRR system is very complex, we do not attempt to directly compute the probability of correct detection of a given aircraft. Instead, several equivalent detection parameters are computed and used to measure the detection performance. One of the most important of these parameters is P_d (i/i-1). This is the probability that aircraft "j" is correctly detected on the i^{th} tracker cycle given that it has already been correctly detected on the $(i-1)^{th}$ tracker cycle.

Table 2.3 gives the false alarm and detection performance of the VSRR system. These results were obtained by assuming a received signal to noise ratio, E/N_o, equal to 9 db (as computed in Table 2.1). The performance is computed for various values of P_f and P_d where P_f and P_d are as defined in Section 2.3, $\overline{N_f}^u$ is an upper bound to $\overline{N_f}^u$, P_d^L (i/i-1) is a lower bound to P_d (i/i-1). While the VSRR system performs at a better figure than these bounds, the bounds are expected to be fairly tight.

As is evident from the table, when the detection threshold is selected such that $P_f = 0.05$, the false alarm performance of the VSRR system is extremely good. However, the detection performance is not acceptable. Lowering the threshold so that P_f increases to 0.1 still gives an acceptable false alarm rate. However, the detection performance, while improved, is still not acceptable. Lowering the threshold further causes both the false alarm and detection performance to degenerate very rapidly. The system ultimately suffers from a great many false alarms which represent a severe computational penalty. The detection parameter, P_d (i/i-1) is not close enough to unity to be operationally attractive for any of the P_f, P_d combinations considered.

In comparing the performance of the VSRR and FSRR systems one cannot recommend one of these systems over the other, assuming $E/N_o = 9$db. At this value of received signal to noise ratio the performance of both systems is unacceptable.

It should be remarked that the VSRR surveillance is extremely complex with respect to the computational power it needs. This complexity arises from the fact that variation of the aircraft codeword period is used to provide unique identity. This implies the need for a complex sorting procedure to obtain an initial track on the aircraft. While implementation of this procedure is feasible, the computational power it requires is quite large.

TABLE 2.3

VSRR SYSTEM PERFORMANCE

E/N_o	P_f	P_d	$\overline{N}_f^u$	$P_d^L(i/i-1)$
9 db	0.05	0.965	$75.5 \cdot 10^{-4}$	0.565
9 db	0.1	0.98	31	0.7
9 db	0.15	0.985	$3.98 \cdot 10^{3}$	0.665
9 db	0.2	0.99	$1.271 \cdot 10^{5}$	0.505
9 db	0.3	0.995	$1.630 \cdot 10^{7}$	0.0695

It should be noted that computational requirements for restart of the VSRR system after a total system failure are modest. Although this system does not automatically reacquire all aircraft within a signature repetition period, (i.e., approximately 2 sec.), it does have the potential to do this within 5 signature repetition periods (approximately 10 seconds). The added delay is due principally to the incorporation of a tracking feature in this system. This feature is necessary because of the variable signature repetition rate character of identification. This tracking feature utilizes memory from one repetition period to another, thus requiring a longer reacquisition time.

This system is designed to provide position updates once every two seconds. Small changes in required update rate have little beneficial effect on system performance. In particular, if the update rate is increased to once every second the signal to noise ratio decreases by 2 db, resulting in an E/N_o of 7 db. On the other hand, a decrease in the required update rate can at most increase the signal to noise ratio by 2 db.

As a final remark, one should note the similarities betweeen the VSRR System and the LIT (Location/Identification Transmitter) type system described by Otten et. al. of TRW*. Both systems assign a unique signature to each aircraft by providing it with a unique codeword-repetition period pair. The VSRR system constructs each codeword from four pseudo-random sequence pulses. There are $(12)^4$ distinct codewords which it employs. It chooses each repetition period from a set of size 100. The LIT system referred to transmits a one pulse codeword and utilizes only 50 distinct codewords. It chooses a repetition period for each aircraft from a set of size 10^4.

As one can readily conclude, the main burdern of unique identity in the VSRR system is carried by the codeword information. The main burden of unique identity in this LIT system is carried by the repetition rate modulation. The implication of this difference is given in the following paragraph.

From the description and analysis of the VSRR System performed in Appendix C, it is evident that the presence of varying repetition rates forces the computational operations needed in the system to become quite

*"Satellites For Domestic Air Traffic Control"--paper given at AIAA 3rd Communications Satellite Systems Conference--April 1970.

involved. In order to obtain initial acquisition of the aircraft, the received signatures must be sorted, which is not a trivial task. However, it does not appear that the presence of varying repetition rates enhances the system performance. The LIT system referred to uses a great many more repetition rates than the VSRR system. Therefore, the sorting problem must be correspondingly more costly, (in terms of computation required). On the other hand, its performance will not necessarily be improved because of this.

On the basis of this brief comparison we can conclude that the VSRR system is more attractive in terms of its complexity than the LIT System mentioned.

2.5 Other Considerations

We have observed that neither the FSRR nor the VSRR air-to-satellite-to-ground system is expected to have an acceptable level of performance. In this section we address the susceptability of these systems to jamming and also consider prospects for improving these systems.

It is evident from the preceding sections that system performance is extremely sensitive to changes in E/N_o. For a first order measure of the jamming susceptability we shall evaluate the jammer ERP required to reduce E/N_o by 3 db. In Table 2.4 we calculate the power level required to increase the effective noise power density by 3 db. Only a 42 dbw ERP facility is required. This facility can be realized with a 3.5 foot antenna with 100 watts of rf power. The cost and operational complexity of a 42 dbw ERP facility are sufficiently small to make such a threat readily available to a large variety and number of groups within the country or close to it. Such a facility is also easily mounted on a small off-shore pleasure craft. Naturally, the jammer's antenna must be pointed at the satellite; however, with the assumed 10^o beamwidth this should not be difficult. As is indicated in Appendix D a single jammer is sufficient to impose a serious penalty in geometric dilution. A few jammers, each directed at different satellites, should be sufficient to completely disable the entire system.

TABLE 2.4

TERRESTRAL JAMMER FOR AIR TO SATELLITE SYSTEM

Jamming power required at the satellite to reduce the effective signal energy to noise power density by 3 db.	-126 dbw	Equals the effective noise in the receiver bandwidth, i.e.,
Satellite antenna gain (-)	-24 db	10° beamwidth
Path loss (-)	+188 db	1.6 GHz, synchronous orbit
Miscellaneous loss (-)	+4 db	
Required Jammer ERP	42 dbw	For example, 100 W of RF Power and a 3.5 foot antenna (22 db gain, 13°)

In examining the prospects for improving this class of systems we can make the following three observations:

1. An increase in pulse energy can at most yield an improvement in E/N_o of 2.5 db because of the multiple access noise. Unfortunately, system performance would remain unacceptable, although somewhat better performance is realized.
2. Some improvement in performance may be realized through improving the signal waveforms and the associated receiver structure.
3. A rapid access ground-satellite-air communications link for use in collision warning and avoidance is a prime candidate for this system. The feasibility of such a link is dependent on the details of the surveillance system and thus is best designed along with a redesign of this system.

We believe, however, that the most essential next step is to try to assess the jamming threat to any air-to-satellite-to-ground surveillance system as contrasted to the above assessment of the jamming threat to these two particular systems. It is difficult to determine at this point whether or not it will be necessary to design an effective air-to-satellite-to-ground surveillance system in order to perform the assessment of the jamming threat.

SECTION 3

SATELLITE-TO-AIR-TO-GROUND SURVEILLANCE SYSTEM

3.1 Introduction

The satellite-to-air- portion of this system is, in a sense, the dual of the air-to-satellite link of Section 2. In particular, it employs a satellite constellation with a minimum of four satellites, each of which transmits one PSK modulated 20 μsec pulse every second. The chip duration is again selected to be 100 nsec. The PSK modulation is assumed identical for all satellites. The pulses are synchronized from satellite to satellite with an accuracy of one part in 10^7; however, a fixed delay of 8 msec between pulse transmissions from different satellites is imposed to ensure that no pulses overlap anywhere over CONUS. At the receiver, a matched filter envelope detector together with satellite ephemeris data, are sufficient to permit aircraft position to be calculated. Two alternatives are considered in this section. In the first, position is calculated on the aircraft and then transmitted to a ground station within line of sight, to provide both a navigation and a surveillance capability. In the second, the time differences are simply transmitted to a ground station within line of sight, to provide surveillance capability only. We have analyzed in detail the performance of the satellite-to-air link, the air-to-ground link and the computational complexity required to realize a navigational capability.

3.2 Satellite-to-Air Link

The down-link path loss calculation is presented in Table 3.1. The pulse energy transmitted by the satellite is assumed to be 9 db higher than that transmitted by the aircraft in the air-to-satellite-to-ground systems. A vacuum tube power amplifier could be used if suitable solid state power amplifiers cannot be developed. The aircraft antenna gain is assumed to be

TABLE 3.1

SATELLITE-TO-AIR LINK CALCULATION

Transmitted Energy	-6 dbJ	See Appendix A
Satellite Antenna Gain	24 db	10^o beamwidth
Miscellaneous Losses	-3 db	Feed and atmospheric losses
Path Loss	-192 db	1.6 GHz, sychronous elliptical orbit (Appendix D)
Aircraft Antenna Gain	-3 db	Elevation angles of 5^o or higher See Appendix A
Received Signal Energy	-181 dbJ	
Received Noise Power Density	-199 dbw/Hz	RFI, thermal and front end noise of 1000^oK
Effective Signal Energy to Noise Power Density	18 db	

-3 db or larger. From Appendix A this is seen to correspond to elevation angles of 5° or higher. (For this system it is not necessary to require a minimum elevation angle of 15° as was required in the air-to-satellite-to-ground systems to limit performance degradation due to the multiple access noise). It therefore follows that the four satellites must be within a cone of half angle 55°, centered at the zenith position, in order to service all aircraft with bank angles no greater than 30°. The geometric dilution and the minimum required number of satellites are expected to be smaller for this system than for those of the previous section.

We see from Fig. 3.1 that with an

$$\frac{E}{N_o} = 18 \text{ db},$$

the system can achieve a pulse detection probability of

$$P_d = 0.9999$$

concomitent with a pulse false alarm probability of

$$P_f = 10^{-12}.$$

It follows that the probability of detecting the required four pulses is

$$P_D = P_d^{\,4} = 0.9996$$

and, if the matched filter is sampled once every 25 nsec, the average number of false alarms per aircraft per second is over bounded by

$$N_f = \frac{P_f}{25 \times 10^{-9}} = 4 \times 10^{-5}.$$

This is an upper bound since it doesn't take account of the constraints between received pulses from successive satellites within the constellation.

With a population of 10^5 aircraft it follows that over any particular one second interval, there will be an average of less than four aircraft which detect one or more false pulses and 40 aircraft which fail to detect a transmitted pulse. For the assumed model it is very unlikely that the same aircraft will detect false pulses and fail to detect the correct pulse during one satellite transmission period. We view this level of performance to be be acceptable.

3.3 Air-to-Ground Link

In this section we discuss the signal structure employed in the air-to-ground link portion of the satellite-to-air-to-ground surveillance system. The performance of this link will also be summarized. The air-to-ground link is considered and analyzed in extensive detail in Appendix E.

As has been stated in Sec. 3.1, each aircraft can calculate its position using the differences in the times of arrival of signals transmitted to it by the satellite constellation. The task of the air-to-ground link is to transmit position data to a ground station. As has been previously stated there are two ways this can be accomplished. The differential times of arrival can be transmitted directly to the ground and position computation carried out on the ground. An alternative to this is to transmit the aircraft position coordinates, which are computed on board the aircraft, to the ground. Both of these transmission methods are considered in Appendix E. In this subsection, we shall only describe position transmission using the second of these alternatives.

On the air-to-ground link position data is transmitted using a modulation format called, "On-Off Keying." In this modulation format a binary digit "1" is transmitted by sending a pulse having a duration of 0.5 μsec. A binary digit "0" is transmitted by having the channel quiet (not transmitting anything) for 0.5 μ sec.

Each aircraft is assigned a unique identification number, some integer from 1 to 10^6. An aircraft relays its position to the ground only <u>upon request</u> from a ground station. When an aircraft receives a request for its position it responds by transmitting to the ground station a codeword consisting of 79 bits. The structure of the codeword is as follows:

1. The first 10 bits are "1's." This is a synchronization prefix which allows the ground station to identify the beginning of the codeword. The On-Off Keying modulation necessitates this.
2. The next block of 20 bits is the expansion to base 2 of the aircraft identification number.
3. The following block of 11 bits represents the aircraft altitude to within an accuracy of 50 feet.
4. The next block of 19 digits represents the difference between the aircraft's longitude and 60° W longitude (which we consider the eastern boundary of CONUS surveillance), to within 0.01 minutes.
5. The final block of 19 bits represents the difference between the aircraft's latitude and 15° N latitude, (which we consider the southern boundary of CONUS surveillance), to within 0.01 minutes.

Each aircraft revises or updates its codeword when it receives a new transmission from the satellite constellation. As has already been stated each aircraft uses its codeword to relay its position to the ground station upon request. A ground station cycles through all aircraft in its area of control making this request and then repeats the procedure. Each interrogation cycle is of the order of a few seconds. After the ground station receives and interprets an interrogated aircraft's codeword it enters its position on a list. This list is updated with each interrogation cycle.

Table 3.2 is an air-to-ground link power budget for transmission of one bit representing the digit "1" in a codeword. E/N_o the received energy to noise power density is 20 db. This corresponds to a received bit error probability of (0.355) 10^{-5}. Using this bit error probability the following lower bound can be computed:

$$\text{Prob}\left(\begin{array}{l}\text{a specific aircraft}\\ \text{position is correctly}\\ \text{updated on an inter-}\\ \text{rogation cycle}\end{array}\middle|\begin{array}{l}\text{a specific}\\ \text{aircraft is}\\ \text{interrogated}\end{array}\right) \geq 0.9996$$

This is a measure of the surveillance performance of the air-to-ground link. This lower bound indicates that the link performance is satisfactory.

TABLE 3.2

AIR-TO-GROUND LINK POWER BUDGET

P_t (peak signal power transmitted)	23 dbw	See Appendix A
Pulse duration	-64 dbsec	0.4 μsec
Aircraft transmitting antenna gain	0 db	
Range loss	-143 db	200 mile maximum slant range, 1 GHz.
Receiver Noise Power density (N_o)	-199 dbw/Hz	RFI, thermal and front end noise (1000^oK)
Miscellaneous losses	-3 db	Feed, atmospheric and signal disadvantage
Receiving antenna gain	14 db	Fan beam 3^o by 9^o
Multipath Fading	-6 db	See Appendix G
Signal Energy to Noise Power Density (E/N_o)	20 db	

3.4 Avionics Computer to Provide Navigation Capability

The computer requirements for on-board navigation in the satellite-to-air system are discussed in this section. A summary of the various computational tasks involved in determining the aircraft position, and estimates of the computer capabilities necessary to update the aircraft position at one second intervals are included in this section. It is shown that the computational tasks are well within the capabilities of a 4096 word, 16 bit minicomputer, e.g., the Nova. A rough estimate of the cost of a special purpose navigation computer is also included. A complete analysis may be found in Appendix F.

The computer receives, at intervals of K_1 seconds, the differential times-of-arrival of ranging pulses from N synchronous satellites. It also receives, at intervals of K_2 seconds, the ephemeris data for the N satellites and an accurate time of day. From these data the computer calculates, every K_1 seconds, an estimate of the aircraft position. For the purposes of this analysis, N has been taken to be five; and K_1, one. K_2 may be thought of as a parameter in the design of the computer, as larger values of K_2 introduce larger errors into the aircraft position estimates. A maximum value of K_2 equal to 100 could possibly be attained.

The computational tasks during each one second interval fall into four classes:

1. Updating the satellite positions.
2. Computing a predicted aircraft position at time t from the estimated positions at times t-2 and t-1, assuming a constant velocity over the interval (t-2, t).
3. Estimating the aircraft position at time t using the most recent pulse arrival time differences and the predicted aircraft position at time t.
4. Converting this estimate from an inertial rectangular coordinate system to a rotating spherical coordinate system (latitude, longitude, and altitude).

It is shown in Appendix F that errors in estimating the satellite ranges introduce errors in the estimated aircraft position in the same manner as do errors in determining the satellite pulse arrival times.

That is, satellite tracking errors are amplified by the geometric dilution of the satellite constellation. The amplification may be an order of magnitude. Thus, satellite tracking errors in the radial direction must be no larger than a few tens of feet.

If the satellites are tracked using a linearized, discrete time approximation to the satellite dynamics, then the tracking error can be conservatively upper bounded by

$$.05\ K_2 + 2^{-(b-30)}\ (.4\ K_2 + .5)\ \text{feet}$$

where b denotes the number of bits used in the computations. Thus, if K_2 is taken to be 50, and 33-bit registers are used, the tracking error can be bounded by five feet.

Another possibility is to use the exact solution to the satellite trajectory. This method requires more computations; but, because it is not a recursive method of tracking the satellites, computational errors do not accummulate. It is shown in Appendix F that the tracking errors are bounded by five feet using this method when K_2 is 100, when 30-bit registers are used, and when the aircraft clock is accurate to 2 parts in 10^6.

The remaining three computational tasks may be performed using 30-bit registers. The most important contributor to roundoff errors in the calculations, a Gaussian solution to set a linear equations, can be shown to introduce no more than 20 feet of error to the aircraft position estimate. This bound is independent of the geometric dilution facotr.

The following constitute a conservative estimate of the navigation computations required to make one position determination.

less than 200 multiplications

less than 50 divisions

less than 200 additions

less than 100 30-bit registers(read-write)

364 22-bit registers of read-only memory

less than 2500 registers for the program (read-only)

A Nova computer with a memory cycle time of 2.6 μ sec. could perform all the computations for each position estimate in less than 50 msec; this corresponds to an idle time of 95%.

While it is difficult to estimate the cost of a special purpose navigation computer, one can expect that by 1990 the cost would be less than $1000, assuming that the computers are to be produced in large quantities.

3.5 Position Estimation Errors

As has been shown in Sections 3.2 and 3.4, there are several contributors to the error in estimating the aircraft position. A first order model for the position estimation error vector, $\underline{\delta}$, is

$$\underline{\delta} = \underline{K}\,\underline{H}\,\underline{\epsilon} + \underline{\delta}c$$

where $\underline{\delta}c$ represents the calculation round-off errors; $\underline{\epsilon}$ is a random vector representing the combined effects of errors in tracking the satellites and errors in measuring the pulse arrival times; and $\underline{H}$ and $\underline{K}$ are matrices, $\underline{H}$ represents the operation of calculating pulse arrival time differences and $\underline{K}$ represents the linearized portion of the estimator. It has been shown in Appendix I that a worst case bound on $\underline{\delta}c$ is

$$\| \underline{\delta c} \| < 20 \text{ feet.}$$

Therefore, the rms position error can be bounded by

$$\| \underline{\delta} \|_{rms} < \| \underline{K} \; \underline{H} \; \underline{\epsilon} \|_{rms} + 20. \qquad (3\text{-}1)$$

The random vector $\underline{\epsilon}$ can be written as

$$\underline{\epsilon} = \frac{1}{c} \, \underline{\epsilon} t + \underline{\epsilon} p + \underline{\epsilon} o + \underline{\epsilon} v \, .$$

In the above, $\underline{\epsilon} t$ represents errors in estimating the satellite ranges and c is the speed of light; $\underline{\epsilon} p$ represents errors in determining location of the peaks in the matched filter output; ϵo represents errors resulting from oscillator inaccuracies; and $\underline{\epsilon} v$ represents errors resulting from motion of the aircraft during reception of the satellite pulses. The mean square value of $\| \underline{K} \; \underline{H} \; \underline{\epsilon} \|$ can be written as

$$E(\| \underline{K} \; \underline{H} \; \underline{\epsilon} \|^2) = E(\| \underline{K} \; \underline{H} \; \underline{\epsilon} p \|^2) + E(\| \underline{K} \; \underline{H} \; \underline{\epsilon} v \|^2) \qquad (3\text{-}2)$$

$$+ E(\| \underline{K} \; \underline{H} \; \underline{\epsilon} o \|^2) + E(\| \frac{1}{c} \, \underline{K} \; \underline{H} \; \underline{\epsilon} t \|^2)$$

$$+ 2\rho \, \| K \; H \; \epsilon o \|_{rms} \cdot \| \frac{1}{c} K \; H \; \epsilon t \|_{rms}$$

where ρ is some number with $|\rho| < |$ representing the correlation between $\underline{\epsilon} o$ and $\underline{\epsilon} t$ (The other $\underline{\epsilon}$'s are assumed uncorrelated).

Each of the above terms may now be bounded using the geometric dilution factor of the satellite constellations, which will be assumed to be 10. Because the value of $\| \delta \|_{rms}$ decreases as more satellites are used, the following analysis is based on the minimum number of satellites, i.e., four.

From Appendix I it follows that for a random vector $\underline{x}$ with zero mean components, but otherwise arbitrary statistics,

$$|| \underline{K} \ \underline{H} \ \underline{x} ||_{rms} \leq k \ || \underline{y} ||_{rms}$$

where $\underline{k}$ is the geometric dilution and $\underline{y}$ is that portion of $\underline{x}$ which is orthogonal to the null space of $\underline{H}$. In the special case where the components of $\underline{x}$ are uncorrelated and have variances all equal to σ^2, then

$$|| \underline{K} \ \underline{H} \ \underline{x} ||_{rms} = k\sigma \text{ feet}$$

If the matched filter output is sampled every 25 nsec, then the components of $\underline{\varepsilon}p$ can be assumed to be uncorrelated and uniformly distributed between -12.5 nsec and 12.5 nsec. Thus, each component of $\underline{\varepsilon}p$ has variance

$$\text{Var} [(\underline{\varepsilon}p) i)] = \frac{(25)^2}{12} = 52 \text{ nsec}^2$$

Consequently,

$$|| \underline{K} \ \underline{H} \ \underline{\varepsilon p} ||_{rms} = 7.21 \text{ k feet} \tag{3-3}$$

Timing errors in the vector $\underline{\varepsilon}v$ are a result of the motion of the aircraft between pulse receptions. If the aircraft is moving at velocity v, where the angle between this motion and the unit vector to the i'th satellite is θ_i, then $\underline{\varepsilon}v$ is of the form

$$\underline{\varepsilon}v = \frac{v}{c}\begin{pmatrix} 0 \\ T_2 \cos\theta_2 \\ T_3 \cos\theta_3 \\ T_4 \cos\theta_4 \end{pmatrix}$$

where T_i is the arrival time (in seconds) of the pulse from satellite i, measured from the time of arrival of the pulse from satellite 1. If one removes the component of ε v that lies in the null space of $\underline{H}$, and uses the fact that all pulses arrive within a 32 msec interval, then it follows that

$$\| \underline{K} \ \underline{H} \ \underline{\varepsilon} v \|_{rms} \leq 2.9 \times 10^{-2} \ v \ k \text{ feet.} \qquad (3\text{-}4)$$

Errors in tracking the individual satellites over intervals of 100 seconds using the exact expressions for the satellite trajectories have rms errors that are proportional to the rms oscillator error (since the real time is needed to calculate satellite positions). The variance of each component of $\underline{\varepsilon}$t is

$$\text{Var}\left[(\underline{\varepsilon} t) \ i \ \right] = 3 \times 10^{12} \ \alpha^2 \text{ feet}^2$$

where α is the rms fractional error in the oscillator. As the components of $\underline{\varepsilon}$ t cannot be assumed to be uncorrelated,

$$\| \frac{1}{c} \ K \ H \ \underline{\varepsilon} t \|_{rms} \leq 3.5 \times 10^{6} \ \alpha \, k \text{ feet.} \qquad (3\text{-}5)$$

Oscillator inaccuracies introduce errors in measuring the times between pulse arrivals. The vector $\underline{\varepsilon}$o is of the form

$$\underline{\epsilon}o = \Delta \begin{pmatrix} 0 \\ T_2 \\ T_3 \\ T_4 \end{pmatrix}$$

where Δ is the random error in the oscillator (Δ rms = α), and T_i is the time of arrival of the i'th pulse. Removing the component of $\underline{\epsilon}o$ the null space of $\underline{H}$, and using the fact that all pulses arrive in a 32 msec interval, it follows that

$$\| \underline{K} \ \underline{H} \ \underline{\epsilon}o \|_{rms} \leq 2.65 \times 10^7 \alpha \text{ k feet.} \qquad (3\text{-}6)$$

If the satellite constellation has geometric dilution k = 10; if the oscillator rms error is $\alpha = 2 \times 10^{-6}$; if the aircraft is moving at velocity $\rho = .5$; then Eqs. (3-1), (3-2), (3-3), (3-4), (3-5), and (3-6) result in

$$\| \underline{\delta} \|_{rms} < 20 + 10 \sqrt{(7.21)^2 + (29)^2 + (7)^2 + (53)^2 + (.5)(7)(53)}$$

$$\| \underline{\delta} \|_{rms} < 648 \text{ feet.}$$

The above estimation error may not be satisfactory. If such is the case, there are several ways to reduce the error:

1. Obtain a lower geometric dilution with a better designed satellite constellation.
2. Improve the oscillator stability.
3. Estimate the aircraft velocity and compensate for it in the position calculations.

The first of these options could be costly, as it could require many more satellites. On the other hand, reducing the oscillator error by a factor of four and compensating for the aircraft motion are considerably less costly.

If one estimates the aircraft velocity by subtracting the position estimates at one second intervals, then the rms error in the velocity estimates is just $\sqrt{2}$ times the rms error in each position estimate. However, the errors in the position due to $\underline{\epsilon}t$ and $\underline{\epsilon}o$ are fairly constant over intervals of several seconds. Thus the error in the velocity estimate, ξ, satisfies

$$\|\underline{\xi}\|_{rms} \le \sqrt{2}\left(20 + 10\sqrt{(7.21)^2 + (2.9 \times 10^{-2}\,\|\underline{\xi}\|_{rms})^2}\right)$$

Thus, by estimating the velocity in this simple manner, the effective aircraft velocity is reduced to

$$\|\underline{\xi}_{rms}\| = 147 \text{ ft/sec.}$$

If the oscillator rms error is now reduced to $\alpha = .5 \times 10^{-6}$, the rms position error is

$$\|\underline{\delta}_{rms}\| < 20 + 10\sqrt{(7.21)^2 + (4.26)^2 + (1.75)^2 + (13.3)^2 + (.5)(1.75)(13.3)}$$

$$\|\underline{\delta}_{rms}\| < 182 \text{ feet.}$$

Thus, these fairly simple changes yield significant improvement.

SECTION 4

AIR-TO-GROUND SURVEILLANCE SYSTEM

4.1 Introduction

In this section we describe and analyze one candidate air-to-ground multilateration system. Each aircraft is assumed to periodically transmit a waveform representing its unique identification and its current barometrically determined altitude. Reception by a minimum of three ground sites permits an aircraft position to be calculated. We again assume that each aircraft has a frequency standard which is accurate to two parts in 10^6, however, it is assumed that each aircraft does not have a real time clock.

The transmitted waveform is assumed to be a sequence of 14 pulses, each of 10μ sec. duration. Each pulse is assumed to be selected from one of eight binary PSK modulated chips, each of duration 100 nsec. Of the 42 bits transmitted the first 20 will contain the aircraft identification while the remaining 22 can be used for altitude reporting and/or communications. It should also be noted that the number of bits transmitted can be increased to handle longer messages. Implications of this will not be pursued in the sequel.

The 140μ sec. transmission is repeated every few seconds. The repetition rate is assumed to be variable and dependent on a number of factors including: aircraft type, neighboring airspace, and the aircraft's current position, velocity and flight plan. It is assumed that average waveform repitition period is 8 sec. in an en route area and 5 sec. in a terminal area.

4.2 Air-to-Ground Link Characteristics

In Table 4.1 we present the link budget for this system. Since the en route and terminal areas are governed by different parameters they are distinguished where necessary.

An rf power of 100w is assumed. Although higher power devices could be utilized, the potential performance improvement is small because of the multiple access noise. Specifically, no improvement can be realized in the terminal area, and at most a 2 db improvement in effective signal to noise ratio can be realized en route. The path loss which has been assumed corresponds to the maximum range of 200 miles en route and 100 miles in the terminal area.

The effect of the multiple access noise is assumed to be that of an equal power white gaussian noise in the receiver bandwidth. The actual degradation is expected to be somewhat worse. Clearly, the multiple access noise increases with increasing message length or frequency. The received signal energy was computed for an aircraft located at maximum range from the ground receiving antenna. In computing the effective multiple access noise it is important to account for the increased multiple access noise due to those aircraft that are closer to this ground receiving antenna. Calculation of this multiple access noise appears in Appendix H. The power advantage of the average aircraft was calculated assuming a uniform distribution of aircraft. This assumption is not truely realistic for the aircraft in the neighborhood of a terminal. Future work on the air-to-ground multiple access problem should use a spatial distribution of aircraft which is obtained from a more realistic traffic model.

It is useful to observe that the ground receiving antenna should not be located in a region where high repetition rate signatures are likely to be transmitted. This would result in a larger multiple access noise.

TABLE 4.1

AIR-TO-GROUND LINK CALCULATION

	En Route	Terminal	
Transmitted Power	20 dbw		Conservative projection for solid state power amplifier
Pulse Duration	-50 dbsec		10μs pulse duration
Aircraft Antenna Gain	2.5 db		See Appendix A
Miscellaneous Losses	-2 db		
Path Loss	-143 db	-137 db	1 GHZ and 200 miles en route and 100 miles terminal
Terrestrial Antenna Gain	3 db		
Received Signal Energy	-169.5 dbJ	-163.5 dbJ	
Receiver Noise Power Density	-199 dbw/Hz		RFI, thermal and front end noise of 1000°k
Number of Users	33 db	36 db	2000 aircraft in terminal area and 4000 en route
Number of pulses Per User	11.5 db		14 pulses per user
Signal Repitition Rate	-9 db sec	-7 db sec	Average surveillance rate 5 sec in terminal and 8 sec en route
Receiver Bandwidth	73 db/Hz		20 MHz
Multiple Access Noise	-207 dbw/Hz	-196 dbw/Hz	Treating the multiple access noise as equivalent white gaussian noise in the band
Advantage of Average Terminal	9.5 db	8.5 db	See Appendix H
Effective Multiple Access Noise	-197.5 dbw/Hz	-187.5 dbw/Hz	
Effective Noise Power Density	-195 dbw/Hz	-187 dbw/Hz	Receiver plus effective multiple access noise
Aircraft Antenna Disadvantage	-3.5db		See Appendix A
Aircraft Power Amplifier Disadvantage	-1 db		See Appendix A
Multipath Fading	-6 db		See Appendix G
Decorrelation Loss	-1 db		See Appendix A
Atmospheric Loss	-1 db		Oxygen loss
Effective Signal Energy to Noise Power Density	13db	11db	

At low elevation angles mutual interference between signals received on a specular (ground) reflection path and the direct path can result in severe multipath fading. By using a sufficiently large vertical aperture the loss can be minimized. The loss due to multipath fading has been evaluated for an idealized propagation model as described in Appendix G. We have assumed in the link budget a loss of 6 db. If an aircraft is always above a particular minimum altitude, one can ensure that the fading loss is no greater than 6 db. Table 4.2 shows this minimum altitude for two values of range and three vertical aperture antenna sizes.

TABLE 4.2

MINIMUM AIRCRAFT ALTITUDE RESULTING IN LESS THAN 6 db MULTIPATH FADING LOSS FOR THREE ALTERNATIVE VERTICAL APERTURE

Vertical Aperture (feet)	Minimum Permitted Elevation Angle	Minimum altitude at 100 miles (feet)	Minimum altitude at 200 miles (feet)
9	2^{o}	20,000	45,000
20	0.75^{o}	8,000	20,000
35	0.5^{o}	5,000	12,000

4.3 Performance Evaluation

In this section, the probability, P_c, of correctly detecting an aircraft and computing its current position is evaluated. Correct detection requires that each of three receivers correctly decode the 14 transmitted pulses, i.e., each of the forty two 10μ sec pulses must be decoded correctly. Thus*

---

* We conservatively assume that each of the three links is equally disadvantaged.

$$P_c = (1 - P_e)^{42}$$

where P_e is the probability that a 10 μ sec pulse is decoded in error. In Figure 4.1 we have plotted the error probability for 8-ary orthogonal PSK modulation with incoherent detection for an additive white gaussian noise channel.

In the terminal area

$$\frac{E}{N_o} = 11 \text{ db}$$

hence

$$P_e = 6.5 \times 10^{-3}$$

and

$$1 - P_c = .24$$

Hence, the aircraft detection probability is only 0.76, which is unacceptable.

For the en route area

$$\frac{E}{N_o} = 13 \text{ db}$$

hence

$$P_e = 1.5 \times 10^{-4}$$

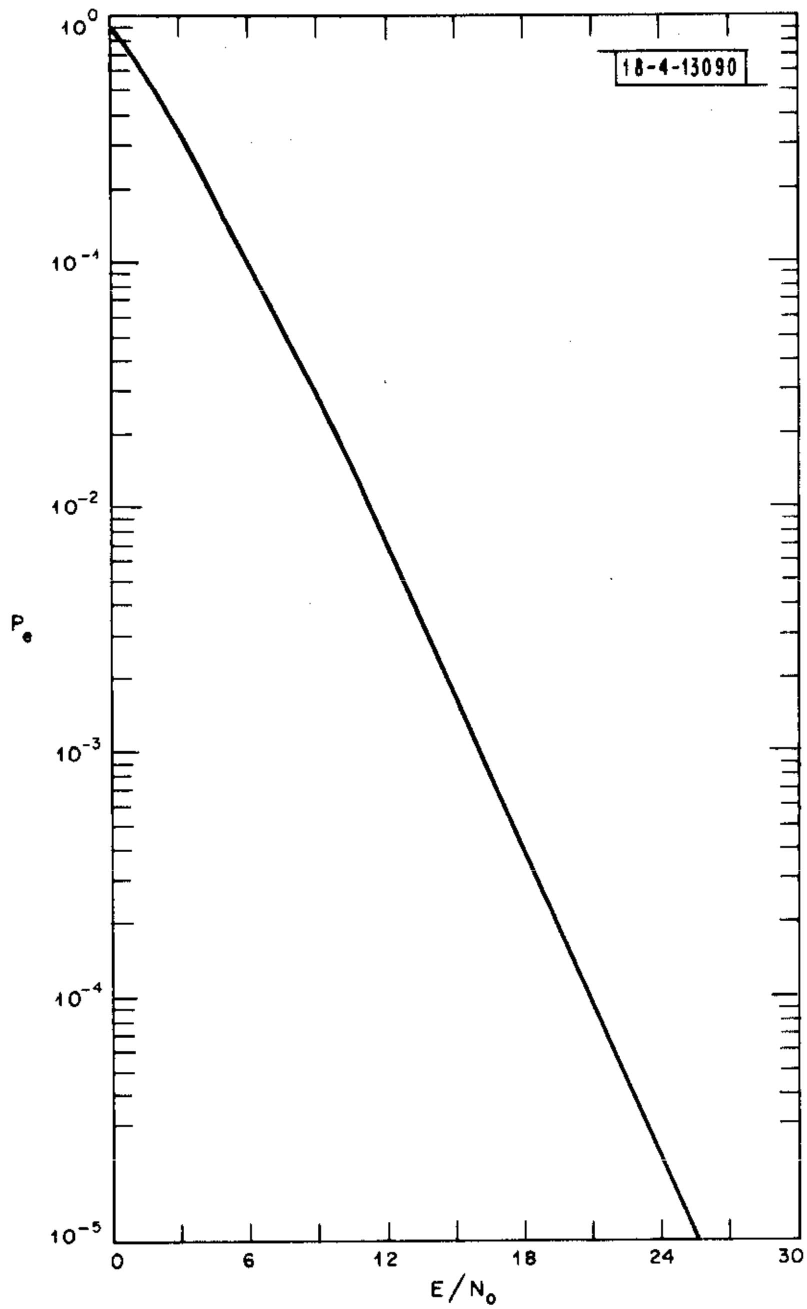

Fig. 4.1. Bit error probability for 8 ary orthogonal code transmission.

and

$$1 - P_c = 6.3 \times 10^{-3}$$

Hence, the detection probability is 0.9937.

The reader might be led to observe that the performance with an E/N_o of 11 db (terminal) is unacceptable while with an E/N_o of 13 db (en route) is tolerable. However, it must be concluded that neither observation is completely valid. Unfortunately, system performance is extremely sensitive to the underlying assumptions. Because these assumptions are so critical and because of the large uncertainty in several of the parameters of Table 4.1, it can only be concluded that further work is required to establish system feasibility.

APPENDIX A

ASSUMED ENVIRONMENT AND TECHNOLOGY

This Appendix is intended to provide a first order model of the assumptions which form a basis for subsequent analysis of candidate fourth generation surveillance systems.

A.1 Traffic Model for CONUS

The traffic model is fundamental to the surveillance systems analyses. The traffic model assumed was obtained from a study of the ATCAC projections for 1995. It is projected that by this time the CONUS aircraft population will be 500,000 with the possibility of growth to one million. 10% of the aircraft population is assumed to be airborne during peak traffic periods. Of 500,000 aircraft, approximately 97% will be general aviation aircraft.

There is a fine structure to the air traffic density over CONUS. This fine structure can best be described by looking at en route surveillance areas of CONUS separately from terminal surveillance areas. The following density figures were obtained from reference 1.

Consider first the situation of en route surveillance. It is estimated that the air traffic density in an en route area will be 50 square miles per aircraft. If CONUS surveillance is maintained by partitioning the country into 200 mile radius discs, then by 1995 it is estimated that approximately 2500 aircraft will be the instantaneous peak population of one of these discs in an en route area. This peak of course, is an average over the entire CONUS en route area.

The Los Angeles Basin provides a good model for worst case traffic condition in a terminal region. The following figures are in reference to this area. Terminal traffic patterns have a fine structure within themselves. The aircraft density very close to the terminal; i.e. within a 50 mile radius is considerably higher than the aircraft density within a 200 mile radius of the terminal. Consider, a disc with center at L. A. International Airport and having a 50 mile radius. By 1995 it is estimated that this disc will have a peak instantaneous population of 1570 aircraft. Now, expand this disc to where it has a 200 mile radius. This should cover the entire Los Angeles Basin. The resultant basin disc is estimated to have a peak instantaneous population of 8400 aircraft. As a general figure, 10,000 aircraft is a fair upper bound to the peak instantaneous aircraft population of the L.A. Basin in 1995.

A.2 Desired Surveillance Performance Characteristics

The required positional accuracy is taken to be a few hundred feet in any direction. This represents a considerable improvement in the azimuthal range accuracy permitted by ground based beacon systems at ranges of one to two hundred miles but is consistent with beacon derived range and barometrically derived altitude accuracy.

The desired surveillance data refresh rate is taken to be once every few seconds. This is consistent with the beacon system capability. We should also like to stress the importance of maintaining full time surveillance on each of the aircraft. This is especially important during maneuver The performance analysis assumes, as a requirement, surveillance of all aircraft during typical maneuvers. In particular we consider aircraft bank angles of 30° or less.

The potentially catastropic consequences of system failures place severe demands on reliability. For this first order model we have not quantified either reliability requirements or the backup capability available through other parts of the fourth generation system. It is observed, however, that the time required to recover from a failure is a critical parameter. A capability for unique aircraft identity is desired but not demanded. The system should achieve a detection probability close to unity and a false alarm probability close to zero.

For this first order model, differences in requirements between different operational areas and different aircraft have been ignored. In no sense should this be construed as an oversight. It is only one of the motivations for a future study.

The potential use of the satellite system for purposes of navigation and communication particularly for IPC is here noted. The specific requirements are not included in the first order requirements model.

A.3 Desired Complexity Characteristics

a. Avionics

Because of the large number of aircraft and the preponderance of general aviation aircraft it is essential to keep the airborne equipment cheap. It should be observed that from the purely economic point of view each dollar saved on the airborne terminals releases, in principal, $500,000 to be spent on other parts of the system. This admittedly simplistic viewpoint serves to emphasize the importance of keeping the avionics cost to a minimum. Maintenance requirements must also be kept minimal.

b. Satellite and Terrestrial

Satellite reliability is important; hence, saving satellite complexity at the expense of the ground processing facility is desired.

A.4 Environmental Effects

a. Doppler Shift Due to Aircraft Motion

Aircraft motion relative to the satellite will cause an apparent shift in frequency. For subsonic aircraft the worst case frequency offset will not exceed one part in 10^6 for a synchronous equatorial satellite.

b. Doppler Shift Due to Satellite Motion

Frequency offset due to satellite motion should contribute a frequency offset less than two parts, in 10^6. See Appendix D.

c. Reflection Multipath

Two types of reflection multipath degrade system performance: specular and non-specular. Specular reflections can degrade performance by three ways:

1) Appear to be an additional target;
2) Degrade signal level by causing mutual interference (often called multipath fading); and
3) Act as an additional source of noise.

Non-specular reflections act as clutter and thus increase the effective noise level.

The multipath fading phenomena in air-ground systems can severely degrade performance. This effect is addressed in detail in Appendix G. Multipath effects due to aircraft structure are included in the pattern of the aircraft mounted antenna.

d. Received Noise

Contributions to receiver noise include galactic noise, earth temperature, P-static, atmospheric noise, preamplifier noise, industrial noise and RFI. The last two are expected to be the dominant contributors. Currently available measurements at L-band are too limited in scope to be used in the design and analysis of a system. For purposes of the first model we assume a noise temperature of $600^{\circ}K$ at the satellite and $1000^{\circ}K$ at an upward looking aircraft. These are not unreasonable assumptions in light of the available data at VHF[1,2]. It must be noted, however, that the noise temperature seen by an aircraft can vary greatly as the aircraft maneuvers near cities, radar sites or TV stations.

e. Refraction Index Variations

Temporal and spatial variations in refractive index introduce several effects which deserve consideration.

1) Time of arrival errors:

The bending of rays through the atmosphere causes larger delays then purely geometric conditions would predict. These effects are largest in air-ground systems operating at low elevation angles. Typical delays, in such a system, to aircraft at cruising altitude are less than 250 nsec at $1/2^{\circ}$ elevation and 200 nsec at 1° elevation. If typical delays are accounted for, the resultant rms error can be reduced to around 15 nsec at $1/2^{\circ}$ and 10 nsec at 1°. Calibration using temperature, pressure and humidity measurements at the ground site can further reduce these to a residual rms error of 2 nsec.[4] The errors are even less at higher elevation angles.

2) Ducting effects

Ducting can result in transmissions at ranges in excess of line of sight. In air to ground systems this can serve to increase the multiple access noise as well as to increase the processing load. These effects are not included in our analysis. They are expected to be of second order in importance.

3) Radio holes

The bending caused by the spatial variation in refractive index can result in areas of significantly lower signal energy than are predicted by a simple spherical spreading argument. The lack of available data has precluded including this effect. We expect this also to be a second order degradation. It should affect only air-ground systems.

A. 5 Technology Constraints

a. Antenna Constraints

The pattern of L-band antennas mounted on an aircraft affects overall system performance. We reject high gain aircraft antennas for these systems because of the required complexity of the pointing and tracking subsystems. To avoid this complexity we propose employing antennas with upper hemispherical coverage. Unfortunately no measurements are currently available for such L-band antennas mounted on aircraft. Theoretical predictions of antenna patterns are of but limited usefulness because of the effect of coupling between the antenna and the aircraft. Our estimates are based on measured patterns at 250 MHz on a C135 (the military version of a Boeing 707). These patterns will be used as a first order estimate of antenna patterns at L-band on general aviation aircraft. Since such aircraft are approximately a factor of five smaller in exterior linear dimensions than a C135, this approach should provide a good estimate of the gross antenna characteristics.

Patterns for three different antenna's are presented in Figures A. 1, A. 2 and A. 3.[3] To a first order there are two important parameters: The minimum gain over the region of interest and the average gain for all aircraft in the system. On these grounds the Lincoln Laboratory crossed slot antenna has a clear advantage. We estimate an average gain of 2. 5db. Assuming a satellite elevation angle of 45^{o} and a maximum aircraft bank of 30^{o}, the minimum gain is estimated to be -1db.

B. Solid State L-band High Peak Power Amplifiers

We consider solid state L-band power amplifiers for the aircraft transmitter portion of the air to satellite to ground surveillance system and

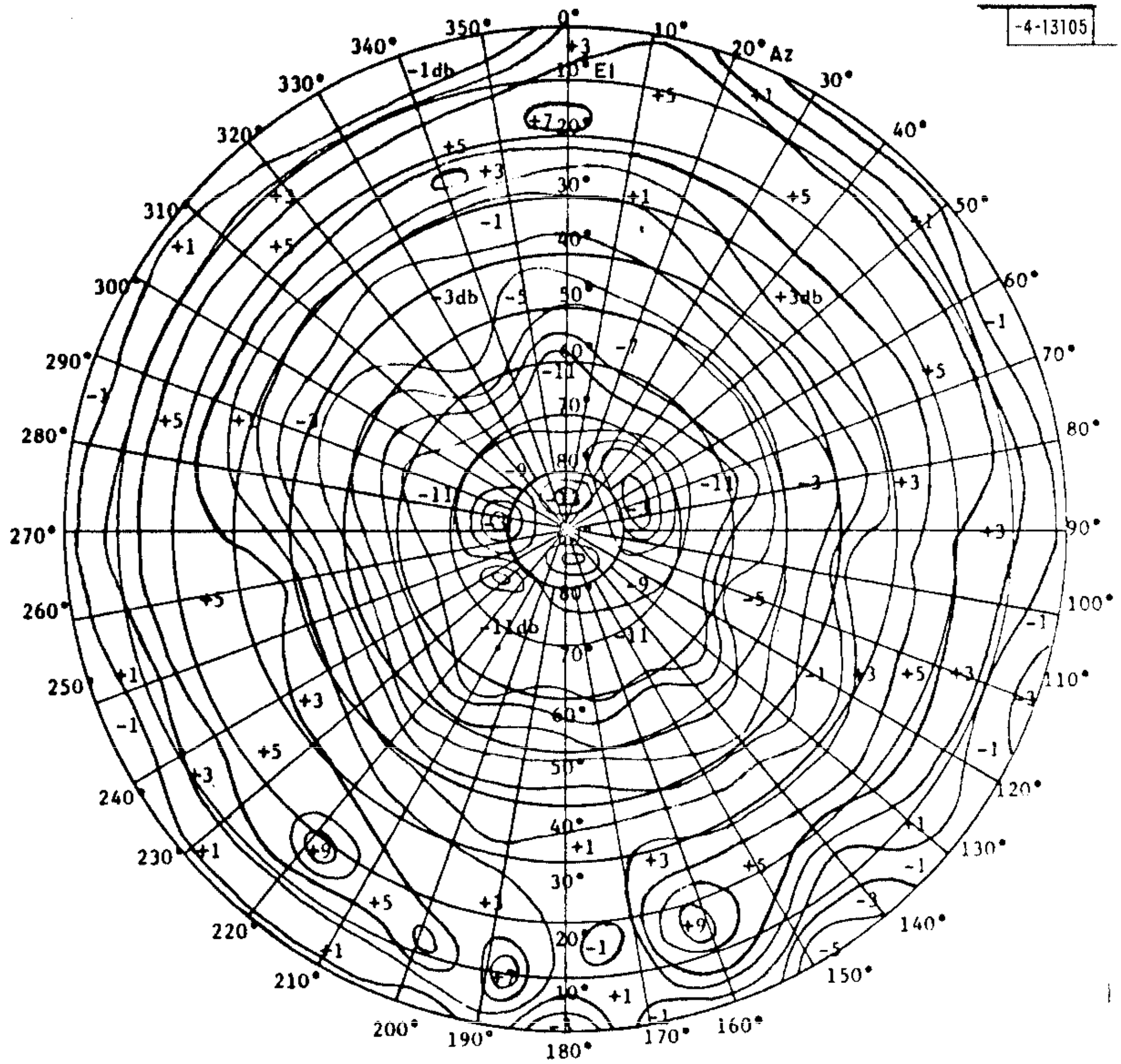

Fig. A. 1. Constant gain contours for UHF blade antenna.

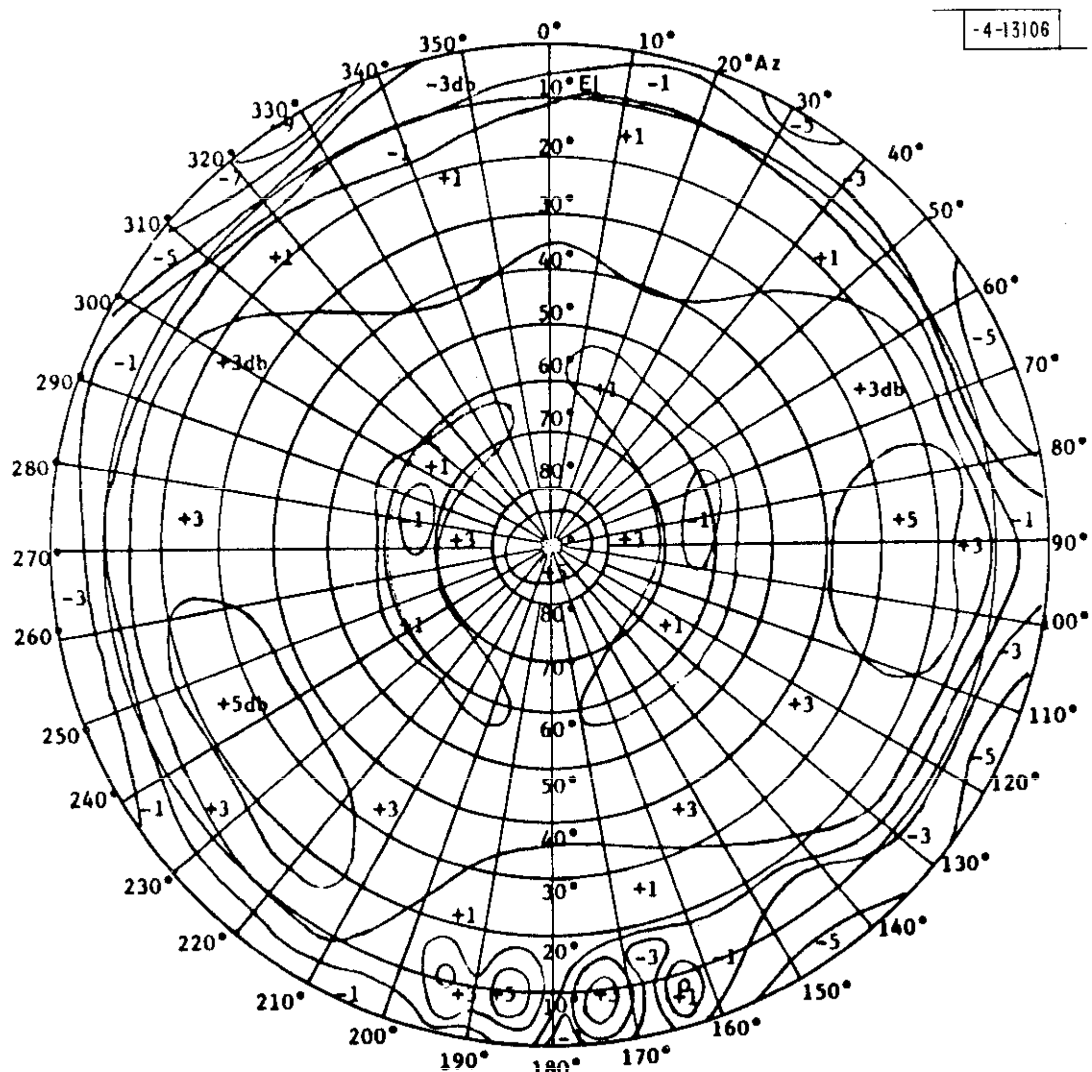

Fig. A.2. Constant gain contours for Lincoln Laboratory UHF crossed slot antenna.

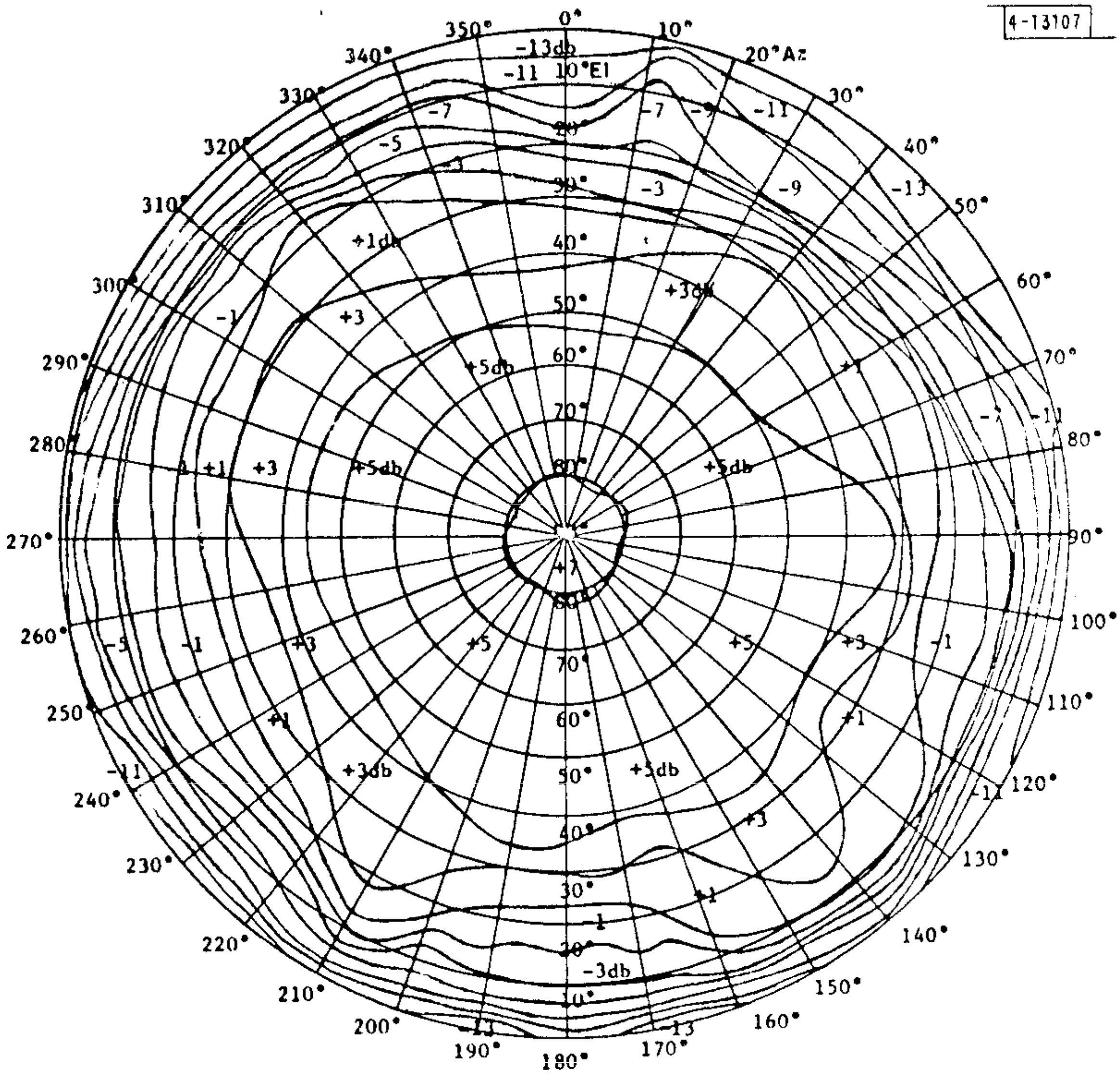

Fig. A. 3. Constant gain contours for UHF crossed dipole antenna.

the satellite portion of the satellite to air to ground system. We summarize here the current state of the art in L-band peak power amplifiers.

Using eight transitors in series it is possible to obtain approximately 800 w of peak power with a pulse duration of up to approximately 20 μsec and an efficiency of around 30%. Duty cycles of a few percent can be achieved. Problems of simultaneously achieving efficient series coupling together with efficient heat dissipation have thus far prohibited possible advantages of stacking additional transitors in series.

Using five avalanche TRAPATT devices in parallel, peak powers of 1.2 kw have been achieved. Pulse durations of 1 μsec are possible with 50% efficiency and a few percent duty cycle. Since the technology of these devices is still new, the prognosis for progress is good.

In light of the above and an operational goal 20 years hence, we feel confident in projecting peak powers of several kilowatts with pulse durations of several tens of microseconds. Efficiencies of 50% and duty cycles approaching 10% would also appear plausable.

One parameter that is especially important in evaluating the performance of air-satellite-ground surveillance systems is the ratio of the power of the aircraft with the lowest power transmitter to the average transmitted power of all of the aircraft. Certainly, this is difficult to assess without considerable experimentation; we optimistically assume -ldb for the probable minimum to average ratio.

C. Solid State L-band CW Power Amplifiers

Airborne solid state power amplifiers with 50 watts of rf power can be obtained today at reasonable cost. Improvement can be anticipated both in cost and power level.

D. Frequency Standards

A local oscillator is an essential complement to the avionics package. Accurate real time clocks are at present too complex and expensive to include in general aviation aircraft. We do not project sufficient progress in this area to propose their inclusion in a system for 20 years hence. Currently, standards with long term stability of two parts in 10^6 can be obtained with electronically compensated crystal oscillators at a cost of a few hundred dollars. A 6 db stability improvement can be achieved with little increase in cost. Since these offsets are comparable to the doppler offset, it is reasonable to configure a system with these standards.

E. Digital Hardware

Over the last decade we have seen a revolution in digital hardware, in terms of speed, power consumption, cost and size. With MOS devices just starting to be used and LSI just beginning, the prognosis for progress is bright. In particular we project significant cost reduction in high production quantities of digital hardware. Consequently, we envision large cost reductions for digital avionics hardware.

A.6 Frequency Offset Losses

In the design of any of the surveillance systems the effect of offsets in frequency between the received waveform and the receiver local oscillator must be taken into account. In this appendix we assume a signature consisting of a number of PSK pulses each of duration τ, with matched filter envelope detection. The total signature is assumed to be of duration T. We assume that no provisions for frequency or time tracking have been made in the receiver. We examine the resultant loss in signal to noise ratio. We assume a frequency offset of 5 parts in 10^6 at 1.6 GHz. This is representative of the systems using satellites and is two thirds larger than that experienced with the air to ground multilateration system.

The decorrelation loss in the detection of a pulse is arrived at through the following argument. Let the received carrier be a sinusoid with center frequency $f_o + \Delta f$, where f_o is the center frequency of the local oscillator and Δf is the offset due to clock instability and motion of the aircraft and satellite. The output of an envelope detector of integration time T is proportional to

$$L = \frac{4}{\tau^2} \left| \int_{-\tau/2}^{\tau/2} \cos 2\pi (f_o \; \Delta f)\, t \; e^{j2\pi f_o t} \, dt \right|^2$$

$$\simeq \left(\frac{\sin \pi \Delta f \tau}{\pi \Delta f \tau} \right)^2 ,$$

thus L is the loss in effective signal power due to frequency off-set. In Table A.1 we present the loss for various pulse durations assuming a frequency offset of 5 parts in 10^6 at 1.6 GHz. It therefore follows that a pulse duration of a few tens of microseconds results in less than a ldb loss with a receiver which does no frequency tracking.

TABLE A.1

DECORRELATION LOSS DUE TO FREQUENCY OFFSET

Pulse duration, τ, in μ sec	Decorrelation Loss in db
36	1
48	2
60	3

Suppose now that the signature consists of a sequence of PSK pulses over a time duration T. Suppose further that the assumed time difference between pulses at the receiver differs from the received waveform by the offset caused by the frequency difference. We examine here the loss in performance resulting from this offset. For an offset of t_o, the resulting loss in effective signal energy is given by

$$L = \left(1 - \frac{t_o}{t_c}\right)^2$$

for randomly selected binary PSK modulation with an assumed chip duration t_c. If the first pulse is used to determine the mask spacing then

$$t_o = 3 \times 10^{-6} T$$

where T is the signature duration and a frequency offset of 3 parts in 10^6 is assumed. In Table A.2 we list the loss for various values of T/t_c. As an example the loss is 1 db for a 100 nsec. chip duration and a 3 msec. signature duration

TABLE A.2

LOSS IN EFFECTIVE SIGNAL ENERGY DUE TO MASK OFFSETS FOR DIFFERENT SIGNATURE DURATIONS T AND CHIP DURATION t_c.

T/t_c	Decorrelation loss in db
4.0×10^4	1
8.6×10^4	2
1.3×10^5	3

*Offsets due to satellite motion can be compensated for and hence are not included.

REFERENCES

1. "Draft — Technical Development Plan for a Discrete Address Beacon System", Volume I, ATC-4, Lincoln Laboratory, M.I.T. (6 August 1971).

2. G. Ploussios, "Noise Temperature of Airborne Antennas at UHF", Technical Note 1966-59, Lincoln Laboratory, M.I.T. (6 December 1966).

3. W. W. Ward, et al., "The Results of the LES-5 and LES-6 RFI Experiments", Technical Note 1970-3, Lincoln Laboratory, M.I.T. (6 February 1970).

4. A. L. Johnson and M. A. Miller, "Three Years of Airborne Communication Testing Via Satellite Relay", Air Force Avionics Laboratory, Technical Report AFAL-TR-70-156, November 1970.

5. R. Crane, Private Communication.

APPENDIX B

PERFORMANCE ANALYSIS OF A FIXED SIGNATURE REPETITION RATE SURVEILLANCE SYSTEM

B.1 Introduction

In this Appendix the performance of a surveillance system which operates by having each aircraft transmit a signature at the same fixed repetition rate will be analyzed. The system will be referred to as the "FSRR system." Bounds to the FSRR system false alarm rate and to the probability of detecting an aircraft on an opportunity to detect will be computed. For convenience we begin by describing the FSRR system.

The FSRR system operates in the following manner. Each aircraft transmits a signature consisting of five pulses as shown in Figure 2.1. Pulse A is an initial synchronization pulse. Pulses B and C are symmetric with respect to a center axis which is placed at a fixed distance from pulse A. This pulse pair can occupy one of 317 possible pair positions around the center line. Similarly, pulses D and E are symmetric with respect to a center axis which also lies at a fixed distance from pulse A. Pulse pair D-E also occupies one of 317 possible positions around its center line.

The five pulses consituting the aircraft signature are modulated with identical pseudo random sequences. The system uses an ensemble of 10 different pseudo random sequences to construct the aircraft signatures. Hence, there are 10^6 (i.e. $10(317)^2$) possible signatures. Therefore, the FSRR system can accommodate 10^6 unique aircraft identification signatures. Each aircraft transmits its signature once every 2.5 seconds. The total signature time width is at most 1 msec. The signature pulses consist of 200 chips of 100 nsec duration. Each chip carries one bit of information in its phase (i.e. a PSK signal).

The aircraft signature is transmitted to and received by each of the four satellites which comprise the system satellite constellation. One of these satellites is designated "master satellite". The remaining satellies are called slave satellites (i.e. "salve 1", "slave 2", and "slave 3").

The received aircraft signatures are retransmitted to the satellite ground stations on the earth. They are received and detected using a bank of 10 matched filters. Each filter is matched to one of the pseudo random sequences used in the signature construction. The detected pulses are stored sequentially in a shift register memory at the ground station. Each of the 10 separate matched filter channels has its own shift register memory. Each stage in the register corresponds to a time difference of 100 nsec (1 chip duration).

The post detection processing is quite simple. It begins on the ground station of the master satellite. Each of the ten shift register memories is handled separately. Consider a particular one of these ten shift register memories. A mask moves sequentially through the stages of the memory. That is, a processor moves sequentially (with increasing time) through the shift register stages checking to see whether or not a received pulse is stored at each stage. If it finds a pulse present it considers this a possible initial synchronization pulse (an "A" pulse) of some aircraft's signature. The processor then sets up B-C and D-E center axes in the shift register memory with respect to the position of this possible "A" pulse. The processor checks to see if there are any B-C and D-E pairs (with respect to the center axes that have been set up) stored in the shift register memory.

If the processor does not find at least one B-C possibility and one D-E possibility, it continues its sequencing through the shift register memory. Otherwise there are 3 possible cases, namely; the processor could find one B-C pair and one D-E pair, the processor could find two B-C possibilities and one D-E possibility or one B-C possibility and two D-E possibilities, the processor could find more than one B-C possibility and more than one D-E possibility. The second and third of these three cases are called "overwrite events". In the second case one overwrite is said to have occurred. In the third case more than one overwrite has occured. The second case is illustrated in Figure B.1.

One or more overwrites implies that the initial synchronization pulses of at least two different aircraft were received simultaneously by the matched filter channel. Hence, the "A" pulse uncovered in sequencing through the shift register memory really corresponds to several different "A" pulses, and corresponding to each B-C -- D-E pair combination there is a different aircraft signature stored in the shift register memory with this same "A" pulse. In the event of one or more overwrites the processor picks two of the signature possibilities at random and only operates on these two. It operates on these separately as if each were uncovered without any overwrites in the masking procedure (i.e., treats each as a first case possibility). We describe now how the processor operates on a first case signature possibility since overwrite processing comes down to this.

Consider the signature of aircraft "j" to have been detected on a shift register memory of the master satellite. Let the shift register stage in which the "A" pulse of "j" is storedbe designated as "T_M". The processor signals the system to interrogate the corresponding shift register memories of three slave satellites as to whether or not the signature of aircraft "j" has been received within $\pm$ 24 msec of T_M. 24 msec is the maximum delay time based upon the geometric structure of the satellite configuration. If aircraft "j's" signature occurs in the memory of each of the slaves within the allowed delay time (determination of the signature presence in the slave memories is similar to the masking procedure in the master satellite), then the FSRR system declares aircraft "j" present in the airspace. It supplies the signature arrival time differences (the time difference between T_M and the "A" pulse storage stage times in the slave memories) to a

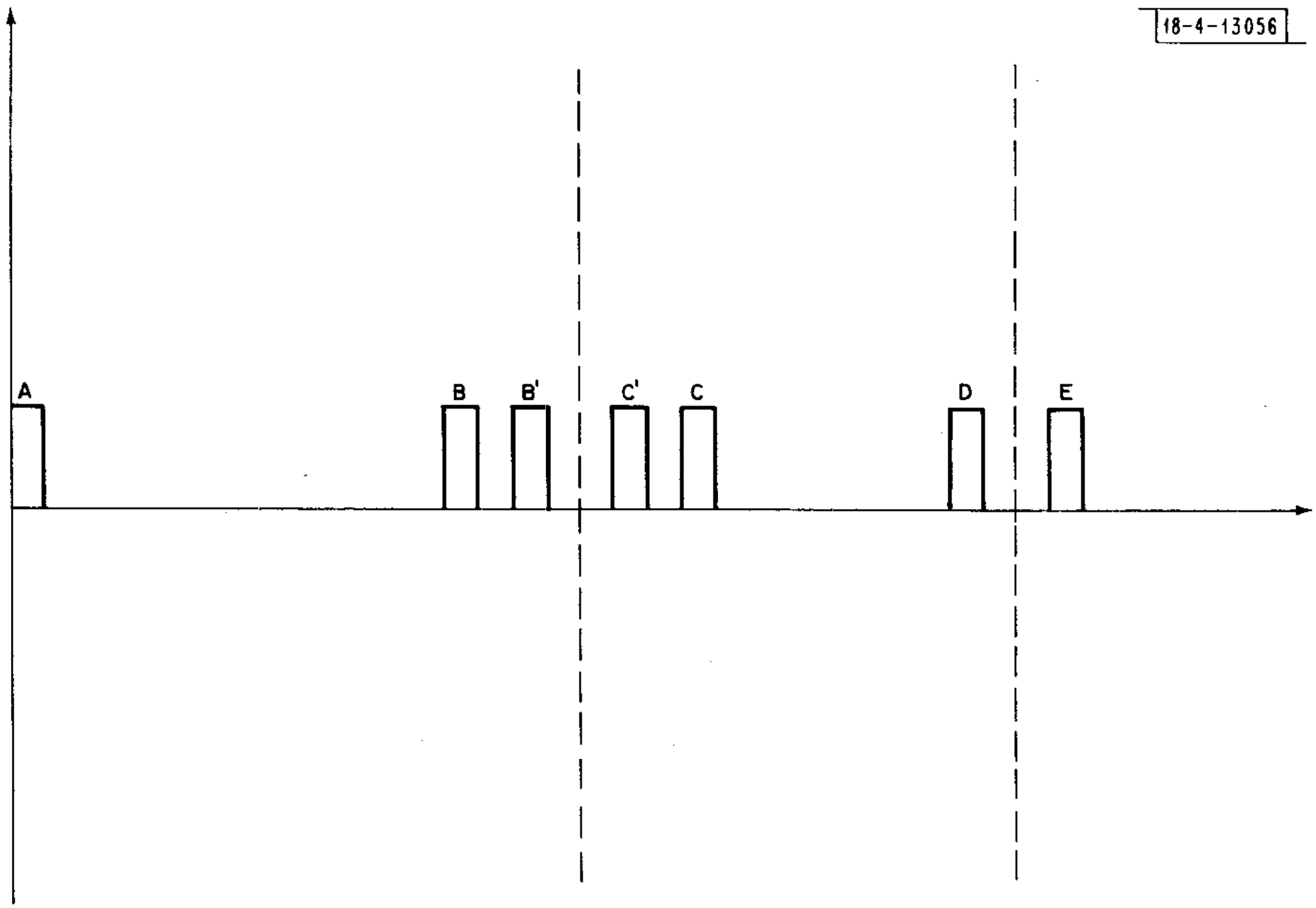

Fig. B.1. The event of an overwrite.

computer which can determine from this information (using the method of Hyperboloids) the position of aircraft "j". Aircraft "j" can then be recorded as being present in the airspace at time T_M at the position computed.

B.2 Causes and Types of Error in FSRR

Error arises in the FSRR surveillance system out of two possible sources; noise and spurious user pulses. Consider a particular matched filter receiving channel. Noise causes error since it may activate the matched filter detector causing the system to declare a signature pulse present when in fact no pulse is present. The noise on a particular matched filter channel is composed of two components. The first component is the ordinary thermal noise input to the matched filter detector. The second component is due to the reception by the matched filter detector of aircraft signatures which are not constructed from the pseudo-random sequence to which the filter is matched. This second component can be thought of as cross-talk. As a starting point of our analysis we shall assume that the output of the matched filter detector due to this second component of noise is in fact white gaussian noise.

The second source of error is the presence on a particular matched filter channel of spurious user pulses. This will now be explained. Because 10^5 different aircraft signatures are constructed from the same pseudo random sequence the "A", "B", "C", "D", or "E", pulse of one of these signatures may be confused with a different order pulse of a different one of these signatures. As an example consider the "A" pulse of 2 different signatures constructed using the same pseudo random sequence. If the signatures arrive at the matched filter detector at appropriate times the pair of "A" pulses could possibly be confused with a B-C pair on a particular mask. This obviously could cause an error in the signature identification procedure in which case we would say that the error was caused by "spurious pulses".

Up until now only the possible causes of errors in the FSRR system have been discussed. Now the types of errors which disturb the performance of the FSRR system will be considered. There are two types of errors; "false alarm errors", and "failure to detect" errors.

By definition, a false alarm error is the following event: for a particular masking time on the master satellite shift register memory the FSRR system announces the presence of a particular aircraft in the airspace when in fact the aircraft is not present. For convenience we shall also define the term "a 'j' false alarm". A "j false alarm" occurs if on a particular masking time on the master satellite shift register memory the FSRR system announces the presence of aircraft "j" in the airspace when in fact aircraft "j" is not present at that time.

A false alarm can occur in many different ways. In fact there are over 60 different ways in which one can occur. Several of the many ways in which a false alarm might occur are described in the following paragraphs.

(1) With an initial pulse at time T_M, 5 noise or spurious user pulses might masquerade as the signature of aircraft "j" on the shift register memory of the master satellite. If this also happens in the shift register memory of each of the slave satellites within $\pm$ 24 msec of T_M then a j false alarm occurs at time T_M.

(2) With an initial pulse at time T_M a valid user signal having the same B-C pair as the signature of aircraft j may be received and detected perfectly. A pair of noise or spurious pulses properly spaced and combined with this signature could masquerade as the signature of aircraft j. If 5 noise or spurious user pulses properly spaced to masquerade as j's signature are received by the shift register memory of each of the salve satellites within $\pm$ 24 msec of T_M then a j false alarm occurs at time T_M.

(3) With an initial pulse at time T_M, 5 noise or spurious user pulses might masquerade as the signature of aircraft "j" on the shift register memory of the master satellite. In addition, "j" might actually be present in the airspace (although not at time T_M) and its true signature might be received and detected and stored in the shift register memories of each of the slave satellites within $\pm$ 24 msec of T_M. This would constitute a j false alarm since aircraft j would be recorded at being present at time T_M at an incorrect position.

By definition a failure to detect error is the following event: Aircraft j is present in the airspace and its signature is received at the ground station of the master satellite at time T_M, yet the system does not declare it present at this masking time and hence does not compute its position. The system misses the aircraft.

There are basically two different reasons for a failure to detect error. They are described in the following paragraphs.

(1) Missing pulses - In order for an aircraft to be declared present its signature has to be detected at the ground station of each of the 4 satellites. This implies that 20 pulses (4 x 5) have to be properly detected. If only one of these pulses is missed because of noise, there will be a failure to detect the aircraft.

(2) Overwrites - The aircraft signatures might be received and detected perfectly. Yet if there is more than one overwrite of it in the shift register memory of the master satellite the aircraft signature could be mistakenly neglected and a failure to detect occur.

B. 3 Parameter Definition

The following parameters occur in the FSRR performance analysis. The figures in parentheses represent the values of these parameters used in the subsequent analysis.

N_T	-	total number of aircraft	(10^6)
N	-	number of aircraft in flight at any time	(10^5)
N_P	-	number of pulses in aircraft signature	(5)
T	-	signature repetition time in seconds	(2.5)
T_p	-	pulse width in seconds	(20μ sec)
T_c	-	chip width in seconds	(100 n sec)
N_c	-	number of codes	(10)
N_I	-	number of pulse pair (B-C or D-E) positions	(317)
P_f	-	per pulse probability of false alarm	
P_d	-	per pulse probability of detection	

B.4 A Lower Bound to the System False Alarm Rate

In this section a lower bound to the rate at which false alarms occur in the FSRR system will be derived. The lower bound will be evaluated for two cases:

1. A received signal to noise ratio of 9 db estimated in the power budget included in the main body of this report and also a signal to noise ratio of 6 dB.
2. A received signal to noise ratio of 13.5 db.

We begin by defining the following probabilities:

$$P_F(T_M) = \text{Prob.}\left(\begin{array}{l}\text{at master satellite masking time } T_M \text{ a false}\\ \text{alarm occurs in the FSRR system}\end{array}\right), \qquad \text{(B-1)}$$

$$P_F(T_M, j) = \text{Prob.}\left(\begin{array}{l}\text{at master satellite time } T_M \text{ a j false alarm}\\ \text{occurs in the FSRR system}\end{array}\right), \qquad \text{(B-2)}$$

$$P(\alpha) = \text{Prob.}\left(\begin{array}{l}\text{noise or spurious user pulses are incorrectly}\\ \text{declared pseudo random sequence pulses at}\\ \text{time t on the matched filter channel which "j's"}\\ \text{signature is detected on}\end{array}\right), \qquad \text{(B-3)}$$

and the following events:

$$r_i = \begin{pmatrix}\text{Aircraft j is present in the airspace, and its signature} \\ \text{is received and detected perfectly by the ground station} \\ \text{of satellite i, and it resides in the shift register memory} \\ \text{of satellite i within} \pm 24 \text{ msec of } T_M\end{pmatrix}, \quad \text{(B-4)}$$

$$n(T_M) = \begin{pmatrix}\text{5 noise or spurious user pulses masquerade as the} \\ \text{signature of the aircraft j with initial pulse } T_M\end{pmatrix}, \quad \text{(B-5)}$$

$$a = \begin{pmatrix}\text{given the condition that a "j" sequence of pulses} \\ \text{(either a true "j" signature or noise or spurious} \\ \text{pulses appearing as "j") is present as an overwrite} \\ \text{on a particular mask, this "j" sequence is chosen} \\ \text{for processing from among all the overwrites}\end{pmatrix}, \quad \text{(B-6)}$$

$$b = \begin{pmatrix}\text{the pseudo j signature represented by } n(T_M) \text{ is picked} \\ \text{for processing from among all overwrites present}\end{pmatrix}. \quad \text{(B-7)}$$

Consider the joint event, E_1, which is the simultaneous occurance of the five events, $n(T_M)$, b, r_1, r_2, and r_3. It is obvious that if E_1 occurs, a j false alarm will occur, hence,

$$P_F(T_M, j) \geq P(E_1) \quad \text{(B-8)}$$

We now evaluate

$$P(E_1) = P(n(T_M)) \; P(a) \; P(r_1, r_2, r_3). \quad \text{(B-9)}$$

First,

$$P(n(T_M)) = P^5 (\alpha). \quad \text{(B-10)}$$

Expanding $P(r_1, r_2, r_3)$ results in

$$P(r_1 \, r_2, r_3) = P(r_3 | r_2, r_1) \; P(r_2 | r_1) \; P(r_1) \,. \quad \text{(B-11)}$$

Now,

$$P(r_1) = P\,(\text{j is in the airspace}) \frac{48 \times 10^{-3}}{T_c} \quad \frac{T_c}{T} \quad P_d^5$$

$$P(r_1) = \frac{N}{N_T} \quad \frac{48 \times 10^{-3}}{T} \, P_d^5 \tag{B-12}$$

If r_1 occurs the signature of aircraft j will be received by the ground station of satellite 2 and 3 within $\pm$ 48 msec. of T_M(since maximum delay time in signature reception from different satellites is $\pm$ 24 msec). Therefore,

$$P\,(r_2 | r_1) = \frac{24 \times 10^{-3}}{48 \times 10^{-3}} \quad P_d^5 = \frac{1}{2} \, P_d^5 \tag{B-13}$$

$$P\,(r_3 | r_1, \, r_2) = \frac{1}{2} \, P_d^5 \tag{B-14}$$

Applying (B-12), (B-13), and (B-14) to (B-11) yields

$$P\,(r_1, \, r_2, \, r_3) = \frac{12 \times 10^{-3}}{T} \quad \frac{N}{N_T} \quad P_d^5 \, . \tag{B-15}$$

A lower bound to P(a) will now be computed. First the following conditional probabilities are

$$P_o(n) = \text{Prob.} \left(\begin{array}{l} \text{exactly n overwrites are} \\ \text{present on the mask at} \\ \text{time } T_M \end{array} \middle| \begin{array}{l} \text{a "j" sequence of pulses} \\ \text{is present as an overwrite} \\ \text{at time } T_M \end{array} \right) \tag{B-16}$$

$$P_1(n) = \text{Prob.} \left(\begin{array}{l} \text{the "j" sequence of pulses} \\ \text{is chosen from among the} \\ \text{n overwrites for processing} \end{array} \middle| \begin{array}{l} \text{a "j" sequence of pulses is} \\ \text{present as an overwrite at} \\ \text{time } T_M\text{, exactly n over-} \\ \text{writes are present on} \\ \text{the mask at time } T_M \end{array} \right) \tag{B-17}$$

The following expansion can be made

$$P(a) = \sum_{n=1}^{N_I^2} P_o(n) \; P_1(n). \tag{B-18}$$

Since in the presence of overwrites the FSRR system operates by choosing only two signatures for processing,

$$P_1(1) = 1,$$

$$P_i(n) = \frac{2}{n} \text{ for } n \geq 2 \tag{B-19}$$

Substituting (B-19) into (B-18) results in

$$P(a) = 2 \sum_{n=2}^{N_I^2} \frac{1}{n} P_o(n) + P_o(1),$$

so that

$$P(a) \geq 2E(1/n) - P_o(1) \tag{B-20}$$

The expectation is conditional on a j sequence of pulses being present on the mask at time T_M.

By Jensen's inequality,

$$E\left(\frac{1}{n}\right) \geq \frac{1}{E(n)} \tag{B-21}$$

Applying (B-21) to (B-20) yields

$$P(a) \geq \frac{2}{E(n)} - P_o(1). \tag{B-22}$$

Evaluating E (n) we obtain

$$E(n) = 1 + E\left(\begin{array}{l}\text{additional number of over-}\\\text{writes of the "j" sequence}\\\text{of pulses}\end{array}\;\middle|\;\begin{array}{l}\text{a "j" sequence of pulses}\\\text{is present at time } T_M\end{array}\right)$$

$$E(n) = 1 + E\left(n_1 \times n_2 \;\middle|\; \begin{array}{l}\text{a "j" sequence of pulses is}\\\text{present at time } T_M\end{array}\right) \qquad \text{(B-23)}$$

$$+ E\left(n_1 \;\middle|\; \begin{array}{l}\text{a "j" sequence of pulses is}\\\text{present at time } T_M\end{array}\right)$$

$$+ E\left(n_2 \;\middle|\; \begin{array}{l}\text{a "j" sequence of pulses is}\\\text{present at time } T_M\end{array}\right)$$

where

n_1 = number of B-C pair positions occupied around the axis set up by the "j" sequence of pulses (in addition to the B-C pair of the "j" sequence.)

n_2 = number of D-E pair positions occupied around the axis set up by the "j" sequence of pulses in addition to the D-E pair of the "j" sequence.

Continuing from (B-23)

$$E(n) = 1 + E\left(n_1 \;\middle|\; \begin{array}{l}\text{a "j" sequence of}\\\text{pulses is present}\\\text{at time } T_M\end{array}\right) E\left(n_2 \;\middle|\; \begin{array}{l}\text{a "j" sequence of}\\\text{pulses is present}\\\text{at time } T_M\end{array}\right)$$

$$+ E\left(n_1 \;\middle|\; \begin{array}{l}\text{a "j" sequence of}\\\text{pulses is present}\\\text{at time } T_M\end{array}\right) + E\left(n_2 \;\middle|\; \begin{array}{l}\text{a "j" sequence of}\\\text{pulses is present}\\\text{at time } T_M\end{array}\right)$$

$$E\left(n_1 \middle| \begin{array}{l}\text{a "j" sequence of} \\ \text{pulses is present} \\ \text{at time } T_M\end{array}\right) = E\left(n_2 \middle| \begin{array}{l}\text{a "j" sequence of} \\ \text{pulses is present} \\ \text{at time } T_M\end{array}\right) = (N_I - 1)P^2(\alpha) \tag{B-25}$$

Applying (B-25) to (B-24) results in

$$E(n) = 1 + (N_I - 1)^2 P^4(\alpha) + 2(N_I - 1) P^2(\alpha) \tag{B-26}$$

Noting that

$$P_o(1) = (1 - P^2(\alpha))^{2N_I - 2}$$

and substituting (B-26) into (B-22) results in

$$P(a) \geq \frac{2}{1 + (N_I - 1)^2 P^4(\alpha) + 2(N_I - 1) P^2(\alpha)} - (1 - P^2(\alpha))^{2N_I - 2}. \tag{B-27}$$

Applying (B-10) and (B-27) to (B-9) and the result to (B-8) yields

$$P_F(T_M, j) \geq \frac{24 \times 10^{-3}}{T} \frac{N}{N_T} P_d^{15} P^5(\alpha)\left(\frac{2}{1 + (N_I - 1)^2 P^4(\alpha) + 2(N_I - 1)P^2(\alpha)} - (1 - P^2(\alpha))^{2N_I - 2}\right) \tag{B-28}$$

The inequality, (B-28) gives a lower bound to $P_F(T_M, j)$. Effort will now be concentrated on determining the average time difference between system false alarms in terms of $P_F(T_M, j)$. The result that will be obtained, when combined with (B-23), will yield a lower bound to the average system false alarm rate.

To begin with the following assumption is made: The events

$$\left\{\begin{matrix}\text{a j false alarm}\\ \text{at time } T_M\end{matrix}\right\}, \quad \left\{\begin{matrix}\text{a k false alarm}\\ \text{at time } T_M{'}\end{matrix}\right\}, \quad \left\{\begin{matrix}\text{an i false alarm}\\ \text{at time } T_M{''}\end{matrix}\right\} \quad \cdots\cdots$$

are independent for any combination of; j, k, i ($j \neq k$ etc) and any combination of T_M, T_M', ...

This assumption provides a workable mathematical structure thus allowing the analysis to proceed. Unfortunately, it is only a first cut approximation to the actual statistical properties of the FSRR system. The true situation in the performance of the FSRR system is obviously one in which there is dependence from false alarm to false alarm. However, if statistical dependence were to be taken into account the analysis would be mathematically untenable. In such a situation one would have to resort to a computer simulation in order to obtain a measure of the system performance.

Proceeding with the analysis, because of assumption (B-24), the expected number of chips between j false alarms is $1/P_F(T_{M,}\ j)$. Translating this into real time units, the expected number of seconds between j false alarms is $10^{-7}\ P_F(T_{M,}\ j)$. Now, the Strong Law of Large Numbers can be invoked.. Consider any ϵ and δ both positive and small. With probability greater than $1 - \delta$ there exists an integer $K(\epsilon)$ such that for all $K \geq K(\epsilon)$, the latest time at which exactly K j false alarms will take place is $\frac{K \times 10^{-7}}{P_F(T_{M,}\ j)} + \epsilon$ seconds after the start of the time segment. In addition, the earliest time at which K j false alarms will take place is $\frac{K \times 10^{-7}}{P_F(T_{M,}\ j)} - \epsilon$ seconds after the start of the time segment.

Consider the symmetry of j and i false alarms, the K^{th} i false alarm will take place between $\frac{K \times 10^{-7}}{P_F(T_{M,}\ j)} - \epsilon$ and $\frac{K \times 10^{-7}}{P_F(T_{M,}\ j)} + \epsilon$ seconds after the time interval began, with high probability. Hence, with high probability KN_T false alarms will take place at approximately $\frac{K \times 10^{-7}}{P_F(T_M, j)}$ seconds after the time interval began. We now compute the average time between false alarms in this interval. Since there are KN_T false alarms in this interval and without loss of generality we can put a j false alarm at the beginning of the internal, the average time between any type of false alarm (i.e. j or otherwise) in the interval is

$$\frac{\frac{K \times 10^{-7}}{P_F(T_M, j)}}{KN_T} = \frac{10^{-7}}{N_T P_F(T_M, j)} \qquad \text{(B-30)}$$

(For simplicity we have suppressed the ϵ and δ and it should be noted that we are looking at false alarm generation at steady state conditions on the system)

Because of assumption (B-29), the quantity in (B-30) is the expected value of the time between system false alarms. This implies that on the average there will be

$$T N_T P_F (T_M, j) 10^7 \qquad \text{(B-31)}$$

system false alarms per epoch (2.5 sec time interval).

Combining (B-28) and (B-31) results in

$$\overline{N}_f \geq 12 \times 10^4 \, N P_d^{15} \, P^5(\alpha) \left(\frac{2}{1 + (N_I - 1)^2 P^4(\alpha) + 2(N_I - 1) P^2(\alpha)} - \left((1-P^2(\alpha)\right)^{2N_I} - 2\right) \qquad \text{(B-32)}$$

where N_f is the average number of system false alarms per epoch.

In the remainder of this section the right hand side of (B-32) will be evaluated for a received signal to noise ratio of 6 db, 9 db, and 13.5 db. Consider first the term P (α) defined by (B-3). Let $P(\alpha_n)$ be the component of P(α) due to noise only. Let $P(\alpha_s)$ be the component of P(α) due to spurious user pulses. P (α) is computed now.

$$P(\alpha_s) = \left(\frac{\text{number of users in flight}}{\text{number of channels}}\right)\left(\begin{array}{l}\text{number of pulses}\\ \text{per signature}\end{array}\right)\left(\begin{array}{l}\text{probability that the}\\ \text{first pulse of a par-}\\ \text{ticular signature}\\ \text{matched to j's channel}\\ \text{activates the matched}\\ \text{filter at time t}\end{array}\right)$$

$$P(\alpha_s) = \frac{N}{\bar{N}} \; 5 \; \frac{10^{-7}}{T} P_d = N5 \frac{10^{-8}}{T} \; P_d \qquad \text{(B-33)}$$

Obviously,

$$P(\alpha_n) = P_f, \text{ (the per pulse false alarm probability)} \qquad \text{(B-34)}$$

hence,

$$P(\alpha) = P_f + 5 \times 10^{-8} \frac{N}{\bar{N}} P_d. \qquad \text{(B-35)}$$

Since the expression on the right hand side of (B-32) is a lower bound to $\overline{N}_f$, we denote it as $\overline{N}_f^L$. Table B.1 has it evaluated for the signal to noise ratios previously mentioned. Both for E/N_o equal to 6 db and equal to 9 db, $\overline{N}_f^L$ is evaluated for several allowable P_f/P_d pairs. For a given E/N_o the allowable P_f/P_d pairs are determined from the Receiver Operating characteristic (ROC) of the matched filter. The ROC is shown in Figure B.2.

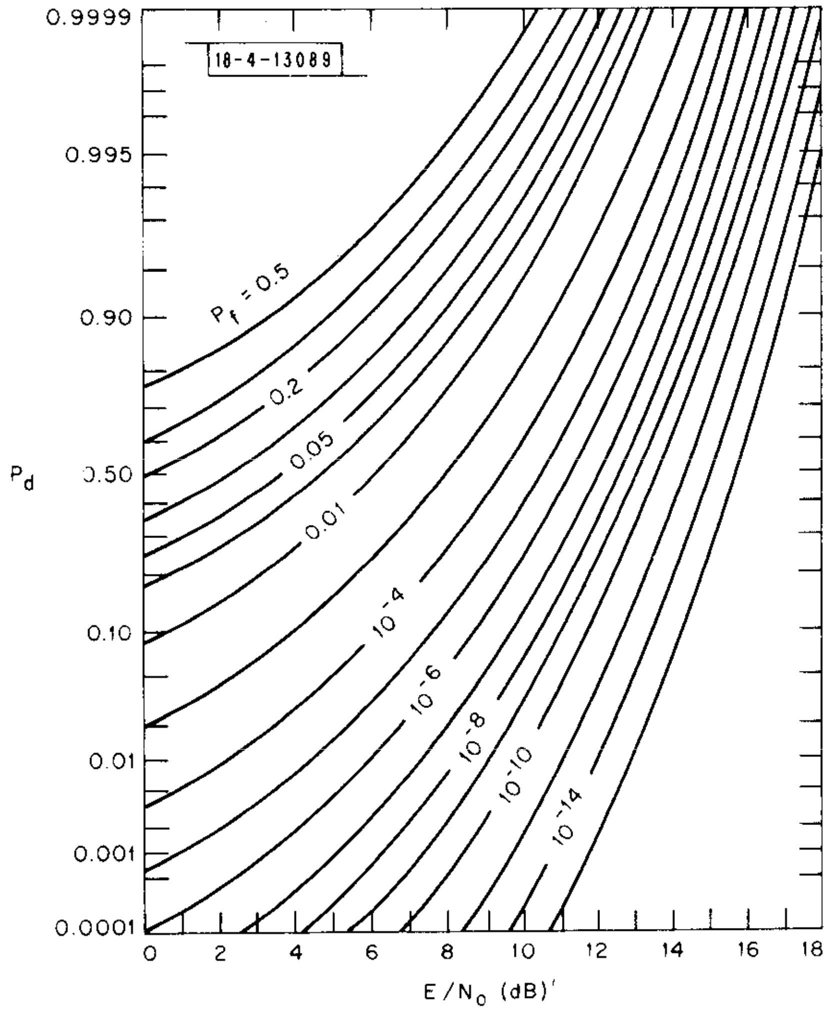

Fig. B. 2. Matched filter receiver operating characteristic.

TABLE B.2

FSRR SYSTEM FALSE ALARM PERFORMANCE

E/N_o	P_d	P_f	$\overline{N_f}^L$
9 db	0.98	0.1	1.038×10^4
9 db	0.99	0.2	3.62×10^4
9 db	0.997	0.3	6.54×10^4
13.5 db	0.9998	0.01	1.126
6 db	0.82	0.1	790
6 db	0.92	0.2	1.23×10^4
6 db	0.94	0.3	2.64×10^4

B.5 Bounds to the System Detection Probability

This section deals with the performance of the FSRR system in detecting the presence of an aircraft at masking time T_M when it is present and should be declared so.

We define a probability of detection,

$$P_D = \text{Prob}\left(\begin{array}{l}\text{aircraft j is declared}\\ \text{present by the system}\\ \text{at time } T_M\end{array}\middle|\begin{array}{l}\text{aircraft j is present in the}\\ \text{airspace and its signature}\\ \text{arrives at the master satellite}\\ \text{with initial pulse at time } T_M\end{array}\right) \tag{B-36}$$

Consider the equivalence of the following two events

$$\left(\begin{array}{l}\text{given that aircraft j is actually}\\ \text{present in the airspace with}\\ \text{initial signature pulse arriving}\\ \text{at master satellite at time } T_M,\\ \text{aircraft j is declared present}\\ \text{by the system at time } T_M\end{array}\right) = \left(\begin{array}{l}\text{The 5 pulses of j's signature}\\ \text{are detected at each of the}\\ \text{satellite ground stations and}\\ \text{the signature of "j" is picked}\\ \text{for processing from among the}\\ \text{overwrites at the master satellite}\\ \text{ground station}\end{array}\right) \tag{B-37}$$

The following equality results when (B-36), (B-37) and (B--9) are combined

$$P_D = P_d^{20}\ P(\alpha) \tag{B-38}$$

Applying (B-27) to (B-38) results in a lower bound to P_D,

$$P_D \geq P_d^{20}\left(\frac{2}{1 + (N_I - 1)^2\ P^4(\alpha)^2 + 2(N_I - 1)\ P^2(\alpha)} - (1 - P^2(\alpha))^{2\ N_I - 2}\right). \tag{B-39}$$

TABLE B.2

FSRR SYSTEM DETECTION PERFORMANCE

E/N_o	P_d	P_f	P_D^L	P_D^U
9db	0.98	0.1	.0768	0.667
9db	0.99	0.2	0.88×10^{-2}	0.82
9db	0.997	0.3	0.22×10^{-2}	0.94
13.5db	0.9998	0.01	0.88	0.99
6db	0.82	0.1	.00207	.0188
6db	0.92	0.2	.00195	.188
6db	0.94	0.2	.00066	.29

Obviously,

$$P_D \leq P_d^{20} \tag{B-40}$$

We now designate the right hand side of (B-39) as P_D^L, and the right hand side of (B-40) as P_D^U. In Table B.2, P_D^L and P_D^U are evaluated for a received signal to noise ratio of 6 db, 9 db and 13.5 db.

B.6 FSRR System Performance Summay

Tables B.1 and B.2 summarize the best possible performance that the FSRR system can achieve. Specifically, the system will actually incur an average number of false alarms (per 2.5 second period) which is greater than the lower bound $\overline{N}_f^L$. In addition, the true system detection probability will be less than the upper bound P_D^U.

The signal to noise ratio of 13.5 db is a very optimistic estimate of the link performance of the FSRR system. When one observes Tables B.1 and B.2 one can indeed conclude that the best possible FSRR system performance will be adequate at this value of E/N_o.

The performance of the FSRR system for received signal to noise ratios of 6 db and 9 db is summarized by the curves plotted in Figure B.3. These curves indicate that the system performance is inadequate for these received signal to noise ratios. The cost of a high detection probability is an enormous false alarm rate. The cost of a low false alarm rate is a very low detection probability. This indicates that it is not possible to obtain acceptable performance from a signal to noise ratio less than or equal to 9 db.

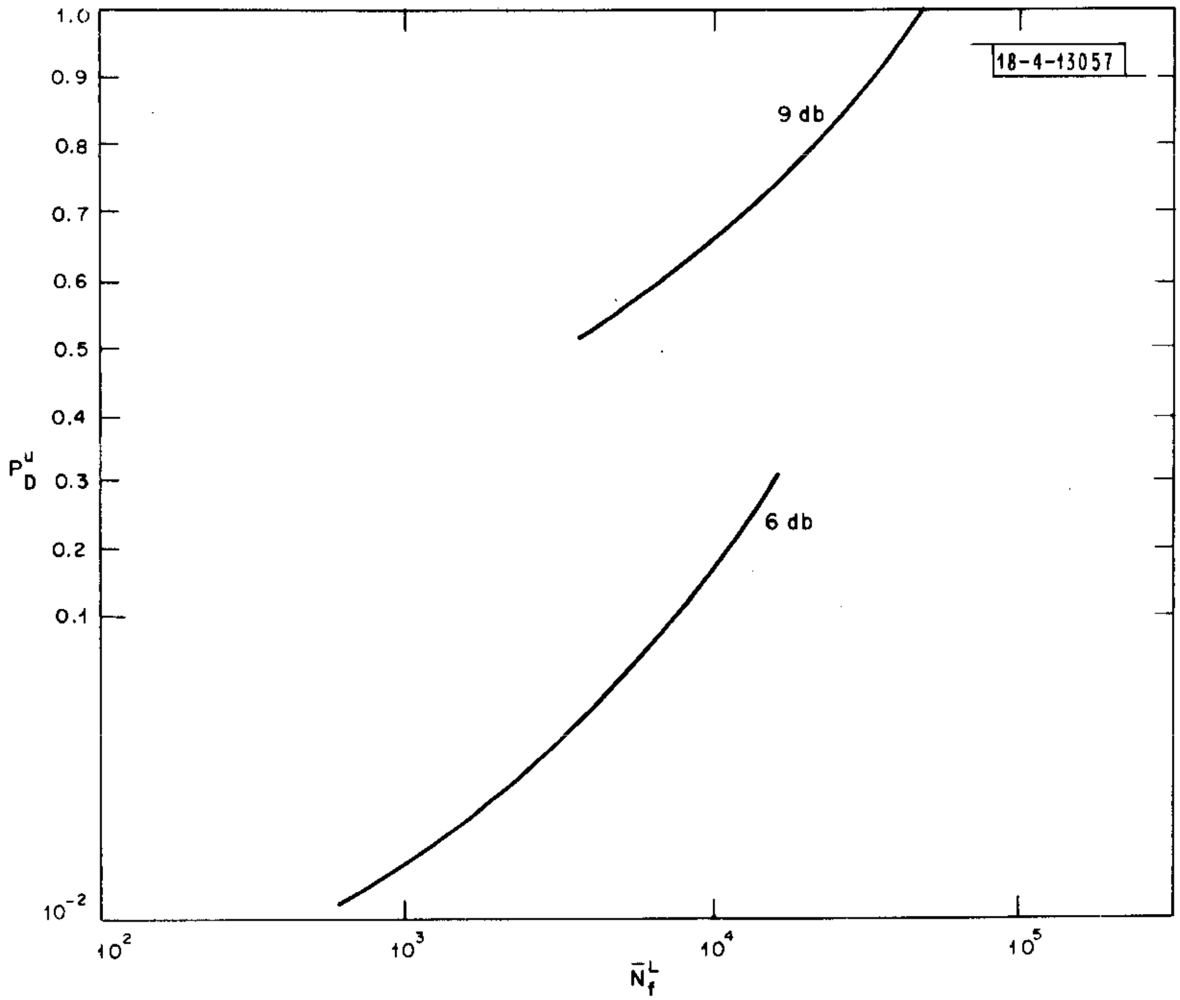

Fig. B. 3. P_D^u vs $\overline{N}_f^L$ for received signal to noise ratio of 9 db and 6 db.

APPENDIX C

OPERATION AND PERFORMANCE OF A VARIABLE SIGNATURE REPETITION RATE SURVEILLANCE SYSTEM

C.1 Introduction

In this Appendix an Air-to- Satellite-to-Ground Surveillance system will be described which operates with each aircraft transmitting a unique signature. The repetition rate of the signature will vary from aircraft to aircraft. This system will be analyzed and a feasibility judgment will be made. Henceforth, the system being considered will be called the VSRR system.

The program of this Appendix will be as follows: First, the aircraft signature design in the VSRR system will be described. The operation of the Air-to-Satellite-to-Ground link and of the satellite ground station will then be detailed. Finally, the performance of the VSRR system will be analyzed.

C.2 Signature Design

Each aircraft will be assigned a codeword and a repetition period. The combination of these two items will comprise the aircraft's VSRR signature.

The codeword will consist of 4 consecutive pulses called respectively; the "A" pulse, the "B" pulse, the "C" pulse, and the "D" pulse. Each pulse is a pseudo random sequence consisting of 511 one hundred nano-second chips (PSK Modulation). Each of the 4 pseudo random sequences is chosen from a different set of 12 such sequences. This implies that there are $(12)^4$ possible codewords. It should be pointed out that it is really not mandatory that the "A," "B," "C," and "D" pulses be strictly adjacent. Delays could be inserted between these pulses. In fact, this would be beneficial from a hardware point of view because of lower demands on the power amplifier. However, in order to keep our system description simple, consider these pulses to be strictly adjacent.

The repetition period of a codeword will have the generic value of x seconds where x is some number in the set $\{2.000, 2.001, \ldots 2.099\}$. The repetition period of a codeword defines a repetition rate. The two terms will be used interchangeably. As is evident, there are 10^2 possible repetition periods.

The combination of codewords and repetition periods permits more than 2×10^6 different signatures. By 1995 it is expected that there will be at most 10^6 aircraft. Thus, in the VSRR system it can be assumed that each aircraft will be assigned a unique signature. A typical VSRR signature is illustrated in Figure 2.2.

C.3 Air-to-Satellite-to-Ground Link

An essential part of the VSRR system will be a constellation of 4 satellites. The satellites will have coverage extending over the entire CONUS. On take off, each aircraft will begin transmitting its signature to each of the 4 satellites in the constellation. Each satellite will transmit each signature it receives to a ground station. The position of a particular aircraft can be computed from the differences between the times at which the aircraft's signature is received at the respective satellites. This of course assumes that the satellite constellation ephermeris data is known.

At the receiver, matched filter detection is used. Since there are 4 pseudo random sequences to a codeword and since each sequence is picked from a set of 12, a bank of 48 matched filters is needed for each of the 4 receivers.

If a pseudo random sequence is detected by a matched filter at a ground station it will be stored on a tape corresponding to that matched filter.* This tape will be partitioned into units corresponding to a time duration of 100 nanoseconds (1 chip duration). Each received pseudo noise sequence will be stored on the tape at a position corresponding to the time its first chip arrives at the ground station.

C.4 Ground Station Procedure - Forming the Acquisition List and the Signature List

This is the first of two sections which will deal with the operating procedure at the ground station of one of the satellites.

First, assume that each aircraft is assigned a unique identification number, say, some integer from 1 to 10^6.

At the ground station each matched filter has a tape associated with it as has already been described. In addition, each of these tapes will also have a processor, henceforth, called a "head" associated with it.

The heads will operate in the following manner. Initially, each head is at the beginning of its tape. At the starting time only the heads operating on tapes corresponding to the "A" pulse matched filters begin to move. Consider just one of these heads, the head operating on the tape corresponding to pulse A_1. This head moves down its tape, chip by chip reading the contents of the tape until it reads an A_1 pulse stored on the tape (the initial chips of the tape will most likely be empty).

When this head reads this A_1 pulse it performs several tasks before continuing its sequential reading of the A_1 tape. Specifically, it orders a special memory unit for the A_1 tape called the "A_1 drum" to come into operation. On one memory track of this drum it stores the time, t_1, at which this first A_1 pulse was stored on the A_1 tape. Remember this is equivalent to its position on the tape. This head then signals each of the heads on the B tapes to come into operation. The A_1 tape then continues its sequential movement.

*For conceptual purposes we shall describe performance as if the storage were on tape. However, in practice disc or core storage would of course be used.

Each head on a "B" tape moves to that position on its tape corresponding to time $(t_1 + 511 \times 10^{-7})$ seconds. Each head then reads the next 511 chips of its respective tape. There will be two possibilities for each head in this reading exercise. Either this 511 chip length contains a complete B pulse or it does not. (If it does not this does not imply that it is completely empty since it could contain a partial B pulse.) If the 511 chip length does not contain a complete B pulse then the head goes back to the beginning of its tape and stays there until it is called into operation again. However, if the 511 chip length does contain a complete "B" pulse it does three things. It first writes this B pulse on a special "B" memory track on the A_1 drum. Secondly, it signals each of the heads on the C tapes to come into operation. Finally, the B head goes back to the beginning of the tape and stays there until it is called into operation again. Assume that pulses; B_1 and B_2 are the only pulses written on the B memory track.

The operation of the C tape heads is practically the same as the B tape heads the only difference being that the C heads begin reading their tapes at a point corresponding to time $(t_1 + 1022 \times 10^{-7})$ seconds. Similarly, the operation of the D tape heads is identical with the only difference being that the D tape heads begin reading their tapes at a point corresponding to time $(t_1 + 1533 \times 10^{-7})$ seconds.

If the entries on the C memory track are C_1 and C_2, and if the entries on the D memory track are D_1 and D_2 then after the D memory track has been filled the A_1 drum will have the following entries:

First memory track:	t_1
Second memory track:	B_1, B_2
Third memory track:	C_1, C_2
Fourth memory track:	D_1, D_2

(Note: Most likely there will not be more than one entry on each track.)

With this A_1 memory drum filled a special operation mode is entered called "the codeword list mode." A special computer utilizes the entries in the A_1 memory drum to make a list called the A_1 - t_1 Codeword List. This list contains the aircraft codewords received by the ground station at time t_1 which had A_1 as their first pulse(assuming perfect detection). Specifically, it contains all codewords that can be constructed from the entries on the A_1 - t_1 drum. In the present example the A_1 - t_1 Codeword List would look as follows:

A_1 - t_1 Codeword List

A_1	B_1	C_1	D_1
A_1	B_1	C_1	D_2
A_1	B_1	C_2	D_1
A_1	B_1	C_2	D_2
A_1	B_2	C_1	D_1
A_1	B_2	C_1	D_2
A_1	B_2	C_2	D_1
A_1	B_2	C_2	D_2

With the "A_1 - t_1 Codeword List" completed the codeword list mode is also completed. A new mode is now entered called "The Acquisition List Mode." The operation of this mode will not be described.

When the Acquisition List Mode is entered the first thing that is done is to erase the A_1 drum. This allows the use of it as a storage memory in other Codeword List formations.

The prime function of the Acquisition List Mode is the filling of two separate memories called: "the Acquisition List" and "the Signature List."

Each entry on the Acquisition List will consist of 12 items. One can think of each item being placed in a different column. The first item in an entry will be an aircraft codeword. The next ten items will be codeword times of arrival in seconds. The last item on the entry will be an address of some other storage memory in which additional times of arrival can be stored for this entry.

Each entry on the Signature List will consist of 5 items. Again one can think of each item as being placed in a different column. The first item will be an aircraft identification number. The second item will be a time in seconds. Each column corresponding to the remaining 3 items will either have a * in it or be blank. These last 3 columns will be called column 3, column 4, and column 5 respectively.

The Acquisition List will have room for $(12)^4$, (the number of codewords), entries. The Signature List will have room for $(10)^6$ entries.

Initially, both the Acquisition List and Signature List will be completely empty. However, for convenience the operations performed on the $A_1 - t_1$ Codeword List, during the Acquisition List Mode, will be described in terms of the Acquisition List and Signature List being partially filled. This will allow a simplifying generalization of the operation of the Mode.

The operation of the Acquisition List Mode is carried out by a special computer called "The Acquirer." The Acquirer goes to the very top of the $A_1 - t_1$ Codeword List. It takes the entry which is there and stores it in a shift register called <u>S</u>. The Acquirer then erases the topmost entry from the $A_1 - t_1$ Codeword List.

Next, the Acquirer moves to the Acquisition List. Starting at the top of the Acquisition List the Acquirer compares the contents of S̲ with the successively lower entries on the Acquisition List. It stops momentarily if it comes to an Acquisition List entry in which the codeword item is identical to the contents of S̲. When this happens the Acquirer cycles through the times listed as the other items for this entry. For each of these items the Acquirer computes the difference between t_1 and it. It lists those differences which are valid values of x, the codeword repetition period. For example this could be (X_1, X_2, X_3). If none of the differences is a value of x then the Acquirer enters t_1 as a time in the first empty time slot on this entry. (If the 10 principle time slots are filled it goes to the address given by the 12th slot and stores it in the first empty space in this storage area). This event is called "Acquisition." On the other hand suppose there are valid repetition periods, (X_1, X_2, X_3) computed.

Corresponding to a codeword "J," and periods X_1, X_2, and X_3 are aircraft signatures Y_1, Y_2, Y_3. The Acquirer computes the sublist of aircraft signatures; Y_1, Y_2, Y_3 and then begins a subcycle. The Acquirer fills up a shift register $\bar{S}$ with Y_1 and erases Y_1 from the sublist. It then moves to the top of the Signature List comparing the contents of $\bar{S}$ with the successively lower entries on the Signature List. If the Acquirer does not find an aircraft identification number on the Signature List which is identical with the contents of $\bar{S}$ then it enters the contents of S in the first empty entry slot on the Signature List, (in the aircraft identification column). In the time portion of this entry it enters the time t_1. In column 3 it enters a *. The Acquirer then returns to the list Y_2, Y_3... and goes through the same procedure.

On the other hand if the Acquirer does find an aircraft identification number on the Signature List which is identical with the contents of $\bar{S}$ then it empties $\bar{S}$, returns to the sublist Y_2, Y_3 ... and continues cycling down through it.

When the Acquirer exhausts the sublist; Y_1, Y_2, Y_3 . . . , it returns to the top of the A_1 - t_1 Codeword List (not the Acquisition List) and continues to cycle down through it going through the same procedure as just described.

Now, if the Acquirer, in one of its cycles down the Acquisition List, goes down the entire list without making any excursions to the Signature List then it places the codeword stored in S in the first empty slot on the Acquisition List, with time t_1, stored in the first time item slot. This event is also called "Acquisition." The Acquirer then returns to the top of the A_1 - t_1 Codeword List and cycles down through it.

Two points should be mentioned before closing this section. First, one might wonder why each entry on the Acquisition List is structured with 10 principle time slots and an address giving a storage area where additional times can be stored if the 10 principle slots overflow. The reason for this is quite simple. There are 10^6 possible aircraft; however, on the average only 10% of them will be in flight at any time. This implies that a given codeword will be received by the ground station at only 10 of the 100 possible repetition rates. Each repetition period corresponds in effect to a separate time slot on an entry on the Acquisition List. On the average only 10 such slots will be needed. Rather than providing a full 100 slots and wasting memory the efficient structure here is designed for the average with a backup memory to take care of overflow if it occurs.

The second point that should be brought up involves the periodic purging of time item entries on the Acquisition List. Many of the time entries on the Acquisition List may become very stale. This may be due to the time entry having been entered by mistake, as a false alarm, and never having been changed. For instance, with an A_1 codeword and t_1 = 10 sec. one might encounter a time item in the J entry giving a time of 2 seconds. Because space on the Acquisition List should be used efficiently, once every 10 seconds a purging routine will go through the entire list and erase all those time items which correspond to times earlier than a certain threshold time, say 5 seconds before.

C.5 Ground Station Procedure - Tracking and Position Computation

In the last section the Acquisition List Mode was described. The operation of the Acquisition List Mode results in the formation of the Signature List. A special computer operates on the Signature List. Its operations are carried out completely in parallel with the other operations at the Ground Station. The computer is called "The Tracker" and its operation results in the position calculation of aircraft in the airspace. The operation of the Tracker on the Signature List will now be described.

The Tracker begins its cycle at the top of the Signature List and observes the first entry. Assume that the aircraft identification portion of this entry is the integer I and that the time item entry is the time t_1 seconds. There are 8 possibilities for the other characteristics of this entry depending upon whether or not columns 3, 4, and 5 are filled with *'s or not. These possibilities are shown in the following table:

	Col. 1	Col. 2	Col. 3	Col. 4	Col. 5
Possibility 1	I	t_1	*		
Possibility 2	I	t_1	*	*	
Possibility 3	I	t_1		*	
Possibility 4	I	t_1	*	*	*
Possibility 5	I	t_1		*	*
Possibility 6	I	t_1	*		*
Possibility 7	I	t_1			*
Possibility 8	I	t_1			

Assume that the signature of aircraft I is composed of codeword J repeated with a repetition period X_1.

Each of the possibilities calls into operation a different mode of the Tracker. Each of the modes will be described separately for each possibility. After a mode is completed the Tracker moves down to the next entry out the Signature List. When it has moved through the entire list it begins its next cycle back at the top. The total cycle time should be of the order of 2 seconds (i.e. signature repetition time).

The Mode for Possibility 1

Possibility 1 comes about if this entry has just been listed on the Signature List by the Acquirer. When the Tracker encounters Possibility 1 the first thing it does is to shift the * contained in column 3 to column 4. The * was previously contained in column 3. The entry in column 2 is t_1, the Tracker uses this to predict that if this entry is not a false alarm the ground station should receive the next codeword emitted by aircraft I during the time interval $[t_1 + x_1 - 40 \times 10^{-7}, t_1 + x_1 + 40 \times 10^{-7}]$, (the $\pm 40 \times 10^{-7}$ takes into account the movement of the aircraft and satellites during the codeword transmission). The Tracker checks the tapes of the pulses making up codeword J to see in fact if the codeword was received at the ground station during this time interval. If the codeword J was not received, this event is called a "cycle loss." Column 3 is kept blank. If the codeword J was received in this interval at time $\underline{t}$ then this event is called "a track." When this happens time t_1 in column 2 is replaced by $\underline{t}$ and a * is entered in column 3.

It is evident that if a cycle loss occurs then Possibility 1 considered now, will become a Possibility 3 on the next cycle of the Tracker through the Signature List. If a track occurs then Possibility 1 will become a Possibility 2.

The Mode for Possibility 2

When the Tracker encounters Possibility 2 the first thing it does is to shift the 2 *'s entered in columns 3 and 4 to columns 4 and 5 respectively.

This leaves column 3 blank. As has already been said, Possibility 2 comes about if a track occurs on a Possibility 1 at this entry during the previous cycle. The Tracker uses this information to predict that if this entry is not a false alarm then the ground station should receive the next codeword emitted by aircraft I during the time interval $[t_1 + x_1 - 40 \times 10^{-7},\ t_1 + x_1 + 40 \times 10^{-7}]$. The Tracker checks the tapes of the pulses making up codeword J to see in fact if the codeword was received at the ground station during this time interval. If the codeword J was not received (a cycle loss) column 3 is kept blank. If the codeword J was received in this interval at time $\underline{t}$ (a track) then time t_1 in column 2 is replaced by $\underline{t}$ and a * is entered in column 3.

It is evident that if a cycle loss occurs the Possibility 2 considered now will become a Possibility 5 on the next cycle of the Tracker through the Signature List. If a track occurs then Possibility 2 becomes a Possibility 4.

The Mode for Possibility 3

When the Tracker encounters Possibility 3 the first thing it does is to shift the * in column 4 to column 5. This leaves column 3 and column 4 blank. Possibility 3 comes about if a cycle loss occurred on a Possibility 1 at this entry during the previous cycle. The Tracker used this information to predict that if this entry is not a false alarm then the ground station should receive the next codeword emitted by aircraft I during the time interval $[t_1 + 2x_1 - 80 \times 10^{-7},\ t_1 + 2x + 80 \times 10^{-7}]$. The Tracker checks the tapes of the pulses making up codeword J to see in fact if the codeword was received at the ground station during this time interval. If the codeword J was not received (a cycle loss) column 3 is kept blank. If the codeword J was received in this interval at time $\underline{t}$ (a track) then time t_1, in column 2 is replaced by $\underline{t}$ and a * is entered in column 3.

It is evident that if a cycle loss occurs, the Possibility 3 considered now, will become a Possibility 7 on the next cycle of the Tracker through the Signature List. If a track occurs then Possibility 3 becomes a Possibility 6.

The Mode for Possibility 4

Possibility 4 comes about if aircraft I has been tracked 3 times in succession. When this occurs it is with high probability that this entry is not a false alarm. When the Tracker encounters Possibility 4 the very first thing it does is to contact the other ground stations and ask each of them two questions:

1. Is aircraft I entered on its Signature List?
2. If it is entered are the entries in columns 3, 4, 5 next to it, all *'s?

If all 3 other satellite receivers answer yes, to both of these questions then the Tracker asks each of these what the item in the time slot of this entry is. Assume that the ground stations answer

$t_1', t_1'', t_1''',$

The interrogating receiver computes the differences $t_1 - t_1'$, $t_1 - t_1''$, $t_1 - t_1'''$. It uses them to compute the position of aircraft I from these differences, and supplies the result to a central surveillance station. This central surveillance station logs the aircraft identification number with the time t_1 and the computed position. The Tracker then continues with the operation it would have gone into immediately if the other ground stations had not answered yes to both questions. This operation is as follows.

The Tracker erases the * in column 5. It then shifts the *'s in columns 3 and 4 to columns 4 and 5 leaving column 3 blank. The Tracker uses this information given by the * positions (before they are shifted) to predict that if this entry is not a false alarm then the ground station should receive the next codeword emitted by aircraft I during the time interval $[t_1 + x_1 - 40 \times 10^{-7}, t_1 + x_1 + 40 \times 10^{-7}]$. The Tracker checks the tapes of the pulses making up codeword J to see in fact if the codeword was received at the ground station during this time interval. If the codeword J was not received (a cycle loss) column 3 is kept blank. If the codeword J was received (a track) in this interval at time $\underline{t}$ then time t_1 in column 2 is replaced by $\underline{t}$ and a * is entered in column 3.

It is evident that if a cycle loss occurs, the Possibility 4 considered now will become a Possibility 5 on the next cycle. If a track occurs Possibility 4 will stay as Possibility 4 on the next cycle.

The Mode for Possibility 5

When the Tracker encounters Possibility 5 the first thing it does is to erase the * in column 5 and shift the * in column 4 to column 5. This leaves column 3 and column 4 blank. As has already been said Possibility 5 comes about if a cycle loss occurred on a Possibility 2 or 4 at this entry during the previous cycle. The Tracker uses this information (given by the * positions before shifting) to predict that if this entry is not a false alarm then the ground station should receive the next codeword emitted by aircraft I during the time interval $[t_1 + 2x_1 - 80 \times 10^{-7}, t_1 + 2x_1 + 80 \times 10^{-7}]$. The Tracker checks the tapes of the pulses making up codeword J to see in fact if the codeword was received at the ground station during this time interval. If the codeword J was not received (a cycle loss) column 3 is kept blank. If codeword J was received in this interval at time $\underline{t}$ (a track) then time t_1 in column 2 is replaced by $\underline{t}$ and a * is entered in column 3.

It is evident that if a cycle loss occurs, the Possibility 5 considered now will become a Possibility 7 on the next cycle. If a track occurs it will become a Possibility 6.

The Mode for Possibility 6

When the Tracker encounters Possibility 6 the first thing it does is to erase the * in column 5 and to shift the * in column 3 to column 4. The Tracker uses the information given by the * positions (previous to shifting) to predict that if this entry is not a false alarm then the ground station should receive the next codeword emitted by aircraft I during the time interval $[t_1 + x_1 - 40 \times 10^{-7}, t_1 + x_1 + 40 \times 10^{-7}]$. The Tracker checks the tapes of the pulses making up codeword J to see in fact if the codeword was received at the ground station during this time interval. If the codeword J was not received (a cycle loss) column 3 is kept blank. If the codeword J was received in this interval at time $\underline{t}$ (a track) then time t_1, in column 2 is replaced by time $\underline{t}$ and a * is entered in column 3.

It is evident that if a cycle loss occurs the Possibility 6 now considered will become a Possibility 3 on the next cycle. If a track occurs it will become a Possibility 2.

The Mode for Possibility 7

When the Tracker encounters Possibility 7 the first thing it does is to erase the * in column 5. Possibility 7 comes about if this entry has suffered exactly 2 cycle losses in a row (no more, no less). The Tracker uses this information to predict that if this entry is not a false alarm then the ground station should receive the next codeword emitted by aircraft I during the interval $[t_1 + 3x_1 - 120 \times 10^{-7}, t_1 + 3x_1 + 120 \times 10^{-7}]$. The Tracker checks the tapes of the pulses making up codeword J to see in fact if the codeword was received at the ground station during this time interval. If the codeword J was not received (a cycle loss) column 3 is kept blank. If the codeword J was received in this interval at time $\underline{t}$ (a track) then t_1 in column 2 is replaced by $\underline{t}$ and a * is entered in column 3.

It is evident that if a cycle loss occurs this Possibility 7 will become Possibility 8 on the next cycle. If a track occurs it will become Possibility 2.

The Mode for Possibility 8

Possibility 8 can only come about if a cycle loss occurs at this entry three times in a row. This is unlikely if this entry is not a false alarm. For this reason when the Tracker encounters Possibility 8 it erases the entire entry from the list. Aircraft I will no longer be tracked at this ground station unless it is reacquired. The Tracker assumes that it has been tracking a false alarm if it encounters Possibility 8.

In carrying out one of the modes the Tracker may look in a time interval for a specific codeword (of the aircraft it is tracking) and find more than one codeword there, one being the valid codeword the others caused by interference. In such a case the Tracker considers only the earliest codeword in the interval and ignores the others.

C.6 Distribution of Ground Station Effort and Computational Cost

In the previous two sections the operation of the Ground Station has been described. The Ground Station effort has been divided into three parts:

(a) the operations on the matched filter tapes

(b) the operation of the Acquisition List Mode

(c) the operations on the Signature List

(a) and (b) are used to accomplish the task of acquiring all the aircraft in the airspace. They are used to find out which aircraft are in the airspace and also to place those aircraft on the Signature List. Assuming perfect detection it takes only one observation of an aircraft's codeword before it is placed on the Acquisition List. Again, assuming perfect detection it takes only one additional observation of an aircraft's codeword before it is placed on the Signature List. Thus, one repetition period (which is at most 2.1 seconds) after an aircraft is first observed it will be put on the Signature List.

(c) is used to track the aircraft in the airspace. The future times of arrival of an aircraft's codeword are predicted based upon past data. If an aircraft is tracked long enough (through 3 repetition periods or equivalently 3 cycles of the Tracker through the Signature List), then its position is computed and recorded. This provides some reliability against the possibility of recording the position of a false alarm.

The event of a system breakdown or failure requires no additional effort on the part of the VSRR system. The Tracker will within 3 cycles have automatically erased the entire Signature List. This List will be refilled with 2.1 seconds (maximum repetition period) by the Acquisition List Mode. Reacquisition of all aircraft (assuming perfect detection) will be accomplished within the time it takes to complete 3 Tracker cycles + 2.1 seconds. Assuming that a Tracker cycle can be made equal to 2.1 seconds reacquisition time will be under 9 seconds.

As has been described, the Ground Station tasks require quite a bit of computational power. The formation of the Codeword Lists, the operation of the Acquirer and Tracker all require extensive computational capability. In the remainder of this section, the quality of computational capability needed to carry out these computations will be estimated.

The Acquisition List, as described in Section 4, had very little structure. Codewords were entered into it at the first available entry namely, the bottom of the list. The computational time needed to carry out the Acquisition List Mode can be greatly reduced if some additional structure is put on this list. Specifically, assume that the Acquisition List is ordered as a lexicon of the codewords. In other words assume that each codeword has a specific address on the Acquisition List. With this structure, whenever a codeword and/or arrival time is entered on the

Acquisition List the Acquirer can go directly to the address of the codeword being considered rather than cycling down the entire list searching for the codeword entry.

Assume that the Acquisition List has the lexicon structure. Consider a specific codeword being operated on during the Acquisition List Mode. The codeword is entered into a shift register, S. The address of the codeword in the Acquisition List is then accessed. Assume this takes Z_1 seconds. After this on the average 10 "subtracts" will be performed to compute possible repetition periods. Assume that each subtract takes Z_2 seconds. The total computation time spent on this one codeword will be $Z_1 + 10Z_2$ seconds.

Assume that there is a peak load of 10^5 aircraft in the airspace at any time. This implies that in approximately every 2 second interval (repetition period) the Acquirer will be processing 10^5 codewords (neglecting false alarms). Thus for every 10^5 codewords processed $10^5 (Z_1 + 10Z_2)$ seconds of computational time will be needed. By 1995 the following values of Z_1 and Z_2 should be realized; $Z_1 = 10^{-7}$ seconds $Z_2 = 2 \times 10^{-7}$ seconds. Therefore, for every 10^5 aircraft processed in the Acquisition List Mode, 0.11 seconds of computation time will be used. This makes acquiring the aircraft a computationally feasible task.

Consider, the operation of the Tracker cycling through the Signature List. There will be a maximum of 10^5 entries on the Signature List. Without any argument we can assume that it is split into a top portion and a bottom portion with a separate Tracker operating on each. This parallel processing will cut the time it takes the Tracker to complete a cycle in half. Let Z_3 be the time that a Tracker spends on one entry on the Signature List. One has then

$$\text{Tracker Cycle Time} = \frac{1}{2}\ 10^5\ Z_3$$

Z_3 is composed of several components. It must take into account the time needed to compute aircraft position if in fact this is carried out when the Tracker is at this entry. Z_3 must take into account time needed for shifting operations and storage of new arrival times. By far the dominant component of Z_3 is the time needed to compute position. This is approximately 10^{-4} seconds assuming a value of $Z_i = 10^{-7}$ seconds. One has then; Tracker Cycle Time = 5 Seconds. By partitioning the Signature List further, the Tracker Cycle time can be reduced to 2 seconds.

C.7 Performance Measures of the VSRR System

As has been described in Section C.5 the Tracker of a satellite receiver moves sequentially down the Signature List of the satellite receiver. If the Tracker comes to an entry (corresponding say to aircraft I) which has been tracked on the previous three cycles then the Tracker contacts the other three ground stations. It inquires of them whether or not the present state of the entry of aircraft I is such that it has been tracked on the last three cycles of the Trackers at these stations? If the other satellite receivers answer affirmatively then the Tracker under consideration requests the values of the current time slot items in the entry of aircraft I. The Tracker then computes the position of aircraft I, supplies the result to a central surveillance station where it is logged with the current time of arrival (at the satellite receiver being considered) of aircraft I's codeword. In this manner the VSRR system maintains the surveillance function.

There are principally two types of errors that can be made in maintaining the surveillance function, "a false Alarm Error," and a failure to detect error."

A False Alarm error can be described as the occurrance of either of the following two events: (Assume that the Trackers at all 4 satellite receivers are synchronized).

(1) the Tracker at one of the 4 satellite receivers (and therefore at all 4 satellite receivers) computes the position of an aircraft which is not in the airspace and supplies it to the central surveillance station.

(2) The Tracker at one of the satellite receivers, computes the position of an aircraft which is in the airspace and supplies it to the central surveillance station; however, the position is not the true position of the aircraft.

Some additional definition of False Alarm type (2) is in order. Consider the following situation. Aircraft I is present in the airspace. Its true codeword is received at all four satellite receivers. It becomes entered on the Signature List at all four receivers with the correct time item entry. It is tracked correctly on all four Signature Lists with a long sequence of its correct positions computed and supplied to the central surveillance station. Now suppose the following event occurs at the end of this long sequence of correct positions. The aircraft codeword is tracked correctly at three of the four receivers. At the fourth receiver interference masquerades as the aircraft codeword and is picked for continual tracking rather than the true codeword. The time item on this fourth Signature List will not be updated correctly, and the position of the aircraft will be computed incorrectly.

As the definition of False Alarm (2) now stands the event described is a false alarm. However, the incorrect time item will be wrong at most by 80 chips, which might cause a position error of at most 1 mile. In addition, the correct codeword would most likely be locked onto again during the next Tracker cycle. In this context it is not fair to count this event as a true false alarm. Adding to the definition of False Alarm (2) we require that at least one of the 4 time items contributing to the position (one on each Signature List) to have been incorrect for at least 3 successive Tracker cycles.

A failure to detect error is the following event: during a Tracker cycle an aircraft which is in the airspace does not have its position computed by any of the 4 trackers or has its position computed with at least one of the time items contributing to the computation to have been incorrect on the three previous cycles.

In the following section an upper bound to the expected number of False Alarms per Tracker cycle will be computed. In Sec. C.9 a lower bound to the probability of failure to detect a given aircraft will be computed. These bounds will give a measure of the error performance of the VSRR system.

In the previous section the Acquisition List was structured somewhat in order to reduce the computational power needed for the VSRR system. Now in order to simplify the analyses in the following 2 sections the Signature List will be structured. From now on it is assumed that an aircraft's identification number will alway be entered onto at a specific entry slot reserved for each aircraft.

C.8 System False Alarm Rate

An upper bound to the system false alarm rate will be computed now. First, some notation will be introduced. Consider a single Tracker cycle. Let

$$\overline{N_f} = E\begin{pmatrix}\text{Total number of false alarms entered at the}\\ \text{central surveillance station by all 4 receivers}\\ \text{during one cycle}\end{pmatrix} \quad \text{(C-1)}$$

then

$$\overline{N_f} = 4E\begin{pmatrix}\text{Total number of false alarms entered at the}\\ \text{central surveillance station by a single receiver}\\ \text{during one cycle}\end{pmatrix} \quad \text{(C-2)}$$

$$\overline{N_f} = 8E \begin{pmatrix}\text{Total number of false alarms entered at the} \\ \text{central surveillance station by one of the} \\ \text{trackers at a single receiver during one cycle}\end{pmatrix} \quad \text{(C-3)}$$

In observing the generation of (C-3) from (C-2) it should be remembered that two trackers operated in parallel at each receiver.

Let the ground stations be numbered from 1 to 4 and consider that Tracker which operates on the top portion of the Signature List of receiver #1. Equation (C-3) can be rewritten as

$$\overline{N_f} = 8E \begin{pmatrix}\text{Total number of false alarms entered at the central} \\ \text{surveillance station by the top Tracker at receiver} \\ \text{\#1}\end{pmatrix} \quad \text{(C-4)}$$

Without loss of generality let the i^{th} slot correspond to the aircraft with identification number "i." Let $\theta(j, i)$ be a characteristic of the Signature List of Ground Station "j." The current entries in columns 3, 4, and 5 of a slot at a particular time will be called the "state of the Slot"

Let

$\theta(j, i) = 1$, if the state of slot i on the top portion of the Signature List of receiver j, is such that there is a * in columns 3, 4, and 5.

$= 0$, otherwise (C-5)

Consider the K^{th} Tracker cycle. Let $\beta(j, i)$ be another characteristic of the i^{th} slot on the top portion of the Signature List of receiver "j" during the K^{th} cycle. Let

$\beta(j, i) = 0$, if the time item of slot i has been incorrect on the K^{th} $(K-1)^{th}$ and $(K-2)^{th}$ Tracker cycles at the receiver

$= 1$, otherwise (C-6)

$\theta(j, i)$ and $\beta(j, i)$ can be used to count false alarms. Specifically, $\theta(j, i)$ can be applied to (3) to yield.

$$\overline{N_f} = 8E\left(\sum_{i=1}^{10^6/2}\left(\prod_{j=1}^{4} \theta(j, i)\right)\left(1 - \prod_{j=1}^{4} \beta(j, i)\right)\right) \tag{C-7}$$

$$\overline{N_f} = 4 \times 10^6 \ E\left(\left(\prod_{j=1}^{4} \theta(j, i)\right)\left(1 - \prod_{j=1}^{4} \beta(j, i)\right)\right) \tag{C-8}$$

The random variable "A" will now be defined

$$A = \left(\prod_{j=1}^{4} \theta(j, i)\right)\left(1 - \prod_{j=1}^{4} \beta(j, i)\right) \tag{C-9}$$

Similarly, the following definitions are made

$$H = \prod_{j=1}^{4} \theta(j, i) \tag{C-10}$$

$$E(A|h, b_1, b_2, b_3, b_4) = E(A|H=h, \beta(1, i) = b_1, \beta(3, i) = b_2, \beta(3, i)=b_3, \beta(4, i) = b_4) \tag{C-11}$$

$$P(h, b_1, b_2, b_3, b_4)=\text{Prob}(H=h, \beta(1, i)=b_1 \ \beta(2, i)=b_2, \beta(3, i)=b_3, \beta(4, i)=b_4) \tag{C-12}$$

The following expansion can now be made

$$E\ (A) = \sum_{h,\, b_1,\, b_2,\, b_3,\, b_4} E(A \mid h, b_1, b_2, b_3, b_4)\ P(h, b_1 b_2 b_3 b_4)$$

$$E\ (A) = \sum_{b_1,\, b_2,\, b_3,\, b_4} E(\ 1 - \underset{j-1}{\overset{4}{\pi}}\ \beta(j, i) \mid 1, b_1 b_2, b_3 b_4)\ P\ (1, b_1 b_2 b_3 b_4) \qquad \text{(C-13)}$$

By symmetry this becomes

$$E\ (A) = P(1,\ 0,\ 0,\ 0, 0),\ + 4\ P\ (1,\ 0,\ 0,\ 0,\ 1) + 6\ P\ (1,\ 0,\ 0,\ 1,\ 1)$$
$$+ 4\ P\ (1,\ 0,\ 1,\ 1,\ 1) \qquad \text{(C-14)}$$

The following term is now defined

$$p\ (b_1) = \text{Prob}\ (\beta(1,\ i) = b_1) \qquad \text{(C-15)}$$

Using the inclusion of event $\{b_1, b_2, b_3, b_4\}$ in b_1, and (C-15)allows (C-16) to be derived from (C-14)

$$E\ (A) \leq 15\ p(0) \qquad \text{(C-16)}$$

Applying (C-16) and (C -9) to (C-8) yields

$$\bar{N}_f \leq 60 \times 10^6\ P\ (0) \qquad \text{(C-17)}$$

The event $\beta(1,\ i) = 0$ implies that on 3 successive Tracker cycles interference masqueraded as the 4 pulse codeword of the signature of aircraft "i." Let

$$P_f = \text{Prob.}\begin{pmatrix}\text{noise causes a receiver matched filter to be activated} \\ \text{and declare a codeword pulse present when in fact it} \\ \text{is not}\end{pmatrix} \quad \text{(C-18)}$$

Since there are 4 pulses to a codeword and a tracking time interval is 80 chips long the following inequality can be written

$$P(0) \le (80 \times P_f^4)^3 = (5 \times 12)\, 10^5 \;\; P_f^{12} \quad \text{(C-19)}$$

$$P\,(0) \le (5 \times 12)\, 10^5\, P_f^{12} \quad \text{(C-20)}$$

Applying (C-19) to (C-17) results in

$$\overline{N_f} \;\le 31 \times 10^{12}\, P_f^{12} \quad \text{(C-20)}$$

Which is the desired upper bound. Let the right hand side of (C-20) be designated by $\overline{N_f u}$. (C-20) can be rewritten as

$$\overline{N_f} \quad \le \quad \overline{N_f u}$$

$$\overline{N_f} \;\le\; 31 \times 10^{\,12}\, P_f^{12} \quad \text{(C-20a)}$$

C.9 Probability of Correct Detection

The "failure to detect" error described in Section 7 implies that the process of detecting and maintaining continuous surveillance on an aircraft is quite complex. For this reason this process will be broken up into several different parameters which together will measure the event of correct detection.

C.9.1 Correct Entrance Onto the Signature List

C.9.1.1 Probability of Correct Entrance

Consider aircraft "i," some aircraft which is actually in the airspace. In order for aircraft i to be detected on a Tracker cycle several properties of aircraft "i's" entry on the four Signature Lists must be satisfied. Columns #3, #4, and #5 of this entry on each Signature List must be filled with *'s. In addition, on each Signature List the time item of this entry must be correct on either the Tracker cycle being considered or on one of the two immediately preceding Tracker cycles. (A time item is correct if it represents the time that the actual codeword of aircraft i was received at a ground station rather than the time interference masquerading as the codeword was received.

Let us fix our attention on one of the Signature Lists. Whether or not the time item is correct depends mostly in the manner in which this entry was most recently entered on the Signature List by the Acquirer. Remember the Acquirer enters the first time item of the entry of aircraft i on the Signature List. Aircraft i is then tracked until columns #3, #4, and #5 of it are blank. It is then erased from the Signature List. Our first task will be to compute, for a specific aircraft, the probability that the first entry in its Signature List slot after system start-up is true. Let R(i) be the event just described relative to aircraft i. Let $\underline{c}$ be the codeword of aircraft "i's" signature.

In order for R (i) to occur the following events must also occur. The first two codewords emitted by aircraft "i" must be perfectly detected. The "$\underline{c}$" codewords emitted by other aircraft, which are received by the ground station before the first codeword of aircraft i (and detected) can not be paired with interference masquerading as codeword $\underline{c}$ or some true but spurious $\underline{c}$ codeword to represent falsely a signature repetition of aircraft "i's" codeword. Finally, interference masquerading as a "$\underline{c}$" codeword and received before the first of aircraft "i's" codewords cannot be paired with interference masquerading as a "c" codeword or some true, but spurious "$\underline{c}$" codeword to represent falsely a signature repetition of aircraft "i's" codeword.

Let P (R (i)) represent the Probability that event R(i) occurs. Similarly, the following notation is introduced:

$$G(n) = \text{Prob.}\left(\begin{array}{l}\text{exactly n true "}\underline{c}\text{" codewords are received before}\\ \text{the first codeword of aircraft "i's" Signature}\end{array}\right) \tag{C-21}$$

$$f(t_1, \ldots t_n) = \text{Prob.}\left(\begin{array}{l}\text{given that exactly n true "}\underline{c}\text{" codewords are}\\ \text{received before the first codeword of}\\ \text{aircraft i's signature, these codewords are}\\ \text{received at times } t_1, \ldots t_n\end{array}\right) \tag{C-22}$$

$$H(m, t_1', \ldots t'_m) = \text{Prob.}\left(\begin{array}{l}\text{exactly m "}\underline{c}\text{" codewords caused}\\ \text{by interference are received before}\\ \text{the first codeword of aircraft "i's"}\\ \text{signature and they are received at}\\ \text{time times } t_1', \ldots t_m'\end{array}\right) \tag{C-23}$$

$$g(K) = \text{Prob.}\left(\begin{array}{l}\text{aircraft "i's" first codeword is received with its}\\ \text{first chip starting during the } K^{th} \text{ 100 n sec in-}\\ \text{terval after the very first "}\underline{c}\text{" codeword is re-}\\ \text{ceived}\end{array}\right) \tag{C-24}$$

$$P(a) = \text{Prob.}\left(\begin{array}{l}\text{interference masquerades as a "}\underline{c}\text{" codeword at}\\ \text{a specific time}\end{array}\right) \tag{C-25}$$

$$P_d = \text{Prob.}\begin{pmatrix}\text{a true codeword input, to the filter it is matched to,} \\ \text{is detected}\end{pmatrix} \quad \text{(C-26)}$$

P(R(i)) can now be represented by the following expansion:

$$P(R(i)) = \sum_{K} \sum_{n} \sum_{m} \sum_{t_i, \ldots t_n} \sum_{t_i, \ldots t'_m} \Bigg(P_d^8 \, g(K) G(n) f(t_1, \ldots t_n)$$

$$(1 - P(a))^n H(m, t'_1, \ldots t'_m) (1 - P(a))^m \Bigg) \quad \text{(C-27)}$$

Identity (C-27) will be simplified now. Assuming that the distribution of the first arrival time of an aircraft's codeword is uniform and that the aircraft transmitters are not synchonized yields:

$$G(n) = \frac{n}{N_{\underline{c}}} \quad \text{(C-28)}$$

Where $N_{\underline{c}}$ is the total number of aircraft in flight which utilize codeword "c" in their signature. With 10^5 aircraft in flight and $(12)^4$ codes N_c can be estimated at 5.

The repetition rate of a signature varies from 2 seconds to 2.1 seconds. Again assuming that the distribution on the first arrival time of an aircraft's codeword is uniform gives

$$g(K) = \frac{1}{2 \times 10^7} \quad \text{(C-29)}$$

For a given K and n, $H(m, t_1', \ldots t_m')$ can be expanded as follows

$$H(m, t_i, \ldots t_m^1) = P^m(a)\,(1-P(a))^{K-n-m} \qquad \text{(C-30)}$$

For a given $t_1, \ldots t_n$ one has

$$f(t_1, \ldots t_n) = (g(K))^n \qquad \text{(C-31)}$$

Applying (C-28) through (C-31) to (C-27) results in

$$P(R(i)) = \sum_{K=1}^{2\times 10^7} \sum_{n=0}^{4*} \sum_{m=0}^{K-n} \sum_{t_1,\ldots t_n} \sum_{t_1',\ldots t_m'} \Big(P_d^8\; g(K)\,\tfrac{n}{5}\, g^n(K)\,(1-P(a))^n$$

$$P^m(a)\,(1-P(a))^{K-n-m}(1-P(a))^m\Big) \qquad \text{(C-32)}$$

(Note: 4* = min (K, 4))

$$P(R(i)) = \sum_{K=1}^{2\times 10^7} \sum_{n=0}^{4*} \sum_{m=0}^{K-n} \binom{K}{n}\binom{K-n}{m} P_d^8\; g^{n+1}(K) P^m(a)(1-P(a))^K \qquad \text{(C-33)}$$

Applying (C-29) to (C-33) yields

$$P(R(i)) = \sum_{K=1}^{2\times 10^7} \sum_{n=0}^{4*} \sum_{m=0}^{K-n} \binom{K}{n}\binom{K-n}{m} P_d^8 \left(\frac{1}{2\times 10^7}\right)^{n+1} P^m(a)(1-P(a))^K$$

$$P(R(i)) = \sum_{K=1}^{2\times 10^7} \sum_{n=0}^{4*} \sum_{m=0}^{K-n} \frac{K!}{n!\ m!\,(K-n-m)!} P_d^8 \left(\frac{1}{2\times 10^7}\right)^{n+1} P^m(a)(1-P(a))^K$$

$$P(R(i)) = P_d^8 \sum_{K=1}^{2 \times 10^7} K! \, (1-P(a))^K \sum_{n=0}^{4*} \frac{1}{n!} \left(\frac{1}{2 \times 10^7} \right)^{n+1} \sum_{m=o}^{K-n} \frac{P^m(a)}{m! \, (K-n-m)!}$$

(C-34)

Now

$$\max_{m=0, \ldots K-n} \frac{P^m(a)}{m! \, (K-n-m)!} \approx \frac{P^{(K-n)\frac{P(a)}{1+P(a)}}(a)}{\left(\frac{(K-n) \; P(a)}{(1+P(a))} \right)! \; \left(\frac{K-n}{1+P(a)} \right)!} \qquad \text{(C-35)}$$

Substituting (C-35) into (C-34) results in the following inequality

$$P(R(i)) \geq P_d^8 \sum_{K=1}^{2 \times 10^7} K! \, (1-P(a))^K \sum_{n=0}^{4*} \frac{1}{n!} \left(\frac{1}{2 \times 10^7} \right)^{n+1} \frac{P^{(K-n)\left(\frac{P(a)}{1+P(a)}\right)}(a)}{\left(\frac{(K-n) \; P(a)}{(1+P(a))} \right)! \; \left(\frac{K-n}{1+P(a)} \right)!} \qquad \text{(C-36)}$$

$$P(R(i) \geq P_d^8 \sum_{K=1}^{2 \times 10^7} (1-P(a))^K \sum_{n=0}^{4^*} \left(\frac{1}{2 \times 10^7}\right)^{n+1} P^{(K-n)\left(\frac{P(a)}{1+P(a)}\right)}_{(a)} \binom{K}{n} \binom{K-n}{\frac{K-n}{1+P(a)}}$$

(C-37)

$$P(R(i)) \geq P_d^8 \sum_{K=1}^{2 \times 10^7} (1-P(a))^K \frac{1}{2 \times 10^7} P^{K\left(\frac{P(a)}{1+P(a)}\right)}_{(a)} \binom{K-n}{\frac{K-n}{1+P(a)}} \qquad \text{(C-38)}$$

Applying Stirlings approximation to $\binom{K}{\frac{K}{1+P(a)}}$ one obtains from (C-38)

$$P(R(i)) \geq P_d^8 \sum_{K=1}^{2 \times 10^7} \frac{1}{2 \times 10^7} \, 2^{K\left(h\left(\frac{P(a)}{1+P(a)}, \frac{1}{1+P(a)}\right) + \frac{P(a)}{1+P(a)} \operatorname{Log} P(a) + \operatorname{Log}(1-P(a))\right)} \qquad \text{(C-39)}$$

where

$$h\left(\frac{P(a)}{1+P(a)}, \frac{1}{1+P(a)}\right) = -\frac{P(a)}{1+P(a)} \operatorname{Log}\left(\frac{P(a)}{1+P(a)}\right) - \frac{1}{1+P(a)} \operatorname{Log}\left(\frac{1}{1+P(a)}\right) \qquad \text{(C-40)}$$

(logarithms are to base 2)

Inequalities (C-39) and (C-40) yield the following lower bound to P(R(i)):

$$P(R(i)) \geq r \qquad \text{(C-41)}$$

where

$$r = P_d^8 \qquad \text{if } P(a) = 0$$

$$r = 0 \qquad \text{if } P(a) = 0$$

$$r = \frac{P_d^8}{2 \times 10^7} 2 \cdot \left(\frac{1 - 2^{2 \cdot 10^7 x}}{1 - 2^x} \right)$$

if $0 < P(a) < 1$

$$x = h\left(\frac{P(a)}{1+P(a)}, \frac{1}{1+P(a)}\right) + \frac{P(a)}{1+P(a)} \text{ Log } P(a) + \text{Log } (1-P(a)) \qquad \text{(C-42)}$$

Before continuing it is convenient at this point to further specify the parameters P(a). P(a) was specified by (C-25).

$$P(a) = \text{Prob}\left(\begin{matrix}\text{interference masquerades as a "}\underline{c}\text{" codeword at} \\ \text{specific time}\end{matrix}\right) \qquad \text{(C-25)}$$

There are two ways in which interference can masquerade as $\underline{c}$ codeword at a specific time. The first way is by direct noise excitation of the matched filter of the $\underline{c}$ codeword. Let the component of P(a) due to this be called P_1. The second way is by spurious pulses. Specifically, a codeword whose "A" pulse agrees with $\underline{c}$ is received at the ground station simultaneoulsy with codewords whose B, C, and D pulses agree with $\underline{C}$'s (however none of these codewords are a $\underline{c}$ codeword). Together these four pulses will appear as if a $\underline{c}$ codeword has appeared at this time at the ground station. Let the component of P(a) due to this be called P_2, One has

$$P(a) = P_1 + P_2 \tag{C-43}$$

Obviously,

$$P_1 = P_f^4 \tag{C-44}$$

Since, there are 12 possible "A" codewords, 12 possible "B" codewords, 12 possible "C" codewords, and 12 possible "D" codewords there are a total of $(12)^3 \times 10^2$ possible signatures which have the same "A" codeword as c. The factor of 10^2 comes from the 10^2 possible codeword repetition rates. Since only 10^5 of a total of 10^6 aircraft are in flight there are approximately $(12)^3 \times 10$ possible signatures in use which have the same "A" codeword as c. Since the repetition time of a signature is between 2 and 2.1 seconds and time is resolved in 100n sec. chips, the probability of one of this $(12)^3 \times 10$ possible signatures arriving at a specific time during a signature repetition interval is $\frac{(12)^3 \times 10}{2 \times 10^7}$

$$P_2 = \left(\frac{(12)^3 \times 10}{2 \times 10^7}\right)^4$$

$$P_2 = (5.6) \times 10^{-13} \tag{C-45}$$

Applying (C-44) and (C-45) to (C-43) yields

$$P(a) = P_f^4 + (5.6) \times 10^{-13} \tag{C-46}$$

P_f^4 will usually be much larger than 10^{-12}. For this reason P(a) and P_f^4 will be used interchangeably.

C.9.1.2 Time for Correct Completion of the Signature List

Consider one of the four Signature Lists on the initial compilation after system start-up. There are 10^5 entries on this Signature List which correspond to aircraft which are actually in the airspace. Of these 10^5 entries at least $r \times 10^5$ of them will have their initial time items correct. The remainder of them, which number at most $(1-r) \times 10^5$, will be filled incorrectly. This can be concluded from lower bound (C-41).

One question that arises immediately is the following. How manyTracker cycles ellapse before some fraction, g, of these 10^5 entries are filled with initial time items correct? Before this question can be answered two other questions must be considered.

First, consider those aircraft present in the airspace which are correctly entered on the Signature List during the first compilation. What is the rate at which these aircraft are dropped from the Signature List? In order for an aircraft to be dropped from the Signature List it must be absent from the tracking interval on three consecutive tracker cycles. The probability of this event is $(1-P_d)^3 (1-P_f^4)^{480}$. Thus, during the fourth tracker cycle of the $r \times 10^5$ correct entries made, on the average $r (1-P_d)^3 (1-P_f^4)^{480} \times 10^5$ will be erased from the Signature List. This will also occur on all subsequent tracker cycles.

Secondly, consider the drop out rate of those entries on the Signature List which really represent false alarms. In order for one of these entries to maintain itself on the Signature List it must be detected in at least one of the first three tracker cycles. The probability that this does not happen is $(1-P_f^4)^{480}$. This implies that during the fourth tracker cycle on the average $(1-P_f^4)^{480} (1-r)\, 10^5$ aircraft which were not entered correctly on the Signature List initially to be listed correctly on it during the fourth Tracker cycle. Utilizing lower bound, (C-41), $r (1-P_f^4)^{480} (1-r)\, 10^5$ of these aircraft will be correctly listed on the Signature List. Therefore, at the end of 4 tracker cycles on the average

$$10^5 \left(r + r(1-P_f^4)^{480} (1-r) - r (1-P_d)^3 (1-P_f^4)^{480}\right) \tag{C-47}$$

of the 10^5 aircraft in the airspace will be entered on the Signature List with initial time slot entry correct.

Let g_1 be the quantity in parenthesis in (C-47). The procedure just described generates an algorithm.

During the 8^{th} Tracker cycle on the average

$$10^5 \left(g_1 + g_1 (1-P_f^4)^{480} (1-g_1) - 3g_1 (1-P_d^3)(1-P_f^4)^{480}\right) \tag{C-48}$$

of the 10^5 aircraft in the airspace will be entered on the Signature List with initial time slot entry correct. Let the quantity in parenthesis in (C-42) be g_2. Replace g_1 in (C-48) by g_2, the resulting value of (C-48) is the number of the 10^5 aircraft in the airspace which will be correctly entered on the Signature List with initial time slot entry correct at the end of 12 tracker cycles. Continuing on in this manner it is possible to compute the number of Tracker cycles until $g \times 10^5$ entries of the Signature List are entered correctly.

C.9.2 Probability of Two Successive Correct Detections

Consider aircraft "i," some aircraft which is actually in the airspace. Assume that aircraft "i" is correctly detected on one tracker cycle, its position being correctly logged at the central surveillance station. Let us ask with what probability will aircraft "i" be correctly detected on the next tracker cycle. Let $P_d(i|i-1)$ be this probability. We shall close this section with the derivation of a lower bound to $P_d(i|i-1)$.

If aircraft i is detected correctly on one tracker cycle, it will be detected correctly on the next cycle if it is just tracked correctly during the next cycle. Using this, the following inequality can be written down

$$P_d\,(i|i\text{-}1) \geq P_d^{16}\,(1-P_f^4)^{320} \qquad \text{(C-49)}$$

This is the desired lower bound. Let us call the right hand side of (C-49) $P_d^L\,(i|i\text{-}1)$. We have then

$$P_d(i|i\text{-}1) \geq P_d^L\,(i|i\text{-}1)$$

$$P_d^L\,(i|i\text{-}1) = P_d^{16}(1-P_f^4)^{320} \qquad \text{(C-49a)}$$

C.10 VSRR System Power Budget

A power budget for the VSRR system is given in Table 2.1. The power budget takes into account both Thermal Noise and Multiple Access Noise. Multiple Access Noise is the interference at the output of a matched filter due to the reception of aircraft codewords which are not matched to it. The power budget just takes into account the Air-to-Satellite uplink. The satellite-to-ground downlink is assumed noiseless.

C.11 VSRR Performance Table

In the previous sections bounds to the performance measures of the VSRR system have been derived. These bounds are summarized by inequalities (C-20a), (C-41), Section C.9.1.2 and inequality (C-49a). They will be evaluated for three values of the pair; P_f/P_d. Remember P_f and P_d are respectively the per pulse false alarm and detection probabilities. The pair values, P_f/P_d, chose are all achievable for the VSRR Effective Signal to Noise ratio of 9 db which was derived in the previous section. The evaluation of just the two bounds, (C-20a) and C-49a), gives a fair description of the system performance.

The evaluation of the system performance bounds is given in the following VSRR Performance Table. As is evident from the table with P_f/P_d = 0.05/ 0.965. The system has an extremely good false alarm performance, but an intolerable detection performance. As P_f increases to 0.1 and P_d increases to 0.98 the false alarm performance is still adequate. However, the detection performance, while improved, is still unacceptable. As P_f increases further both the false alarm and detection capabilities degenerate.

An optimum surveillance system should operate with the system detection probability as a monotonically <u>increasing</u> function of the average number of false alarms. If this is true, then one can trade detection performance for false alarm performance and vice-versa. As is evident from Table C.1, the VSRR system does not have this performance. In the range in which the average number of false alarms is small the detection performance does improve when the false alarm tolerance is increased. However, a peak is soon reached. When the system allows larger and larger numbers of false alarms, the detection performance decreases rather than increases. Thus, the VSRR system is extremely sensitive to large numbers of false alarms and its performance degenerates because of them. This is understandable. If a large number of false alarms is tolerated the Tracker will soon lose track of a true aircraft and detection errors will occur. Since, only one listing of an aircraft occurs on the Signature List, a high pulse detection probability will not even improve the system detection probability in this case.

In comparing the VSRR system to the FSRR system (analyzed in Appendix B), one cannot report favorably on one system relative to the other. A E/No = 9db the VSRR system has a low false alarm rate at least for P_f = 0.1. FSRR had a very high false alarm rate not only for P_f=0.2 and 0.3, but also for P_f=0.1. On the other hand the detection probabilities of the FSRR system while not extraordinarily good were better than that achieved by a VSRR.

TABLE C.1

VSRR SYSTEM PERFORMANCE TABLE

P_f	P_d	$\overline{N_f}^u$	$P_d^L(i\|i-1)$
0.005	0.965	75.5×10^{-4}	0.565
0.1	0.98	31	0.7
0.15	0.985	3.98×10^{3}	0.665
0.2	0.99	1.271×10^{5}	0.505
0.3	0.995	1.630×10^{7}	0.069

APPENDIX D

SATELLITE CONSTELLATIONS FOR MULTILATERATION SURVEILLANCE SYSTEMS

The performance of an aircraft surveillance or navigation system employing satellite multilateration depends to a large extent on the satellite constellation. In this Appendix we present two constellation candidates, each consisting of twelve satellites. These can provide surveillance coverage of the continental U.S. via an aircraft-to-satellite-to-ground system. A first order analysis of the geometric dilution (ratio of rms aircraft positioning errors to rms range signal timing errors) that may be expected from these constellations is also presented.

The aircraft-to-satellite-to-ground surveillance systems under consideration are of the hyperbolic ranging type. That is, comparison of the times-of-arrival at two satellites, of a signal emitted from the aircraft, determines the location of the aircraft on some hyperbolic surface. Three such hyperbolic surfaces, determined by three pairs of satellites, intersect at two points. Of these two points the one which is closer to the earth determines the aircraft position. To locate an aircraft with this method it is necessary to have three independent pairs of satellites. Thus, a minimum of four satellites is required. If more than four satellites are available, they all may be utilized with a resultant decrease in the aircraft positioning error.

Two factors determine the number of satellites that may be used in locating an aircraft: the density of satellites in the constellation, and the size of the solid angle that is illuminated by the aircraft transmitting antenna. The latter of these is determined by the aircraft antenna pattern, which may be assumed to illuminate a cone of half-angle 75°. However, as the aircraft may bank as much as 30° in any direction, the region of space that is consistently illuminated is a cone with a vertical axis and a half-angle of 45^{o}.

The basic requirement, therefore, is that at any point in the continental U.S. there must be at least four satellites at elevations of 45^{o} or more. The constellations presented in this appendix have been designed so that at least five satellites are at elevations greater than 45^{o}. The additional satellites provide an increase in surveillance accuracy and provide backup satellites in case of a failure.*

D.1 Satellite Equations of Motion

The satellite position in its orbital plane may be specified (see Fig. D.1) by the radius r (from the center of the earth) and the angle V, known as the true anomaly, measured from the perigee[1]:

$$r(t) = R(1 - e \cos E(t)) \tag{D-1}$$

$$V(t) = \cos^{-1}\left(\frac{\cos E(t) - e}{1 - e \cos E(t)}\right) \tag{D-2}$$

In the above, R is the semimajor axis (about 26,000 miles for a synchronous orbit), e is the eccentricity of the orbit, and E(t) is the eccentric anomaly which satisfies the functional equation

$$E(t) - e \sin(E(t)) = \frac{2\pi t}{T} \tag{D-3}$$

where T is the period the orbit. Both V(t) and E(t) are measured in radians. Passage through the perigee occurs at times $t = 0, \pm T, \pm 2T, \ldots$

It should be observed that E(t), and thus also V(t), increases most rapidly at the perigee, and least rapidly at the apogee. Thus, if the perigee is positioned above a point in the southern hemisphere, the satellite will spend a greater percentage of its time over the northern hemisphere than

*If the satellites were to be used in a satellite-to-air-to-ground system, one would require four satellites (plus a spare) to be at elevations greater than 35^{o}. Clearly the constellations described herein satisfy this condition.

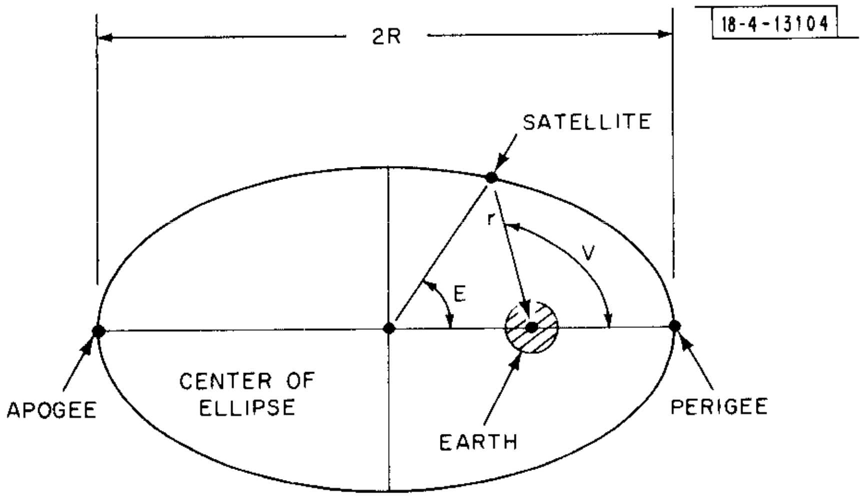

Fig. D. 1. Orbital geometry.

over the southern hemisphere. This characteristic is desirable for coverage of the U.S., and becomes more pronounced as the eccentricity e increases.

A visual aid to the analysis of a particular satellite constellation is the set of ground tracks of the satellite orbits, i.e., the latitudes and longitudes of the sub-satellite points as functions of time. If a satellite is in synchronous orbit with the sub-perigee point at the southernmost point of the ground track, then the latitude $\lambda(t)$ and the west longitude $\gamma(t)$ of the sub-satellite point can be shown to be

$$\lambda(t) = -\frac{180}{\pi}\sin^{-1}(\sin i \cos V(t)) \qquad \text{(D-4)}$$

$$\gamma(t) = \Gamma_o + 15t - \frac{180}{\pi}\tan^{-1}(\sec i \tan V(t)) \qquad \text{(D-5)}$$

In the above Γ_o is the west longitude of the sub-perigee point and i is the inclination of the orbit, i.e., the angle between the angular momentum vectors of the satellite and the earth (with respect to the earth's center). Γ_o, $\lambda(t)$, and $\gamma(t)$ are measured in degrees; i, in radians; and t, in hours. It is assumed that $0 \leq i \leq \pi/2$, i.e., that the satellite is in a posigrade orbit.

From the above expressions it is clear that the maximum and minimum latitudes of the ground track are $\frac{180i}{\pi}$ and $-\frac{180i}{\pi}$, respectively; that is, the orbital inclination determines the "length" of the ground track. Similarly, it can be shown from Eqs. (D-2), (D-3), and (D-5) that the eccentricity of the orbit roughly determines the "width" of the ground track. If Γ_e denotes the longitude at which the ground track crosses the equator from south to north, then a measure of the width of the ground track is $2(\Gamma_o - \Gamma_e)$ (For orbits of very low eccentricity, $2(\Gamma_o - \Gamma_e)$ can be very much less than the actual ground track width). The relation between e and $(\Gamma_o - \Gamma_e)$ is given in Figure D.2. From this figure it is seen that the eccentricity needed to produce a given value of $(\Gamma_o - \Gamma_e)$ is approximately

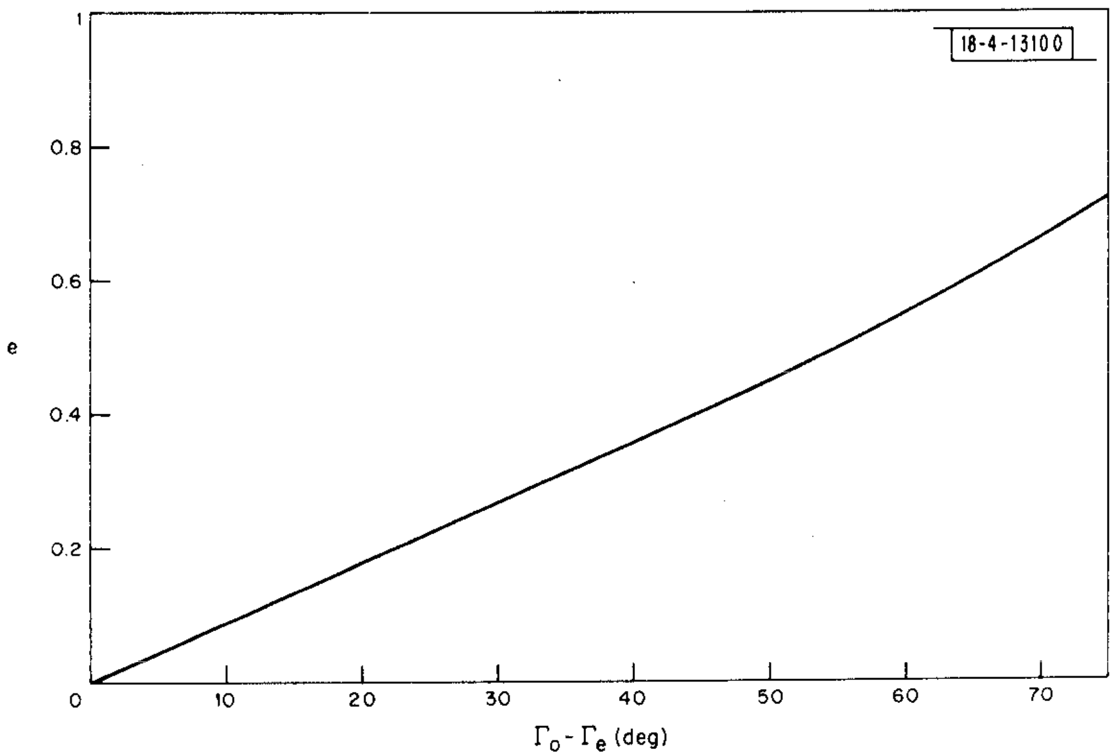

Fig. D. 2. Eccentricity vs the longitudinal difference between the subapogee point and the equatorial crossing.

$$e \cong 8.08 \times 10^{-3} (\Gamma_o - \Gamma_e) + 2.10 \times 10^{-5} (\Gamma_o - \Gamma_e)^2$$

As has been previously stated, the required objective is to have at least five satellites at elevations of 45° or more at each point in the continental U.S. at all times. If the aircraft is at latitude λ_a and west longitude γ_a, then satellite k, at latitude λ_k, west longitude γ_k, and radius r_k, is at elevation α_k, where

$$\cos \alpha_k = r_k \left[\frac{1 - (\cos \lambda_a \cos \lambda_k \cos(\gamma_a - \gamma_k) + \sin \lambda_a \sin \lambda_k)^2}{1 + r_k^2 - 2 r_k (\cos \lambda_a \cos \lambda_k \cos(\gamma_a - \gamma_k) + \sin \lambda_a \sin \lambda_k} \right]^{1/2}$$

In the above, r_k is measured in earth radii (R in Eq. (1) equals 6.6166 earth radii). Thus, in order for the angle of elevation of satellite k, as seen from the aircraft, to be 45° or more, it is necessary that

$$r_k^2 - 2(r_k \cos \Delta_k - \frac{1}{2})^2 < \frac{1}{2} \qquad \text{(D-6)}$$

The angle Δ_k is given by

$$\Delta_k = \cos^{-1}(\cos \lambda_a \cos \lambda_k \cos(\gamma_a - \gamma_k) + \sin \lambda_a \sin \lambda_k) \qquad \text{(D-7)}$$

and is equal to the arc of a great circle connecting the aircraft and the sub-satellite point.

Given a satellite constellation, Eqs. (D-1), (D-2), (D-4), (D-5), (D-6), and (D-7) may be used to determine which of the satellites are at elevations 45° or more as seen from a particular location (λ_a, γ_a) at a particular time t.

D.2 Orbit Stability

Unfortunately, it is not possible to design a synchronous orbit with a perfectly stable ground track, i.e., a ground track that remains constant over a period of several years. The sources of orbit instabilities are celestial bodies such as the sun and the moon, and perturbations in the earth's gravitational field due to bulges, principally at the equator. The orbit perturbations due to the sun and the moon are quite small, and are periodic with periods of 180 days and 14 days, respectively;[2] these perturbations are not bothersome. The orbit perturbations due to the earth's bulge, on the other hand, can produce gross shifts of the ground track over a period of years.

The two main effects of the equatorial bulge on a satellite orbit are[3] a slow precession of the orbit angular momentum vector about the earth's axis, and a gradual rotation of the perigee position in the (precessing) orbital plane. The result of the precession is that the longitude of the subperigee point increases at a rate of

$$\dot{\Gamma}_o \cong 1.34 \times 10^{-2} \frac{\cos i}{(1 - e^2)^2} \text{ degrees/day}$$

where i is the orbit inclination, and e, the eccentricity. The position of the perigee rotates in the orbital plane at a rate of

$$.67 \times 10^{-2} \frac{(5 \cos^2 i - 1)}{(1 - e^2)^2} \text{ degrees/day} \qquad \text{(D-8)}$$

The following observations can now be made. First, for both circular orbits (with e = 0) and eccentric orbits the effect of the precession on the ground track can be exactly cancelled simply by slightly decreasing the period of the orbit, i.e., by decreasing the satellite altitude. Secondly, the effect of perigee rotation on a circular orbit simply introduces a slowly time varying time delay in the ground track; but since the ground track is symmetric, this is not bothersome. Finally, for an eccentric orbit, the perigee rotation would eventually bring the sub-perigee point to the northern hemisphere, which is undesirable. However, from Eq. (D-8) it is clear that when the inclination is

$$i = \cos^{-1}\left(\frac{1}{\sqrt{5}}\right) = 1.107 \text{ radians} = 63.4 \text{ degrees}$$

then this perigee rotation effect is nonexistent.

In summary, synchronous orbits with good stability, and thus of use to a surveillance system, are (1) circular orbits of any inclination, and (2) eccentric orbits of inclination 63.4°.

D.3 Doppler Shifts Introduced by Satellite Motion

If the aircraft transmits at a center frequency f_o, then the frequency of the signal received by a satellite is

$$f_o\left(1 - \frac{\underline{u}'\underline{v}}{c}\right)$$

where $\underline{u}$ is the unit vector pointing from the aircraft to the satellite, $\underline{v}$ is the velocity of the satellite relative to the aircraft, and c is the speed of light. The portion of the frequency shift due to aircraft motion is bounded by $10^{-6}f_o$; it would be desirable if the portion due to satellite motion were of comparable size. While such is not the case for a highly eccentric orbit, it can be shown that the frequency shifts from all aircraft whose antennas illuminate the satellite fall in an interval of length comparable to $10^{-6}f_o$. The satellite may then compensate for an average Doppler shift.

If the aircraft were at the subsatellite point, it can be easily shown that

$$\underline{u}'\underline{v} = \frac{2\pi R}{T} \frac{e \sin E(t)}{1 - e \cos E(t)}$$

The maximum value of this quantity occurs when $\cos E(t) = e$ (or, equivalently when $\cos V(t) = 0$) and is

$$(\underline{u}'\underline{v})_{max} \cong 10^4 \frac{e}{\sqrt{1 - e^2}} \text{ feet/sec}$$

Thus the Doppler shift, due to satellite motion, at the sub-satellite point is bounded by

$$\left| f_o \frac{\underline{u}'\underline{v}}{c} \right| \le 10^{-5} \frac{e}{\sqrt{1 - e^2}} f_o$$

For an eccentricity of 0.6 this Doppler shift is $7.5 \times 10^{-6} f_o$.

The satellite can be designed to compensate for the Doppler shift due to an aircraft transmitting from the sub-satellite point. Thus, what is of interest is the additional Doppler shift that results when the aircraft is not at the sub-satellite point. This can be bounded as follows. The quantity $\underline{u}'\underline{v}$ is given by

$$\underline{u}'\underline{v} = ||\underline{v}|| \cos\theta$$

where θ is the angle between $\underline{u}$ and $\underline{v}$, and has some nominal value θ_o at the sub-satellite point. The value of θ differs most from θ_o when the aircraft is a distance from the sub-satellite point such that the elevation of the satellite is 45^o. If this distance corresponds to an arc length Δ of a great circle, then it follows that

$$|\theta - \theta_o| \leq 45^o - \Delta$$

The value of Δ is about 38.9° when the satellite crosses the minor axis of the orbit, and is slightly larger at the apogee, and slightly smaller at the perigee. Thus, the maximum deviation of θ from θ_o is approximately

$$|\theta - \theta_o|_{max} \cong 6.1^o$$

Thus $|\cos\theta - \theta_o|$ can be approximately bounded as

$$|\cos\theta - \cos\theta_o| = |\cos\theta_o \cos(\theta - \theta_o) - \sin\theta_o \sin(\theta - \theta_o) - \cos\theta_o|$$

$$< |\sin\theta_o \sin(6.1^o)|$$

$$< .11$$

It follows that

$$|\underline{u}'\underline{v} - \|\underline{v}\| \cos\theta_o| < .11 \|\underline{v}\|$$

The magnitude of the satellite velocity in the northern hemisphere is bounded by

$$\|\underline{v}\| < 10^4 \sqrt{\frac{1 + e^2}{1 - e^2}} \text{ feet/sec}$$

and at the apogee it is only

$$\|\underline{v}\| \cong 10^4 \frac{\sqrt{1 - e^2}}{1 + e} \text{ feet/sec}$$

Thus, the Doppler shift differs from its nominal value by an amount which is bounded by

$$1.6 \times 10^{-6} f_o$$

throughout the northern hemisphere, and by

$$0.55 \times 10^{-6} f_o$$

in the vicinity of the apogee, when the eccentricity is 0.6. As e decreases, the northern hemisphere bound decreases, although the bound near the apogee increases.

D. 4 The Satellite Constellation Candidates

In this section are presented the two constellation candidates. Both constellations have good orbit stability and acceptable Doppler shift characteristics. The geometric dilution, i.e., the factor by which timing errors are multiplied to produce errors in estimating the aircraft position, of both constellations is about one order of magnitude. However, if a vital satellite becomes inoperative, the geometric dilution in some regions of the U.S. can increase by an additional order of magnitude.

The two constellations are depicted in Figs. D. 3 and D. 4. In each of these figures the sub-satellite points at time t = 0 are indicated by triangles. The dots on these figures indicate the sub-satellite points at intervals of one hour. It should be noted that the period of constellation 1 is four hours, and that the period of constellation 2 is eight hours.

Constellation 1, shown in Fig. D. 3, consists of 12 satellites, each of which is in an orbit of eccentricity .4 and inclination 63.4°. It should be noted that no two of these satellites are in the same orbital plane, although for each satellite there corresponds another satellite for which the orbital plane differs by only 5°.

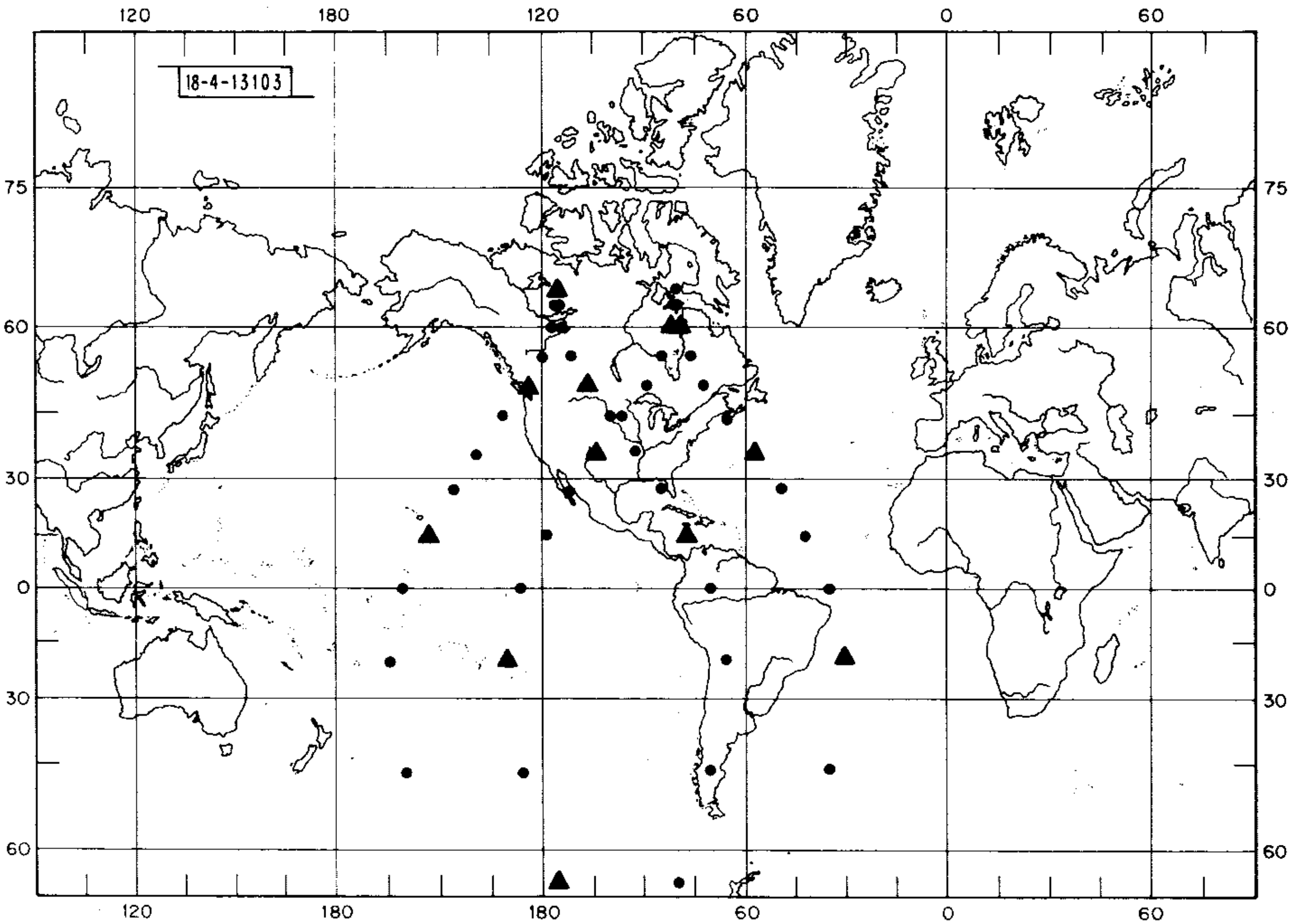

Fig. D. 3. Satellite constellation 1.

Constellation 2 depicted in Fig. D.4, consists of 12 satellites, six of which are in orbits of eccentricity .6 and inclination 63.4°, with the remaining six being in circular orbits of inclination 35°. As in constellation 1, no two satellites are in the same orbital plane.

A limited analysis of the geometric dilution* resulting from these constellations has been performed as follows. A hypothetical aircraft was located at latitude 45°, west longitude 120°. Then, at hourly intervals, the geometric dilution was found, first using all the satellites at elevation 45° or more, and then deleting from this set of satellites that one which was thought to have the most effect on the geometric dilution. The results for constellation 1 are shown in Table D.1; those for constellation 2 are shown in Table D.2. As is evident from these results, the geometric dilution for both constellations is quite sensitive to the loss of a vital satellite.**

These two satellite constellations represent only a first order attempt at the design of an efficient constellation with good geometric dilution. There appears to be no method, other than trial and error, for arriving at a satellite constellation that is sufficiently stable and posesses good geometric dilution properties with relatively few satellites.

---

*See Appendix I for the method of calculating geometric dilutions and some remarks on the geometric dilutions that can be attained with four satellites.

**If the satellites were to be used in a satellite-to-air-to-ground system, smaller geometric dilutions could be obtained from each of these constellations. This is because a 55° half-angle cone encompasses more satellites giving better coverage than does a 45° half-angle cone.

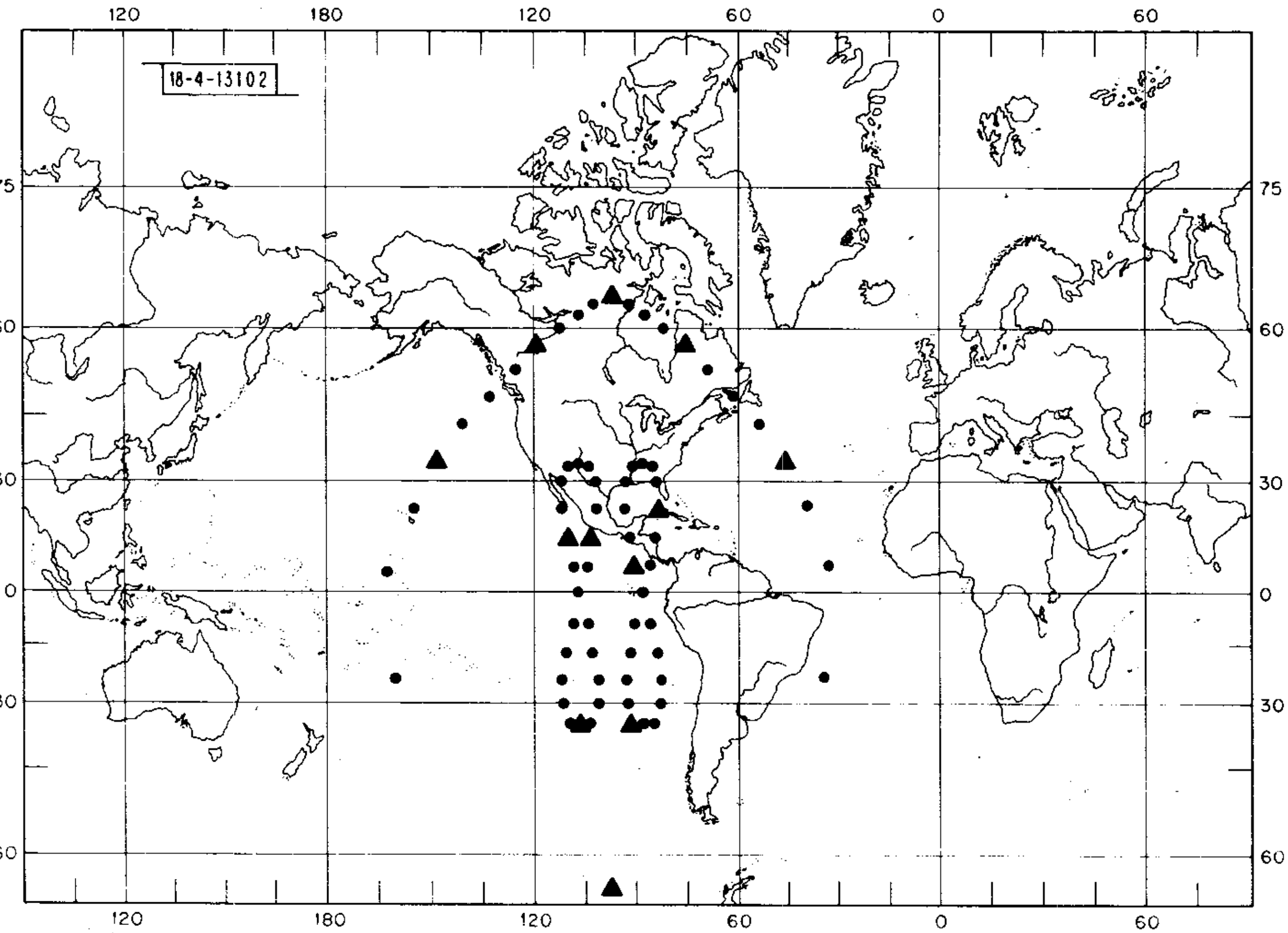

Fig. D.4. Satellite constellation 2.

TABLE D.1

GEOMETRIC DILUTION WITH CONSTELLATION 1 AND AIRCRAFT AT LATITUDE 45°, LONGITUDE 120°

Time	Satellite	Lat.	Long.	Geometric Dilution with all satellites	Geometric Dilution without satellite 1
t = 0	1	14.9	152.7	5.4	30.4
	2	51.0	123.2		
	3	63.4	115.0		
	4	51.0	106.8		
	5	36.6	101.8		
	6	60.1	80.5		
	7	60.1	79.5		
t = 1	1	27.0	109.8	17.9	18.2
	2	44.5	129.5		
	3	62.6	114.6		
	4	56.2	111.6		
	5	27.0	85.3		
	6	44.5	65.5		
	7	62.6	80.4		
	8	56.2	83.4		
t = 2	1	14.9	117.7	8.9	11.9
	2	36.6	93.2		
	3	36.6	136.8		
	4	60.1	114.5		
	5	60.1	115.5		
	6	63.4	80.0		
	7	51.0	71.8		
	8	51.0	88.2		
t = 3	1	27.0	144.8	7.6	278.5
	2	56.2	118.4		
	3	62.6	115.4		
	4	44.5	100.5		
	5	44.5	94.5		
	6	62.6	79.6		
	7	56.2	76.6		

TABLE D.2

GEOMETRIC DILUTION WITH CONSTELLATION 2 AND AIRCRAFT AT LATITUDE 45°, LONGITUDE 120°

Time	Satellite	Lat.	Long.	Geometric Dilution with all satellites	Geometric Dilution without satellite 1
t = 0	1	35.3	148.2	11.0	45.0
	2	16.7	111.7		
	3	16.7	102.3		
	4	23.9	82.3		
	5	57.3	118.6		
	6	63.4	97.5		
	7	57.3	76.4		
t = 1	1	24.2	155.5	5.8	13.3
	2	53.7	125.4		
	3	63.0	102.1		
	4	60.0	82.5		
	5	8.5	104.4		
	6	16.7	92.7		
	7	23.9	112.7		
t = 2	1	49.1	132.8	19.1	63.7
	2	29.8	112.2		
	3	61.9	107.0		
	4	61.9	88.0		
	5	23.9	93.7		
	6	49.1	62.2		
t = 3	1	43.2	141.5	12.7	200.7
	2	60.0	112.5		
	3	63.0	92.9		
	4	53.7	69.6		
	5	29.8	93.2		
	6	33.6	110.1		

REFERENCES

1. Dubyago, A. D., The Determination of Orbits, MacMillan, 1961, (Ch. 2).

2. Cook, G. E. and Scott, D. W., "Lifetime of Satellites in Large-Eccentricity Orbits", Planetary Space Science, Vol. 15, p. 1552, Pergeman Press.

3. Shapiro, I. I., Jones, H. M., and Perkins, C. W., "Orbital Properties of the Westford Dipole Belt", Proc. of IEEE, Vol. 52, 5, p. 472, (May 1964).

APPENDIX E

OPERATION AND PERFORMANCE OF THE AIR-TO-GROUND COMMUNICATION LINK IN THE SATELLITE-TO-AIR-TO GROUND SURVEILLANCE SYSTEM

E.1 Preliminaries

In this Appendix the Air-to-Ground link of the Satellite-to-Air-to-Ground Surveillance System is considered. Its mode of operation is described and its performance is analyzed. Computations will show that such a link is indeed feasible.

It is assumed that there is a population of 10^6 aircraft. Each aircraft is assigned a unique integer from 1 to 10^6 called its identification number.

A satellite constellation consisting of four satellites transmits four pulse trains (one from each satellite) to each aircraft. The pulse period in each of the pulse trains is of the order of a few milliseconds.

Calling the satellites: Sat 1, Sat 2, Sat 3, Sat 4, each aircraft can successively decode each set of four corresponding pulse trains (one from each of the satellites) that it receives, and can then compute three independent time differences:

$$\Delta_{12} = t_1 - t_2,$$

$$\Delta_{23} = t_1 - t_3,$$

$$\Delta_{34} = t_1 - t_4,$$

where

t_1 = time aircraft receives pulse train from Sat 1,

t_2 = time aircraft receives corresponding pulse train from Sat 2,

t_3 = time aircraft receives corresponding pulse train from Sat 3,

t_4 = time aircraft receives corresponding pulse train from Sat 4.

Consider aircraft "j". In a surveillance system this aircraft must relay the values of Δ_{12}, Δ_{23}, Δ_{34} to the ground. Knowing these values from aircraft "j" and the satellite constellation ephermeris data, the ground station can then compute the position of aircraft "j" by the method of hyperboloids. The results of such position calculations then provide the surveillance data base for ground based ATC functions. As another option, the computation of the aircraft position could take place on the aircraft itself, with the computed position subsequently relayed to the ground. However, it will be assumed, for the present, in the analysis performed here that the position calculation takes place on the ground.

E.2 Structure of the Aircraft Position Data

Each aircraft wishes to convey to the ground station four items of information: its identification number and the values of Δ_{12}, Δ_{23}, Δ_{34}. In order to accomplish this it will transmit a codeword to the ground and have the ground terminal compute these items from the codeword. This codeword will only be transmitted when requested by the ground station. The requesting or interrogation procedure will be discussed in a later section. Since the set (Δ_{12}, Δ_{23}, Δ_{34}) is changing with each new set of pulses received from the satellite constellation, the downlink codeword which is kept ready to be transmitted when the aircraft is interrogated, will have to be recomputed or updated every second. In this section, the structure of this codeword will be described.

The Air-to-Ground downlink will transmit the aircraft codewords using a very basic modulation format called, "ON-OFF Keying". In this modulation format a binary digit "1" is transmitted by sending a pulse having a duration of 0.5μ sec. A binary digit "0" is transmitted by having the channel quiet (not transmitting anything) for 0.5μ sec.

The downlink codeword must contain the identification number of the aircraft. This can be represented by a block of binary digits giving the expansion to base 2 of this identification number. Since the identification number is some integer from 1 to 10^6, a block of 20 binary digits will suffice to represent it.

The downlink codeword must also contain the values of the time difference, Δ_{12}, Δ_{23}, Δ_{34}. Due to the geometry of the satellite constellation, the maximum value that either Δ_{12}, Δ_{23}, Δ_{34}, can have is 16 milliseconds. These time differences will be quantized in steps of 25 nano-seconds. Thus, they can be transmitted to the ground by transmitting the integers; $\Delta_{12}/25 \times 10^{-9}$, $\Delta_{23}/25 \times 10^{-9}$, $\Delta_{34}/25 \times 10^{-9}$. These integers in turn can be represented in the downlink codeword by a binary sequence giving their expansion to base 2. Since the maximum value of Δ is 16×10^{-3}, a block of 20 binary digits will suffice to represent the integer $\Delta/25 \times 10^{-9}$.

The previous data computations and modulation description serve as arguments for the following description of the aircraft downlink codeword structure.

Each aircraft codeword consists of 90 binary digits. The first 10 binary digits in the codeword are ten "1's". This is synchronization prefix necessary because of the "ON-OFF Keying" modulation used. The receiver has to be able to discern where each codeword begins. Since absence of any pulse in the channel is used to represent a "0," the receiver has to be able to decide when the channel is truely quiet due to the absence of a codeword in it, and when the channel is quiet due to a "0" being transmitted. This initial synchronization prefix will allow this discernment. The next block of 20 digits is the expansion to base 2 of the aircraft identification number. The remaining 3 successive blocks of 20 digits are, respectively, the expansions to base 2 of Δ_{12}, Δ_{23}, Δ_{34}.

It has already been stated that each codeword will be transmitted only upon request from the ground. Each codeword will be recomputed or updated as each successive set of Δ's, (Δ_{12}, Δ_{23}, Δ_{34}) is generated.

E. 3 Structure of the Ground Based Portion of the Surveillance System

Each aircraft in flight will be interrogated from the ground and in turn will transmit its codeword to the ground. In order to accomplish this two-way task, the ground network must be organized in some type of order. In this section the geometry of the ground portion of the Air-to-Ground link will be described in detail.

The ground network will operate by covering the entire CONUS (continental United States) with discs having a 200 mile radius. At the center of each disc will be a ground station. There will be ground communications between the ground stations (for instance, by telephone).

Each ground station will be responsible for maintaining the surveillance function and providing navigation aid to all aircraft (of which it has knowledge) which lie within the 200 mile radius hemisphere centered at the ground control station.

In order to provide an aid to the interrogation of all the aircraft positioned within each hemisphere, it is necessary to put some fine structure on the geometry of each hemisphere. This will now be done.

Consider a specific 200 mile radius hemisphere. It is first subdivided by 200 equally spaced concentric hemispherical shells centered at the ground station. Thus, the shells will be spaced 1 mile apart. Let the volumes created between the successive shells (also between the outer hemispherical surface and the largest shell, and the small shell and the ground control station disc) be called "regions." Consider these regions ordered from 1 to 200 with region 1 being bounded by the ground station disc and the smallest hemispherical shell, region 2 being bounded by the smallest hemispherical shell and the next smallest hemispherical shell, ... etc. The subdivision of the hemisphere by shells is illustrated in Figure E.1 and Figure E.2.

Each of the regions subdividing the hemisphere can be further subdivided. Consider a particular region and consider a cross section of it taken perpendicular to the disc. The cross section is shown in Figure. E.3. From the projection of the ground station shown in Figure E.3, let rays be extended intersecting both surfaces of the region cross section. Let the rays be equally spaced around the cross section every 6^{o} with the ray being extended along the disc. This situation is illustrated in Figure E.4 which shows that the intersection of 2 consecutive rays with the region cross section produces a curvilinear quadralateral shown darkened in Figure E.4. When this curvilinear quadralateral is rotated through all of the cross sections of the region perpendicular to the disc, it produces a ring which is 1 mile deep and 6^{o} thick. Thus, the region can be divided into rings. There will be 15 rings to a region. Assume these are ordered with ring "1" being that ring closest to the "disc end" of the region, ring 2 next closest, etc.

Each ring can be further divided into cells. Consider a specific ring. Both the outer and inner base paremeters of the ring are circles. This is evident from the top view of the ring shown in Figure E.5. Let radial lines or rays drawn from the common center of these circles intersect the circles at 1^{o} intervals. The result is illustrated in Figure E.6. Let these rays be moved through entire thickness of the ring. In other words, let each ray generate a plane which is perpendicular to the base of the ring. The intersection of the resultant planes with the ring subdivides the ring into units which we shall call cells. These cells are 1^{o} wide, 6^{o} deep and 1 mile long.

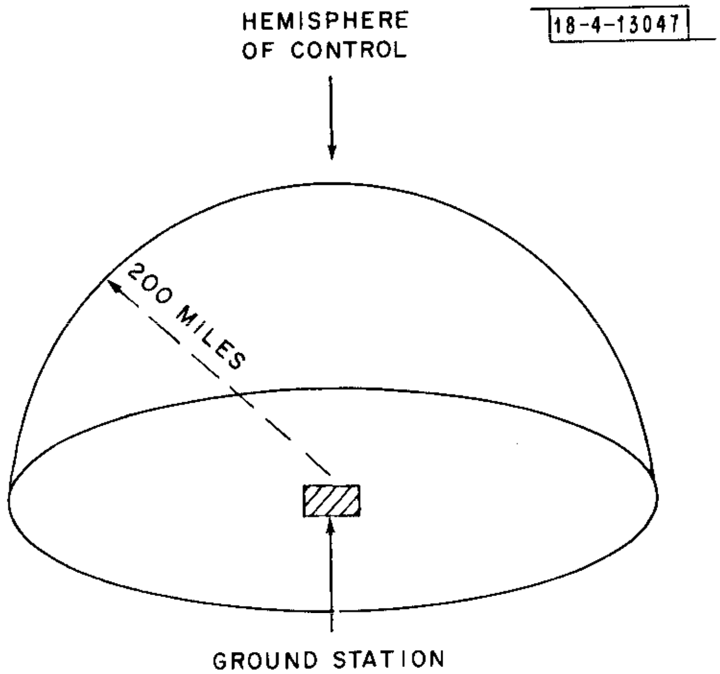

Fig. E.1. Ground station and hemisphere of control.

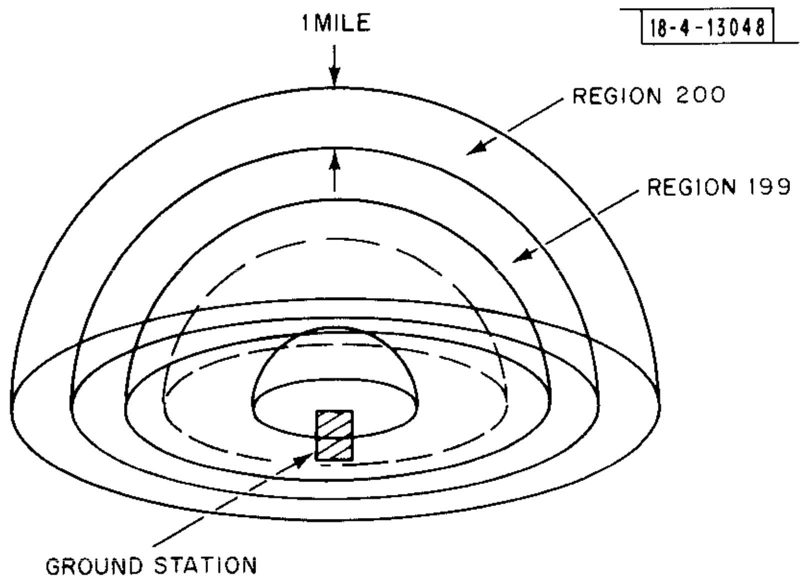

Fig. E.2. Subdivision of hemisphere of control into regions.

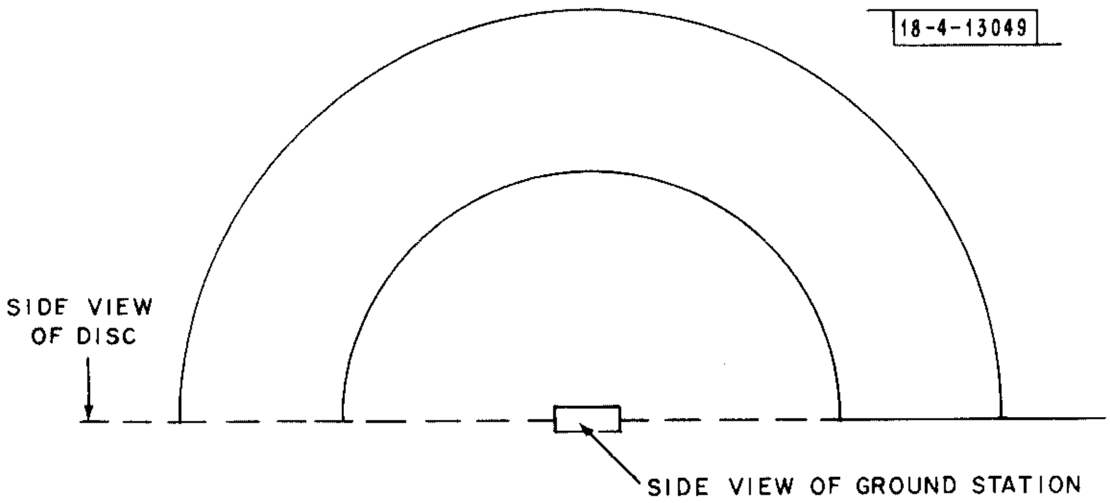

Fig. E.3. Cross section of a region.

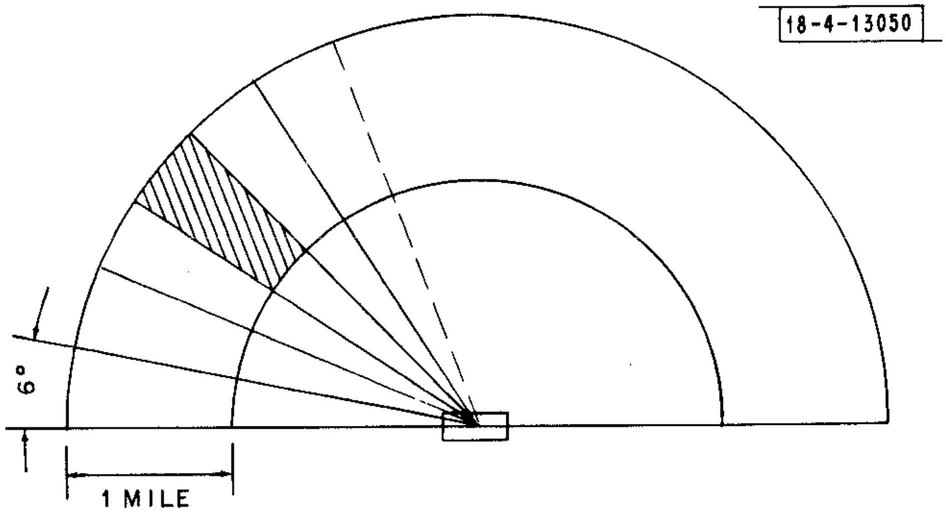

Fig. E.4. Subdivision of region cross section by rays.

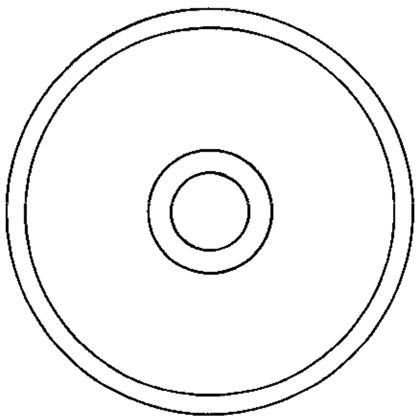

Fig. E.5. Top view of a ring.

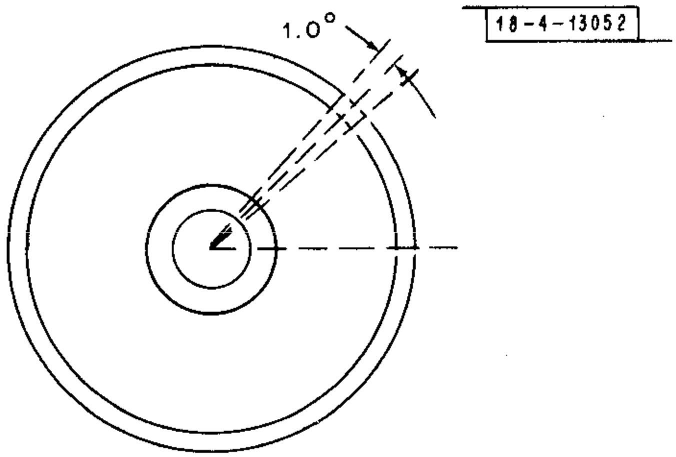

Fig. E.6. Ring being divided into cells.

Assume they are ordered from 1 to 360 in some manner. The subdivision of a ring into cells by the rays mentioned is illustrated in Figure E. 6.

Having introduced the geometric figures of "region," "ring," and "cell," we can now quantize the position of each aircraft in the hemisphere of control into the triplet

$$\underline{P} = (P_1, P_2, P_3)$$

where

P_1 = region aircraft lies in

P_2 = ring of the region aircraft lies in

P_3 = cell of the ring of the region aircraft lies in.

It should be emphasized that $\underline{P}$ is not the true position of the aircraft, but just a quantization of it. Hence, more than 1 aircraft might have the same value of $\underline{P}$. It should also be noted that many of the discs covering the CONUS may intersect, so each aircraft may lie in the hemisphere of control of several different ground stations. In maintaining a surveillance function this causes no additional procedures to be developed. In maintaining a navigation function, one of these ground control stations will have to exert final authority based on some predetermined rule.

E. 4 Communications and Data Management

In the past two sections consideration has been given to both the structure of the codeword that the aircraft will transmit to the ground when interrogated and the structure of the airspace under the responsibility of each ground station. This has all been a prelude to the discussion of this section, which will deal with the actual operation of the Air-to-Ground Link. Consider a specific ground station and the hemisphere of its responsibility. Every 2. 5

seconds this ground station will begin an "Interrogation-Reception-Logging Cycle". In this section, the procedure during such a cycle will be described in detail.

At the beginning of the cycle, the ground station consults a list which has on it all of the aircraft in the hemisphere of the ground station (known to the ground station) and also the aircraft positions during the previous 2 1/2 second cycle stored in terms of the P triplet. The list is called the "Interrogation List".

There are three possible reasons for an aircraft being on this list at the beginning of the cycle.

1. It could have been on the list at the previous cycle and not have been erased from the list during that cycle (reasons for erasure will be taken up later).
2. It could have been put on the list at the request of another ground station (i. e. using ground communications, another ground station could signal the ground station under consideration that a specific aircraft is entering its hemisphere) and should be included on its Interrogation List.
3. It could be put on the list at the request of the aircraft itself signaling over an RF link (i. e. the aircraft could be entering the CONUS from a transoceanic flight in which it had not been under a ground station's responsibility).

The interrogation list has its entries ordered in terms of their regions first, then their rings, and finally their cells.

The control station cycles through the list interrogating each aircraft in the following manner: The ground station has a phased array antenna which forms 15 beams. The beams are 9° deep and 3° wide. Each corresponds to a different ring of each region (i. e. beam 1 corresponds to ring 1, beam 2 corresponds to ring 2, etc. . .). The ground station begins with the outermost region (region 200). Each beam is aimed at the respective ring of the region to which it corresponds and begins interrogating those aircraft which reside in this ring on a cell-to-cell basis.

Specifically, consider beam 1. It will first look up on the Interrogation List the first aircraft which resides in ring 1 of region 200, and it will then aim itself at the cell position listed for this aircraft. It will then interrogate the aircraft by sending up the signal K(t) which is an ON-OFF Keying signal consisting of 30 binary digits. The first 10 binary digits are 10, "1's". The remaining 20 binary digits are the expansion to base 2 of the aircraft identification number. The signal K(t), if received correctly by the aircraft transponder, causes this transponder to be activated and transmit the most recently updated aircraft codeword to the ground control station. The ground control station searches for the codeword reply of the aircraft by using a range gating method. In other words, it looks for a reply in a specific slot of time based upon the region in which the aircraft was listed.

There are several possibilities in this codeword search. First, the aircraft codeword could be the only codeword received in the time slot and received perfectly, then no other digits exist in the time slot. Second, the aircraft codeword could be received perfectly in the time slot yet other digits could exist in the time slot (due to noise or other interference). Third, the aircraft codeword may not be received perfectly (due to noise or other interferance).

Since the ground station knows that each aircraft codeword must begin with a synchronization prefix of 10 "1's", it adopts the following strategy. In the codeword search, it looks for the first sequence of 10 consecutive "1's" in the time slot. If it finds this, it considers the 20 digits after this prefix. Since it knows which aircraft it interrogated, it can compare this 20 bit sequence with the aircraft identification number. If they agree, it declares that the aircraft codeword has been extracted. The following 60 digits are then interpreted. The aircraft position is then calculated and logged on a list called the "Logging List" along with its identification number and the absolute time at which the downlink transmission occurred. If no first sequence of 10 consecutive "1's" is found or if such a sequence is found but the following 20 digits do not agree with the identification number of the aircraft being interrogated, an entry is still made into the "Logging List" giving the identification number of the aircraft, absolute time, and a remark that its position was not updated during this cycle. This event is called "cycle loss." (The aircraft is lost on this cycle).

Beam 1 then continues, looks up the next aircraft on the Interrogation List residing in region 200, aims itself at its cell position and interrogates it in the same manner as before. All other beams continue in like manner allowing parallel processing until region 200 is completely interrogated. They then continue cycling down through all the regions.

At the end of the interrogation, the ground station updates all of the entries on the Interrogation List using the Logging List (i. e. it updates all aircraft positions). The ground station then considers all of the aircraft listed whose positions lie on the boundary of the hemisphere of control (i. e. on the outer hemisphere and on the base-the ground). Again using the previous logging lists, the ground station can discern whether these aircraft are moving out of the hemisphere of control or landing. If it is the former of these, it employs ground communications to inform those ground stations into whose hemisphere specific aircraft are moving, that these aircraft should be added to their Interrogation Lists and it also supplies them with their most recent position. The ground control station then erases these aircraft from its own Interrogation List. If an aircraft is touching ground, it is likewise erased from the Interrogation List.

Finally, the ground control station adds to its own Interrogation List all aircraft it learns are entering the hemisphere, learning this either from other ground control stations or from the aircraft itself by an RF link.

One item should be noted. When a beam is interrogating an aircraft it is aimed at the aircraft, (region, ring, cell), position which the aircraft occupied during the previous cycle. The aircraft's position has changed from this previous position and as such its (region, ring, cell) coordinates may have changed. However, due to aircraft dynamics, they cannot have changed much. Since the beam dimensions ($3^{\circ} \times 9^{\circ}$) are considerably wider than the cell widths ($1^{\circ} \times 6^{\circ}$), the aircraft transponder will still be excited even though pointing accuracy is not perfect. Similarly, if an aircraft is lost on a cycle due to noise or other interference, it may still be recovered in the next cycle even though the beam is aimed at an old position.

Figure E. 7 gives a system representation of the entire interrogation procedure.

E. 5 Air-to-Ground Link Power Budget and Probability that a Bit is Received in Error

The interrogation procedure is at the heart of the Air-to-Ground Link performance. As a prelude to analyzing the performance of this procedure, an Air-to-Ground Link Power Budget is given in Table E-1, for the transmission of one bit representing the digit "1" in a codeword. The power budget indicates a received signal energy-to-noise power density ratio E/N_o, of 20 db. In absolute terms $E/N_o = 100$.

For ON-OFF Keying modulation

$$\frac{1}{2} e^{-\frac{E}{8N_o}} \leq P_e \leq e^{-\frac{E}{8N_o}}$$

where P_e is the probability that a bit (either a "0" or a "1") is received in error. Evaluating this at $E/N_o = 20$ db yields:

$$P_e \approx (0.355)\, 10^{-5} \qquad \text{(E-1)}$$

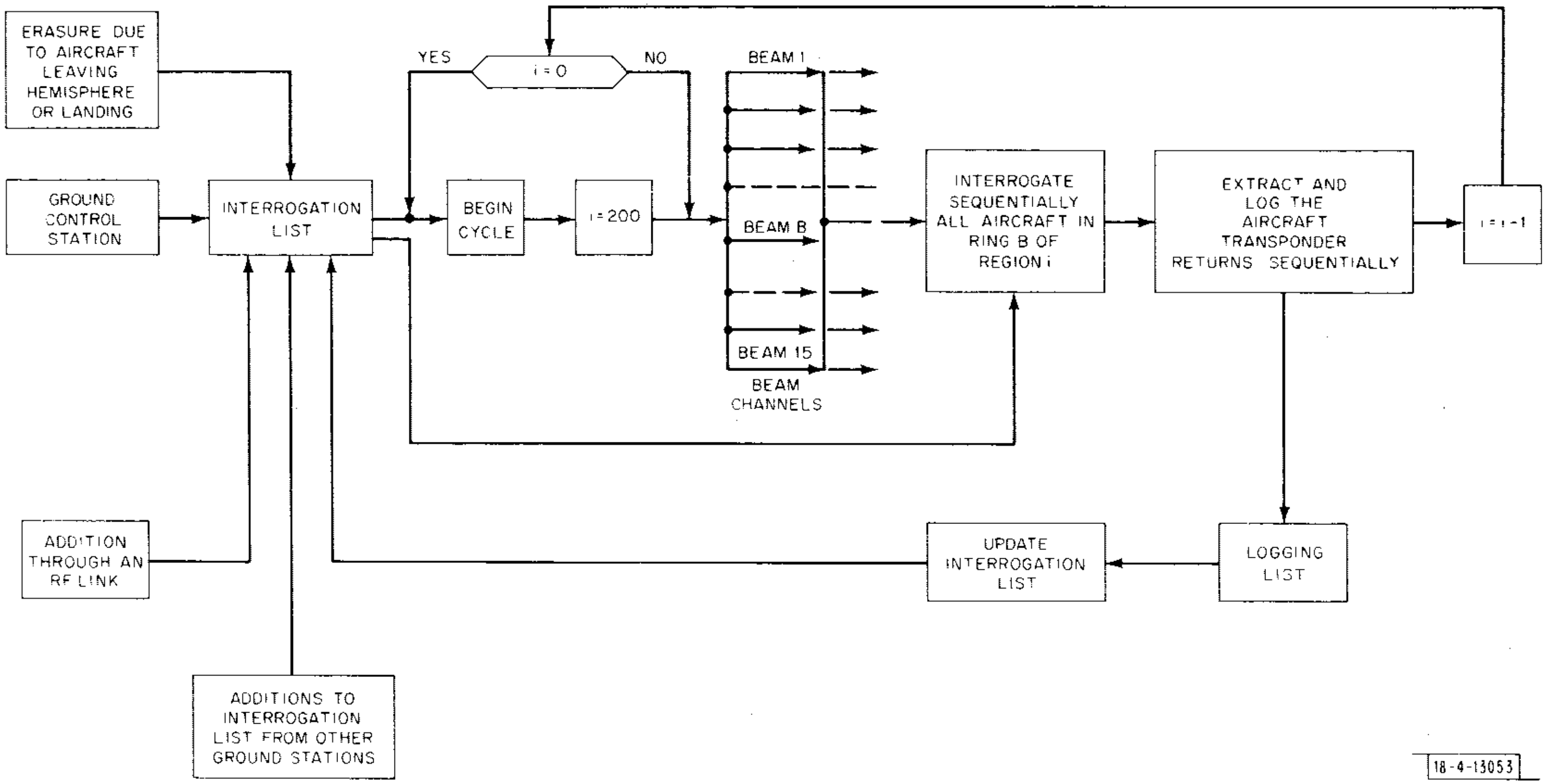

Fig. E.7. System representation of interrogation procedure.

TABLE E.1

AIR-TO-GROUND LINK POWER BUDGET

Item	Value	Reference
P_t (peak signal power transmitted)	23 dbw	
Chip Duration	-64 db-sec	
Aircraft Transmitting Antenna Gain	0 db	
Range Loss	-143 db	200 mile maximum slant range, 1 GHz
Receiver Noise Power Density (N_o)	-199 dbw/Hz	RFI, thermal and front end: noise (1000°K)
Miscellaneous Losses	-3 db	Feed, atmospheric and signal disadvantage
Receiving Antenna Gain	14 db	Fan beam 3° x 9°
Multipath Fading	-6 db	See Appendix G
Signal Energy to Noise Power Density (E/N_o)	20 db	

E. 6 Performance Analysis of the Air-to-Ground Link

In this section the performance of the Air-to-Ground Link will be analyzed.

E.6.1 Range Gating and Types of Interference

In the description of the interrogation procedure given in Section 4 it was remarked that a range gating procedure is utilized in obtaining the received aircraft codeword. In other words, the received codeword will be searched for in a specific slot of time. The length of this time slot will now be specified.

In a single 2.5 second cycle a given aircraft will at most move 5/12 miles(assuming a 600 mph velocity). It is likely that by 1995 aircraft will at most travel 1 mile in a 2.5 second cycle; hence at best it will move from the region it was logged at in the previous cycle into one of the 2 adjoining regions. The range interval (measured from the ground station) that it might lie in, extends for 3 miles. Thus, when a ground control station interrogates a specific aircraft it can expect to observe the beginning of the aircraft codeword somewhere in a time slot equal to the length of time necessary for a wave to propagate 3 miles. This is 16.2μ sec. Extending this out to the nearest 0.5μ sec., the beginning of the aircraft codeword return will lie in a time slot 16.5μ sec. long.

As described in Section E.2 the aircraft downlink codeword consists of 90 binary digits. Each digit is represented by an 0.5μ sec. chip (ON-OFF Keying modulation). Since the beginning of the codeword will be received somewhere in a time slot 16.5μ sec. wide, the entire codeword can be searched for in a time slot 61.5μ sec. long. In the absence of any interference, an aircraft codeword received in one of these 61.5μ sec. long time slots (henceforth called "region bins") might appear as in Figure E.8.

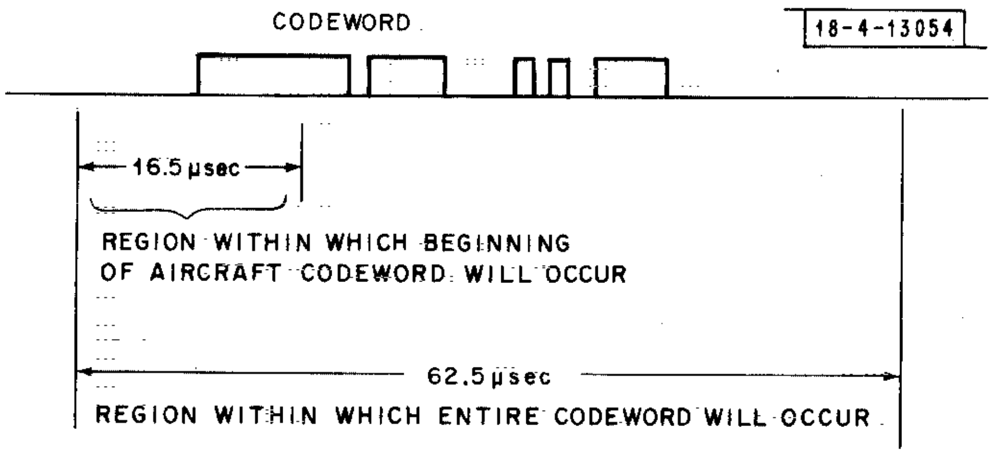

Fig. E.8. Received codeword in region bin in absence of interference.

Of course, interference might be generated in each region bin from two different sources:

1. Thermal noise might represent itself as bits of an aircraft codeword causing problems and/or errors in the reception-processing of the aircraft codeword.
2. Cross-Beam Interrogation - An aircraft could lie in the intersection of two hemispheres of control. It may be interrogated by a beam from one control station while it is in the view of, but not interrogated by, a beam from another control station. In such a situation its aircraft codeword would appear in the beam channel of some other aircraft which is being interrogated and interfere with that aircraft's codeword being transmitted. This type of interference can be eliminated by having the interrogation from neighboring control station be synchronized so that an aircraft in the hemisphere intersection will not lie in the view of beams from each control station.

E.6.2 Probability of Correct Synchronization

As described in Section E. 4, during the interrogation procedure, the ground control station searches in the region bin for the first sequence of 10 consecutive "1's", and considers this the synchronization prefix of the codeword of the aircraft which it has interrogated.

The ground control station will recognize the correct synchronization prefix and not a noise sequence disguised as the synchronization prefix if the region bin from its start until the beginning of the codeword is empty of noise masquerading as message "1's", and if the synchronization prefix of the aircraft codeword is received without error. Since the start of the codeword will occur in the first 16.5μ sec. of the region bin, the portion of the region bin prior to the reception of the aircraft codeword being free of noise digits corresponds to n "0's" being received correctly where n is less than or equal to 33. Let

$$P(\text{synch}) = \text{Prob.} \begin{pmatrix} \text{Ground control station} \\ \text{locks onto the correct} \\ \text{synchronization prefix} \end{pmatrix} \qquad (E\text{-}2)$$

Utilizing (E-1) and the previous discussion

$$\begin{aligned} &P(\text{synch}) \geq (1-P_e)^{33}\,(1-P_e)^{10} \\ &P(\text{synch}) \geq (1-(0.355 \times 10^{-5}))^{43} \approx 0.999864 \qquad (E\text{-}3) \\ &P(\text{synch}) \geq 0.999864 \end{aligned}$$

It should be noted that the probability of correct synchronization is actually much higher than the lower bound given by (E-3). Since the ground station knows which aircraft it is interrogating, in order to really lose synchronization, noise must not only masquerade as the synchronization prefix, but also as the aircraft identification number. This makes P(synch) much larger than the (E-3) lower bound. However, for present purposes, this lower bound will suffice.

E. 6. 3 Probability of Updating the Aircraft Position in the Logging List

As described in Section 4, once the synchronization prefix is established, the ground station considers the 20 digits received after the prefix. Since the ground control station knows which aircraft it is interrogating, it can compare this 20 bit sequence with the aircraft identification number. If the two sequences agree, the ground control station declares the aircraft codeword extracted and proceeds to compute the new aircraft position (from the remainder of the codeword) and update the position in the logging list. Thus,

$$\text{Prob.} \left(\begin{matrix} \text{aircraft codeword} \\ \text{is extended} \end{matrix} \;\middle|\; \begin{matrix} \text{correct} \\ \text{synchronization} \\ \text{prefix is found} \end{matrix} \right) = (1-P_e)^{20},$$

$$(1-(0.355 \times 10^{-5}))^{20} \approx 0.999937 \qquad (E\text{-}4)$$

and

$$\text{Prob.}\left(\begin{array}{l}\text{aircraft position}\\\text{is updated on}\\\text{Logging List}\end{array}\middle|\begin{array}{l}\text{correct}\\\text{synchronization}\\\text{prefix is found}\end{array}\right) = 0.999937 \qquad \text{(E-5)}$$

E.6.4 Probability that the Correct Aircraft Position is Logged in the Logging List

On a given aircraft interrogation if the correct synchronization prefix is found and the aircraft codeword is extracted, the only question remaining is with what probability the correct aircraft position will be logged in the Logging List. This, of course, is the probability that the last three blocks of 20 digits making up the codeword will be received without error, since it is these digits which contain the aircraft position information. Hence,

$$\text{Prob.}\left(\begin{array}{l}\text{correct aircraft}\\\text{position is logged}\\\text{onthe Logging List}\end{array}\middle|\begin{array}{l}\text{correct synchronization}\\\text{prefix is found and}\\\text{aircraft codeword is}\\\text{extracted}\end{array}\right) = (1-P_e)^{60} = (1-(0.355 \times 10^{5}))^{60}$$

$$= 0.99981 \qquad \text{(E-6)}$$

E.6.5 Probability that Aircraft Position will be Updated Correctly Given that the Aircraft is being Interrogated

The results of (E-3), (E-5) and (E-6) may now be combined to yield

$$\text{Prob.}\left(\begin{array}{l}\text{Aircraft position is}\\\text{updated correctly}\\\text{on a cycle}\end{array}\middle|\begin{array}{l}\text{Aircraft}\\\text{is being}\\\text{interrogated}\end{array}\right) \geq (0.999864)\,(0.999937)\,(0.99981)$$

$$\geq (0.9996) \qquad \text{(E-7)}$$

which represents adequate performance on the part of the interrogation procedure.

E.7 Estimated Number of Ground Control Stations Needed

In setting up the Air-to-Ground Link, the CONUS must be covered by discs. Each disc has a 200 mile radius with a ground control station at its center. This area of the CONUS is 3, 542, 559 square miles. This corresponds to the area of 81 of the 200 mile radius discs. Of course, in order to have the CONUS completely covered by discs many of these discs will have to overlap. Hence, more than 81 discs will be needed. However, it can safely be assumed that at most a few hundred discs, and therefore ground stations, will be needed to cover CONUS. This is an entirely reasonable cost to bear.

E.8 Performance of the Air-to-Ground Link when Position is Calculated Incorrectly

Consider the following event during the interrogation procedure of the Air-to-Ground link: An aircraft is interrogated, and when its codeword is extracted, several of the last 60 digits of its codeword are received incorrectly. If this event occurs, the aircraft position that is logged will be incorrect. When the aircraft is interrogated during the next cycle, the beam will be pointed at a wrong position and it is unlikely that the aircraft transponder will be excited and give a codeword return. In this case, the aircraft will suffer a cycle loss and in fact will be permanently in a cycle loss loop for all of the following cycles. Such an event, although it may be rare, would be a disaster as far as keeping the aircraft under surveillance is concerned.

The possibility of an aircraft entering a cycle loss loop can be eliminated to some extent by a simple improvement in the interrogation procedure, namely keeping a "Position Difference Table." This will now be described.

Every time an entry is made in the Logging List, the position difference between the entry and the last entry for the aircraft (i. e. that on the previous cycle) should be calculated. This position difference should be logged with the aircraft identification number and cycle time in a table called the "Position Difference Table." If an aircraft suffers a cycle loss, the last entry in the Position Difference Table is looked up. If this entry was small (i. e. below some threshold) nothing is done. If this entry was large, the position entered on the Interrogation List is computed from the last position listed on the Logging List before the large position difference occured. (i. e. 3 cycles back). This most likely will be close to the true position of the aircraft and will prevent the formation of a cycle loss loop. However, the only way to measure the effectiveness of this method is by simulation.

E.9 Air-to-Ground Link Procedure During System Start-Up

Consider the operation of the Satellite-to-Air-to-Ground Surveillance system when it is starting up. This could be either at the beginning of its lifetime or at some time immediately after the entire system has failed (both of these events will be considered equivalent). During the Start-Up each ground station must comehow learn the identity and positions (regions, ring, cell) of all aircraft in its hemisphere of control. Each ground control station must in a sense initialize its Interrogation List. In this section the procedure which the Air-to-Ground Link utilizes in order to initialize the Interrogation List is described. The procedure is sequential in nature and operates with the cooperation of the aircraft.

E.9.1 Aircraft Start-Up Signal

As an aid in the Start-Up procedure, each aircraft is assigned a "Start-Up Signal." The Start-Up Signal consists of 6 pulses. Each pulse is a 200 chip long (each chip being 100 nsec) pseudo random sequence picked from a set of 10 possible pseudo-random sequences. Each pseudo random sequence corresponds to a different integer from 0 to 9. Thus, the sequence of 6 pulses comprising the Start-Up Signal can and is put in correspondence with the aircraft identification number, and can thus serve to identify the aircraft.

E. 9. 2 Start-Up Procedure

The Start-Up procedure will now be described. The antenna beams normally used during the regular interrogation procedure are used in parallel. Remember each antenna beam corresponded to a different ring. It interrogated each cell on the ring sequentially for a given region and then moved on to a different region. During the Start-Up procedure each beam considers all regions simultaneously and moves sequentially around its ring cell by cell and in this way operates instead on a sequence of wedges of the airspace rather than individual cells.

Consider the operation of one antenna beam now on one particular wedge. After moving into the wedge the beam transmits a special signal to all occupants of the wedge. The signal consists of 20, "1's" and is called the "General Call Codeword." When the transponder of each aircraft in the wedge receives the General Call Codeword it does two things:

1. It switches itself to a special "Start-Up Mode"; and
2. It responds by transmitting back to the ground control station the first pulse of the aircraft's Start-Up Signal.

The ground station receives these returns using matched filter receivers. It also orders these pulses on a special list called List 1. The ground control station considers the first pulse on the list and transmits it to all aircraft in the wedge. This pulse is received by the transponders of all these aircraft. However, the "Start-Up Modes" of these transponders are designed in such a way that there will only be a response from transponders of aircraft with the first pulse of their Start-Up Signal identical with this received pulse. The transponders of these aircraft will respond with the second pulse of their Start-Up Signal. The ground control station receives these second pulses using matched filtered receivers. It then logs the "first pulse" transmitted and the "second pulse" received on a special list called List 2. The ground control station cycles through the other entries on List 1 making the appropriate entries into List 2. At the end of this cycle it has a list of the first two pulses of the Start-Up Signal of every aircraft in the wedge it is illuminating.

The ground control station then considers the first entry on List 2 and transmits these two pulses to all aircraft in the wedge. Again the Start-Up Mode is designed in such a way that only the transponders of those aircraft will respond which have the first two pulses of their Start-Up Signal identical with these two received pulses. The transponders of these aircraft will respond with the third pulse of their Start-Up Signal. The ground control station receives these pulses using matched filter receivers. It then logs the first two pulses transmitted with the third pulse received on a special list called List 3. The ground control station cycles through the other entries on List 2 making the appropriate entries on List 3. At the end of this cycle it has a list of the first three pulses of the Start-Up Signal of every aircraft in the wedge it is illuminating.

The procedure continues on in this manner constructing List 4, List 5, and List 6. List 6, of course, will contain the Start-Up Signals of all aircraft in the wedge being illuminated by the beam. The aircraft identification numbers are computed from this list and entered in the first Interrogation List. The ground station considers the first of these numbers and transmits it to all aircraft in the wedge. Only the aircraft having this identification number responds and it responds with its most recent downlink codeword. The ground control station computes the aircraft position from this codeword, quantizes it into a (region, ring, cell) coordinates and lists these quantized coordinates next to the corresponding aircraft identification number on the first Interrogation List. The ground control station then considers the second identification number on the Interrogation List and follows the same procedure. After cycling down the entire list it has the aircraft identification numbers and quantized positions of all aircraft in the wedge. It then broadcasts an "All Clear Codeword" (to all aircraft in the wedge) consisting of a sequence of 15, "1's." This signals all aircraft transponders to switch off the special "Start-Up Mode" and to ignore any General Call Codewords received during the next 30 seconds. The beam then moves to the next wedge. After this procedure is completed by all beams cycling through all wedges, the first Interrogation List is completed and the first interrogation cycle can be started using this Interrogation List.

E.9.3 An Upper Bound to the Amount of Time Needed for Start-Up

The feasibility of the Start-Up procedure described in the previous section depends in large part on the amount of time it takes to compile the entire Interrogation List. Obviously, if a very large amount of time is required when the Interrogation List is finally completed, some of its entries may be too stale to use in the first Interrogation cycle. This may result in cycle loss loops occurring from which no exit is possible. In this section an upper bound to the total amount of time that the Start-Up procedure requires will be computed. Worst case conditions will be assumed. The figure resulting will be acceptable for the total system performance.

Consider a ground control station and its hemisphere of control carrying out the Start-Up procedure. Assume the worst case aircraft population of the hemisphere of control, namely 10^4 aircraft, which have to be logged on the first Interrogation List. Since all rings are being operated on by beams in parallel, the amount of Start-Up time is at most the maximum time that a beam might require to complete its operation on its ring.

Consider a typical beam operating on its ring. Assume that there are Y aircraft residing in this ring. An upper bound to the amount of time taken to log all of these planes on the interrogation list will first be computed.

The first item to be computed is the amount of time taken by the beam to interrogate the empty wedges. If a wedge is empty, the following is the beam procedure. The beam is aimed along the wedge. It transmits the General Call codeword which is 2 μ sec. long. The ground control station waits the maximum delay time for a response. Since the wedge is empty, no response will be obtained (ignoring false responses due to noise). The beam then proceeds to the next wedge. The hemisphere of control is 200 miles in radius. Thus, the maximum delay time is 2.16 milliseconds and hence the maximum amount of time it takes for a beam to carry out the Start-Up procedure in an empty wedge is 2.162 milliseconds. Since each wedge is 1° long, there is a maximum of 360 empty wedges on each ring. Therefore, the maximum amount of time the beam takes to interrogate all empty wedges on its ring is 0.78 seconds.

Now the question of how long the beam takes to operate on wedges which are not empty will be taken up. Assume that non-empty wedges are ordered in some manner. Let Y_i be the number of aircraft in the i^{th} such wedge. The ground control station first forms List 1 by transmitting 20μ sec. General Call Codeword, and then waiting the maximum delay time of 2.16 milliseconds for a relay. The total time taken for the formation of List 1 is 2.162 milliseconds.

The ground control station then proceeds to form List 2 from List 1, List 3 from List 2, ..., List 6 from List 5. In order to form List j from List j-1, (j=2, ... 6), the ground control station transmits each entry on List j-1, (i.e. j-1 pulses), waits the maximum delay time of 2.16 milliseconds and logs all the replies. Since there are Y_i aircraft in the wedge being operated on, the maximum length of List j-1 is Y_i. Hence, the maximum amount of time it takes to form List j from List j-1 is upper bounded by

$$(Y_i)\,(j-1)\,(2.16)\,10^{-3} \text{ sec.}$$

This implies that the maximum amount of time that it takes to form List 1 through 6 is upper bounded by

$$2.162 + \sum_{j=2}^{6} Y_i\,(j-1)\,(2.162)\,10^{-3} \text{ sec.}$$

which itself is upper bounded by

$$(16\,Y_i)\,(2.162)\,10^{-3} \text{ sec.}$$

After List 6 is compiled, the aircraft identification numbers are computed. These are transmitted sequentially with the ground control station waiting for the aircraft codeword reply from each before transmitting the next. The total amount of time this takes is

$$Y_i\,(2.169 \cdot 10^{-3}) \text{ sec.}$$

Finally, the All Clear Codeword is transmitted which is 1.5μ sec. long. Altogether an upper bound to the amount of time the beam spends on this wedge is

$$34.5 \cdot Y_i \cdot 10^{-3} \text{ sec.}$$

The total amount of Start-Up time needed to operate on all non-empty wedges is therefore upper bounded by

$$\sum_i 34.5\ Y_i \times 10^{-3} = 34.5\ 10^{-3} Y \text{ sec.}$$

assuming Y aircraft in the ring. Taking into account the time spent on operating on empty wedges, the maximum time spent on the entire ring is upper bounded by

$$34.5 \times 10^{-3}\ Y + 0.78 \text{ sec.}$$

If there are 10^4 aircraft in the entire hemisphere of control a reasonable estimate is that Y is at most 1000. In this case the Start-Up time is not more than 36 seconds which is a feasible figure for operation.

By making a slight change in the Start-Up procedure it is possible to reduce the Start-Up time by a few seconds and also simplify the Start-Up procedure. In the worst case of 10^4 aircraft in the hemisphere of control, and most likely during typical cases, List 1 and List 2 will be completely filled after being formed. In other words, every code will be entered on List 1 (it will have 10 entries) and every two-sequence combination will be entered on List 2 (it will have 100 entries). One may then simplify the Start-Up procedure by assuming Lists 1 and 2 completely filled to begin with. The Start-Up procedure would operate by first transmitting the General Call Codeword to all aircraft in the hemisphere. The Ground Control station would then immediately begin cycling through the completely filled List 2. The maximum amount of time this cycling will take will be 0.2 seconds. The Start-Up procedure will be simplified and the net Start-Up time, (particularly during worst case conditions) may be reduced. From now on this simplification will be assumed to have been incorporated into the Start-Up procedure.

E.9.4 Interference Effects During the System Start-Up Procedure

In this section the question of interference during the Start-Up procedure will be addressed. Interference comes from three sources; thermal noise, multiple access noise, destructive interference of pseudo random sequence pulses matched to the same filter.

Thermal noise, the first interference phenomenon, can be suppressed with sufficient signal energy. Multiple access noise is due to the following event. The pseudo random sequences transmitted by the aircraft are received not only by the matched filters to which they are matched, but by all the other matched filters at the ground control station. When a matched filter is excited by a pseudo random sequence to which it is not matched, the matched filter output looks like gaussian noise. This is multiple access noise. It cannot be suppressed by raising the signal energy, since this type of interference increases as signal energy increases.

The last type of interference mentioned is similar to specular multipath and will be called Pseudo Specular Multipath. Consider the Start-Up procedure being carried out by a particular beam in a particular wedge. Suppose on one of the downlink transmissions, two aircraft transmit the same pseudo random sequence down to the ground control station. If the two aircraft are close enough, the two pulses may be received within 4 chips (400 nano-seconds) of each other by the matched filter. In this case the two pulses might destructively interfere causing the matched filter not to have two sharply peaked autocorrelation functions as its output, but rather a degraded version of this. If this output is so degraded that the decision threshold on the output of the matched filter is not exceeded, an error might be introduced into the Start-Up procedure and aircraft may not be logged on the Interrogation List. Fortunately, the possibility of this last type of interference occurring is very slight as is shown by the following argument.

Suppose a wedge is being operated on during the Start-Up procedure. Specifically, suppose certain aircraft are transmitting pseudo random sequence pulses in the compilation of one of the lists and two of these aircraft transmit the same pseudo random sequence pulse. In order for these two identical pulses to be received within a 4 chip time delay the ranges of the two aircraft from the ground station can differ by at most 7.45×10^{-2} miles. Consider now the wedge sliced perpendicular to its axis at 2 points, 7.45×10^{-2} miles apart. A curvilinear box is formed by the slices. The two aircraft must lie in such a box. Since the wedge is 1^{o} wide and 6^{o} deep with a wedge radius of 200 miles, one can infer that in order for the 2 aircraft to interfere they must lie within a common volume of size 5.5 cubic miles.

The volume of the entire hemisphere of control is 16.7×10^{6} cubic miles. Assuming the worst case of 10^{4} aircraft in the hemisphere of control and assuming them uniformly distributed throughout this volume implies that the probability of one aircraft being in a specific 5.5 cubic mile volume is $(0.333)\,10^{-2}$. The probability of 2 aircraft being in a specific 5.5 cubic mile volume is 1.11×10^{-5}. If a specific 5.5 cubic mile volume is occupied by 2 aircraft, the probability that they are both transmitting during the compilation of List 1 is at most 1. If they are both transmitting, the probability that they are both transmitting the same pseudo-random sequence pulse is 0.1. Combining these parameters yields

$$\text{Prob.}\left(\begin{array}{l}\text{conditions arise in} \\ \text{a specific 5.5 mile}^3 \\ \text{volume in the wedge to} \\ \text{cause Pseudo Specular} \\ \text{Multipath}\end{array}\right) \leq 1.11 \times 10^{-6}$$

The volume of a wedge is 4.9×10^{3} cubic miles. This implies that

$$\text{Prob.}\left(\begin{array}{l}\text{conditions are in the}\\ \text{wedge such that}\\ \text{Pseudo Specular Multipath}\\ \text{occurs during a}\\ \text{downlink transmission}\end{array}\right) \leq 5.5 \times 10^{-3}$$

This figure is small enough so that this type of interference can be ignored.

The downlink power budget (Table E.2) gives a measure of the interference consisting of thermal noise and multiple access noise during one downlink transmission of a pseudo random sequence pulse. The average received signal energy is computed from the transmitted signal energy, the transmitting and receiving antenna gain, the path loss and the miscellaneous losses. The thermal noise power density is computed directly from the receiver front end noise temperature. The calculation of the multiple access noise energy is more involved. The average energy received over any 500 nano sec time period at a matched filter from any particular mismatched user is first computed. This computation is carried out assuming that all replies to an interrogation during the Start Up Procedure are received within a 2.17 milliseconds period following the initiation of the interrogation. Furthermore, it is assumed that the replies are uniformly distributed in this 2.17 millisecond period. The average number of mismatched codes into a particular matched filter as a result of a single interrogation during the Start-Up Procedure is then calculated. These two parameters are combined to give the average energy received from all mismatched codes at a particular matched filter during any 500 nano-sec interval as a result of interrogation during Start-Up Procedure. This parameter has the same units as noise power density and is combined with the thermal noise power density to give an equivalent noise power density. This in turn is combined with the average received signal to give the resultant E/N_o.

It should be noted the multiple access noise is not gaussian in nature. This is due to this noise being composed of only a relatively few mismatched codes. Hence, the equivalent noise power density cannot be thought of as an equivalent power gaussian source. However, for purpose of this first order analysis we shall treat this as a gaussian channel. A gaussian channel operating with an E/N_o of 17dB will have a bit error probability less than 10^{-5}.

E.9.5 Using the Start-Up Procedure for System Monitoring

As has been mentioned in Section 4, during the normal operation of the interrogation procedure there are three ways in which an aircraft may become entered on the Interrogation List at the beginning of a cycle.

1. It could have been on the list during the previous cycle and not have been erased from the list during that cycle.
2. It could have been put on the list at the request of another ground station (i.e. using ground communications, another ground station could signal the ground station under consideration that a specific aircraft is entering its hemisphere and should be entered on its Interrogation List).
3. It could be put on the list at the request of the aircraft itself signaling over an RF link (i.e. the aircraft could be entering the CONUS from a transoceanic flight in which it had not been under a ground control station's responsibility).

Now the following event may occur. An aircraft may enter the hemisphere of control without its identification number having been entered on the Interrogation List. This may occur for a variety of reasons. For example, an aircraft may enter the CONUS from a transoceanic flight and forget to notify the ground control station of the hemisphere it enters.

TABLE E. 2

LINK POWER BUDGET DURING AIR-TO-GROUND START UP

Item	Value	Reference
Chip Power	18.5 dbw	When a "1" is transmitted
Chip Duration	-63 db sec	
Chip Energy	-44.5 dbJ	When a "1" is transmitted
Pseudo Random Sequence Length	23 db	
Average Signal Energy Transmitted Per Pulse	-24.5 dbJ	
Range Loss	-143 db	200 mile maximum slant range, 1 GHz
Aircraft Transmitting Antenna Gain	0 db	
Receiving Antenna Gain	14 db	Fan beam, 3° by 9°
Miscellaneous Losses	-3 db	Feed, atmospheric, and signal disadvantage
Average Received Signal Energy	-156.5 dbJ	
Thermal Noise Power Density	-199 dbw/Hz	RFI, Thermal and front end noise (1000°K)
Average energy transmitted from any particular mismatched user	-60.9 dbJ	
Average number of mismatched codes per matched filter channel	19.5 db	10^4 aircraft assumed in a hemisphere, LIST 2 assumed filled to begin with 100 entries, 10 different codes
Average energy transmitted from all mismatched codes in a particular matched filter channel	-41.5 dbJ	
Average energy received from all mismatched codes in a particular matched filter channel	-173.5 dbJ	
Equivalent Noise Power Density	-173.5 dbw/Hz	
E/N_o	12 db	

If an aircraft is not entered on the Interrogation List, surveillance will not be maintained over its flight and the result might be disastrous. Thus, it would be desirable if the Ground Control Station could run through a periodic check to determine whether there are aircraft in its hemisphere which for one reason or another have not been entered on its Interrogation List, and then include these aircraft on the Interrogation List.

The ground station can carry out this periodic check quite easily by making use of the Start-Up Procedure. This will now be described. Once per minute the ground station will go into a Monitor Mode. The station will have its antenna cycle through each wedge of the hemisphere. The operation on each wedge is as follows. The ground station transmits a "Monitor Codeword" consisting of 25, "1's." All aircraft residing in the wedge receive this codeword and do one of 2 things:

1. If an aircraft's transponder has been activated by the ground station within the last 10 seconds (in other words if it is on the Interrogation List) the aircraft transponder goes into a special Monitor Mode and simply ignores the Monitor Codeword and all other commands it receives until it receives a special "All Clear Codeword" consisting of 35, "1's". The transponder then switches back to normal mode operations.

2. If an aircraft's transponder has not been activated by the ground control station within the last 10 seconds (in other words the aircraft is not on the Interrogation List) the transponder goes into a special Monitor Mode. It transmits back the first pulse of its Start-Up Signal. The ground control station receives these using matched filters. The rest of the Start-Up procedure is then completed (including the construction of List 1 and List 2, no abbreviated procedure). The identification number and positions of the aircraft responding are entered on the Interrogation List. The "All Clear Codeword" is then transmitted by the ground station and all transponders switch back to normal mode operations.

In general, very few aircraft will come under category 2, above. Thus, this entire procedure will take very little time. Certainly it will not take as much time as a general "Start-Up" and it does afford quite a bit of protection vis à vis maintaining truely complete surveillance overall aircraft in the airspace.

E.10 Aircraft Codeword Design When Position Is Computed On Board the Aircraft

The Air-to-Ground link has so far been described as operating with the aircraft transmitting to the ground control station a codeword which represents the difference in times of arrival between the pulses the aircraft receives from the different satellites. The ground control station then computes the aircraft position from these times of arrival differences by using the method of Hyperboloids. This is carried out, of course, assuming that the ground station has the satellite ephermis data.

Since determining the aircraft position from the differences in times of arrival is a very simple computational operation, it could be carried out on board the aircraft as well as at the ground station provided the cost of a small computer is small when the fourth generation system is implemented. The aircraft position would then be incorporated into the aircraft codeword (rather than time of arrival differences) and transmitted to the ground control station. In this section the aircraft codeword structure needed to accomplish transmission of the aircraft position will be described.

As before, since ON-OFF Keying modulation is being used, a synchronization prefix is needed. The first 10 digits of the aircraft codeword will be 10, "1's", and will be used for synchronization. Again, as before, the next block of 20 digits in the aircraft codeword will be the expansion to the base 2 of the aircraft identification number. One of the simpliest ways to represent an aircraft's position is by the three coordinates, (altitude, longitude, latitude). This representation will be used. Altitude should be to within an accuracy of $\pm$ 50 feet. Longitude and Latitude should be to within an accuracy of $\pm$ 0.01 arc minutes.

In 1995 the maximum aircraft altitude will still most likely be less than 60,000 feet. Quantizing the altitude in steps of 50 feet yields 1200 quantization levels. Each quantization level can be represented by a binary sequence of length 11. Hence, an aircraft's altitude, to within an accuracy of 50 feet, can be represented by a block of 11 binary digits.

The CONUS lies within the region bounded by 60° W. Longitude and 135° W. Longitude. An aircraft's longitude can be transmitted simply by transmitting the difference between it and 60°. The range of the difference will be 75°. Quantizing each degree of longitude into steps of 0.01 arc minutes yields 4.5×10^{5} quantization levels. Each quantization level can be represented by a binary sequence of length 19. Hence, an aircraft's longitude, to within an accuracy of 0.01 minutes, can be represented by a block of 19 digits.

The CONUS lies within the region bounded by 15° N Latitude and 60° N Latitude. An aircraft's latitude can be transmitted simply by transmitting the difference between it and 15°. The range of the difference will be 45°. Quantizing each degree of latitude into steps of 0.01 minutes yields 2.7×10^{5} quantization levels. Each quantization level can be represented by a binary sequence of length 19. Hence, an aircraft's latitude, to within an accuracy of 0.01 minutes, can be represented by a block of 19 digits.

Combining these computations the aircraft codeword structure is now explicity described.

1. The first 10 digits are "1's" representing a synchronization prefix.

2. The next block of 20 digits are the expansion to base 2 of the aircraft identification number.

3. The following block of 11 digits represents the aircraft altitude to within an accuracy of 50 feet.

4. The next block of 19 digits represents the difference between the aircraft's longitude and 60° to within an accuracy of 0.01 minutes.

5. The final block consists of 19 digits. It represents the difference between the aircraft's latitude and 15° to within an accuracy of 0.01 minutes.

The total codeword length is 79 digits. This compares favorably with the situation in which time of arrival differences are transmitted. In that case the aircraft codeword was 90 digits long. Of course, one may argue that the aircraft codeword reduction on the downlink will be more than balanced by the need to transmit satellite ephermeris data to the aircraft on the uplink. However, this is really not a fair comparison because the ground control station has a tremendous amount of transmitter power so the uplink transmission of satellite ephermeris data is no burden to it.

In addition to the codeword length reduction gained by transmitting aircraft position, the aircraft has the advantage of having its own satellite derived position estimate available for navigation.

APPENDIX F

COMPUTER REQUIREMENTS FOR ON-BOARD NAVIGATION

In this Appendix an estimate will be made of the complexity of a computer needed to perform on board satellite navigation. It is assumed that:

(1) Every K_1 seconds the aircraft computer receives the times-of-arrival of ranging pulses from N synchronous satellites.

(2) Every K_2 seconds the aircraft computer receives satellite ephemeris data (position and velocity) for N satellites, as well as an accurate time of day.

The received data are then used to compute, (every K_1 seconds) an estimate of the aircraft's position via hyperbolic ranging techniques. This estimate should be accurate to within several hundred feet. For the purposes of this Appendix, K_1 will be taken to be one, and K_2, approximately one hundred. N will be a minimum of four, and possibly as large as six, depending on the density of the satellite configuration and the shape of the receiver antenna pattern.

Specifically, the following parameters are of interest:

(1) The required sizes of the various storage registers, in bits;

(2) The number of airthmetic operations (adds, multiplications, and divides) required for each aircraft position estimate; and

(3) The memory requirements of the computer.

While it appears that by 1990 a special purpose computer would be most suited to this task, the following analysis is intended to demonstrate that the computing load may be easily handled by any 4096 word, 16 bit minicomputer currently available.

F.1 Derivation of the Estimation Equations

It is convenient at this point to introduce the following notation:

$\underline{p}(t)$ = actual position of aircraft at time t.

$\hat{\underline{p}}(t)$ = estimated position of aircraft at time t.

$\underline{p}^*(t)$ = predicted position of aircraft at time t based on $\underline{p}(u)$, $u = t - K, t - K + 1, \dots t - 1$.

$\underline{s}_i(t)$ = actual position of satellite i at time t.

$\hat{\underline{s}}_i(t)$ = estimated position of satellite i at time t.

$\underline{v}_i(t)$ = actual velocity of satellite i at time t.

$\hat{\underline{v}}_i(t)$ = estimated velocity of satellite i at time t.

$\underline{\tau}(t)$ = vector of times-of-arrival of satellite ranging pulses at aircraft during the time interval (t-1, t).

$\hat{\underline{\tau}}(t)$ = measured value of $\underline{\tau}(t)$.

All of the above, with the exception of $\underline{\tau}(t)$ and $\hat{\underline{\tau}}(t)$, are vector elements of a three-dimensional, geocentric, inertial rectangular coordinate system. $\underline{\tau}(t)$ and $\hat{\underline{\tau}}(t)$ are N-vectors, where N is the number of satellites.

The times of transmission of the ranging pulses from the N satellites are such that during each one second interval the N pulses arrive at the aircraft in sequential order (1, 2, ... N) with no interference between adjacent pulses. If N equals four, then one can arrange to have all the pulses arrive in their correct order within a 32 msec interval, regardless of the location of the aircraft over the continental U. S. On the other hand, if N is larger than four, then the size of the interval increases proportionally. Since an aircraft moves at moderate speed, its displacement during 32 msec is significantly less than the acceptable error in estimating its position; and, as a result, the aircraft can be considered to be motionless during the reception of each set of N pulses. If satellite "i" transmits at time $t - \delta_i$, where t is the time-of-arrival of the last of the N pulses, then

$$\|\underline{s}_i(t - \delta_i) - \underline{p}(t)\| \simeq c\,[\tau_i\,(t) - (t - s_i)]$$

where $\|\underline{x}\|$ denotes the length of the vector $\underline{x}$, c is the speed of light, and $\underline{\tau}_i(t)$ is the i'th component of $\underline{\tau}_i(t)$.

The above equation can be put in a more compact form by defining the N-vector valued function $\underline{f}\,(\underline{p},\ t)$ whose i'th component is

$$f_i\,(\underline{p},\ t) \;=\; \|s_i(t - \delta_i) - \underline{p}(t)\|, \quad i = 1, 2, \ldots N$$

It now follows that

$$\underline{f}\,(\underline{p},\ t) \cong \; c\,\underline{\tau}\,(t) + c\delta - ct\,\underline{1}$$

where $\underline{\delta}$ is an N-vector with components $\delta_1, \ldots \delta_N$ and $\underline{1}$ is an N-vector, each of whose component is 1. If the exact times of pulse transmissions, $t - \delta_i$, were known and were compared with the times of arrival $\tau_i(t)$, one could use this last equation to determine $\underline{p}(t)$. However, as the aircraft does not have a precision clock (with accuracy of a few parts in 10^9), time differences are employed by operating on both sides of this equation with the (N-1) by N matrix $\underline{H}$:

$$\underline{H} = \begin{pmatrix} 1 & -1 & 0 \ldots & 0 \\ 0 & 1\ -1 & 0 \ldots & 0 \\ \vdots & & & \\ 0 & 0 \ldots & 0\ 1 & -1 \end{pmatrix}$$

Noting that

$$\underline{H}\ \underline{1} = \underline{0}$$

it follows that

$$\underline{H}\ \underline{f}(\underline{p}, t) = c\,\underline{H}\,\underline{\tau}(t) + c\,\underline{H}\,\underline{\delta}$$

The (N-1) - vector $\underline{H}\,\underline{\tau}(t)$ has as components differences of times-of-arrival, $\tau_i(t) - \tau_{i+1}(t)$, which may be accurately measured to within a few nanoseconds by a clock with accuracy of a few parts in 10^6. Also, the vector $\underline{H}\,\underline{\delta}$ has as components the inter-transmission times $\delta_i - \delta_{i+1}$ which may be assumed to be known on the aircraft, as they are fixed constants.

One may now use the measured differences of pulse times-of-arrival $\underline{H}\,\hat{\underline{\tau}}(t)$ to determine the estimated aircraft position $\hat{\underline{p}}(t)$. That is, $\hat{\underline{p}}(t)$ is defined as that vector which minimizes the quantity

$$\|\underline{H}\,\underline{f}(\hat{\underline{p}}(t), t) - c\,\underline{H}\,\hat{\underline{\tau}}(t) - c\,\underline{H}\,\underline{\delta}\|^2$$

If $\underline{f}(\hat{\underline{p}}(t), t)$ is linearized about the predicted position $\underline{p}^*(t)$ as follows:

$$\underline{f}(\hat{\underline{p}}(t), t) = \underline{f}(\underline{p}^*(t), t) + F\,(\hat{\underline{p}}(t) - \underline{p}^*(t))$$

then the problem becomes one of minimizing

$$\|\underline{H}\,\underline{F}\,(\hat{\underline{p}}(t) - \underline{p}^*(t)) - c\,\underline{H}\,\hat{\underline{\tau}}(t) - c\,\underline{H}\,\underline{\delta} + \underline{H}\,\underline{f}\,(\underline{p}^*(t), t)\|^2$$

In the above, $\underline{F}$ is the matrix of partial derivatives of $\underline{f}(\underline{p}^*, t)$ with respect to the components of $\underline{p}^*$:

$$\underline{F} = \frac{\partial \underline{f}(\underline{p}^*, t)}{\partial \underline{p}^*}$$

The above quantity is minimized by requiring that*

$$(\underline{F}'\underline{H}'\underline{H}\,\underline{F})\,(\hat{\underline{p}}(t) - \underline{p}^*(t)) = \underline{F}'\underline{H}'(c\underline{H}\hat{\underline{T}}(t) + c\,\underline{H}\,\underline{\delta} - \underline{H}\underline{f}(\underline{p}^*(t), t)) \qquad \text{(F-1)}$$

where the prime," '," denotes matrix transposition. By straightforward differentiation one can easily show that

$$F = -\begin{pmatrix} \underline{u}_1' \\ \underline{u}_2' \\ \vdots \\ \underline{u}_N' \end{pmatrix}$$

where $\underline{u}_i$ is the unit 3-vector pointing from $\underline{p}^*(t)$ to $\underline{s}_i(t - \delta_i)$. It should be noted that $\underline{F}$ is a function of both the predicted aircraft position $\underline{p}^*(t)$ and the position of the i'th satellite at the time it sends its pulse. However, as the aircraft has only an estimate $\hat{\underline{s}}_i(t - \delta_i)$ of this position, the estimate is used in the construction of $\underline{F}$.

---

*One should compare Eq. (F-1) with Eqs. (I-7), (I-9), and (I-10) of Appendix I. The slight difference between the estimates described in this Appendix and in Appendix I is a result of modeling the errors in $\hat{\underline{T}}$ differently. In Appendix I the components of $\hat{\underline{T}} - \underline{T}$ are assumed uncorrelated; here, the components of $\underline{H}(\hat{\underline{T}} - \underline{T})$ are assumed uncorrelated.

A true statistical model for all the measurement errors (timing errors, satellite tracking errors, and errors due to atmospheric refractions) should be developed in order to determine the optimal aircraft position estimation equations. Such a study should be included in any second order attempt at improving the performance of the avionics computer.

The computational steps involved in producing the estimate $\hat{\underline{p}}(t)$ may now be listed as:

(1) Computation of $\underline{p}^*(t)$ from $\hat{\underline{p}}(t-1)$, $\hat{\underline{p}}(t-2)$, ... $\hat{\underline{p}}(t-K)$.

(2) Computation of the estimated satellite positions $\hat{\underline{s}}_i(t-\delta_i)$, $i = 1, 2, \ldots N$.

(3) Computation of the components of $\underline{f}(\underline{p}^*(t), t)$:

$$f_i(\underline{p}^*(t), t) = \|\hat{\underline{s}}_i(t-\delta_i) - \underline{p}^*(t)\|$$

(4) Computation of the unit vectors $\underline{u}_i$:

$$\underline{u}_i = \frac{1}{\|\underline{s}_i(t-\delta_i) - \underline{p}^*(t)\|}(\underline{s}_i(t-\delta_i) - \underline{p}^*(t))$$

and matrix $\underline{H}\,\underline{F}$.

(5) Solving for the difference between $\hat{\underline{p}}(t)$ and $\underline{p}^*(t)$:

$$(\underline{F}'\underline{H}'\underline{H}\,\underline{F})(\hat{\underline{p}}(t) - \underline{p}^*(t)) = \underline{F}'\underline{H}'(c\,\underline{H}\,\hat{\underline{\tau}}(t) + c\,\underline{H}\,\hat{\underline{\delta}} - \underline{H}\,\underline{f}(\underline{p}^*(t), t))$$

and thus the estimate $\hat{\underline{p}}(t)$.

(6) Expressing $\hat{\underline{p}}(t)$ in a geocentric, rotating, spherical coordinate system, i.e. in terms of latitude, longitude, and altitude.

F.2 Computation of $\underline{p}^*(t)$

The predicted position $\underline{p}^*(t)$ depends to some extent on the model that one chooses to use for the aircraft flight dynamics. If the previous estimates $\hat{\underline{p}}(t-K)$, $\hat{\underline{p}}(t-K+1)$, ... $\hat{\underline{p}}(t-1)$ are available, then one can fit a (K - 1)'th order polynomial to these points and extend this polynomial one second in time to obtain $\underline{p}^*(t)$. For the special case where K equals three, this amounts to assuming that the aircraft acceleration changes vary little from t - 3 to t; when K equals two, the assumption is that the aircraft velocity is roughly constant from t - 2 to t.

If this constant velocity assumption is used, then the predicted position $\underline{p}^*(t)$ has a particularly simple form:

$$\underline{p}^*(t) = 2\,\hat{\underline{p}}(t-1) - \hat{\underline{p}}(t-2) \qquad \text{(F-2)}$$

One can bound the error that results from this prediction under the assumption that $\hat{\underline{p}}(t-1)$ and $\hat{\underline{p}}(t-2)$ are good estimates by noting that it is reasonable to assume that the aircraft acceleration is bounded in magnitude by approximately one g = 32 ft./sec^2. If the aircraft undergoes this maximum acceleration over the interval $(t-2, t)$, then it is easy to see that the predicted position $\underline{p}^*(t)$ given by Eq. (F-2) will be off by at most 32 feet, a perfectly acceptable error. Errors in the estimates $\hat{\underline{p}}(t-1)$ and $\hat{\underline{p}}(t-2)$ add to the error in $\underline{p}^*(t)$, but such errors would be present in other prediction schemes.

One should note that Eq. (F-2) gives a good prediction of $\underline{p}(t)$ because the time interval between new positional estimates is only one second. If, on the other hand, position estimates were to be made only every ten seconds, then the error in $\underline{p}^*(t)$ due to acceleration could be as large as 3200 feet.

The computation requirements for Eq. (F-2) are very simple: All that is necessary is to perform 3 shifts and 3 adds.

F.3 Updating the Estimated Satellite Positions $s_i(t - \delta_i)$

The position and velocity vectors for each satellite satisfy the following set of differential equations:

$$\dot{\underline{s}}(t) = \underline{v}(t)$$

$$\dot{\underline{v}}(t) = -\left(\frac{2\pi}{T}\right)^2 \frac{R^3}{\|\underline{s}(t)\|^3}\,\underline{s}(t) \qquad \text{(F-3)}$$

where R is the radius of a synchronous circular orbit (about 26,000 miles) and T = 1 day = 86,400 seconds. The solution for $\underline{s}(t)$ traces out an ellipse with the earth at one focus.

If one defines the x axis of the coordinate system to be coincident with the major axis of this ellipse, and the z axis to be perpendicular to the plane of the ellipse, then the solution to Eq. (F-3) is

$$\underline{s}(t) = \begin{pmatrix} s_x(t) \\ s_y(t) \\ s_z(t) \end{pmatrix} = R \begin{pmatrix} \cos \varphi(t) - e \\ \sqrt{1 - e^2} \sin \varphi(t) \\ 0 \end{pmatrix}$$

$$\underline{v}(t) = \begin{pmatrix} v_x(t) \\ v_y(t) \\ v_z(t) \end{pmatrix} = \frac{2\pi R}{T} \begin{pmatrix} -\dfrac{\sin \varphi(t)}{1 - e \cos \varphi(t)} \\ \sqrt{1 - e^2} \dfrac{\cos \varphi(t)}{1 - e \cos \varphi(t)} \\ 0 \end{pmatrix} .$$

In the above, e is the eccentricity of the orbit (between 0 and .4 for most synchronous navigation satellites) and $\varphi(t)$ is the eccentric anomaly, which satisfies the following equation

$$\varphi(t) - e \sin \varphi(t) = \frac{2\pi}{T} (t - t_p) \qquad \text{(F-4)}$$

(t_p is the time of passage through the perigee).

In terms of a more general rectangular coordinate system, the solutions $\underline{s}(t)$ and $\underline{v}(t)$ are of the form

$$\underline{s}(t) = R\,\underline{P}\begin{pmatrix}\cos\varphi(t) - e \\ \sqrt{1-e^2}\,\sin\varphi(t) \\ 0\end{pmatrix}$$

$$\underline{v}(t) = \frac{2\pi R}{T}\,\underline{P}\begin{pmatrix}-\dfrac{\sin\varphi(t)}{1-e\cos\varphi(t)} \\ \sqrt{1-e^2}\,\dfrac{\cos\varphi(t)}{1-e\cos\varphi(t)} \\ 0\end{pmatrix} \qquad \text{(F-5)}$$

where $\underline{P}$ is a suitable orthogonal matrix, i.e. $\underline{P}'\underline{P} = \underline{I}$, representing a rotation of coordinates. The angle $\varphi(t)$ again satisfies Eq. (F-4).

As explained in the introduction, the aircraft computer must be able to compute the satellite positions at one second intervals over periods of time equal to about 100 seconds, at which point new, correct satellite ephemeris data are received. Equations (F-4) and (F-5) could be used to compute these positions; a simple calculation reveals that the accuracy of the aircraft clock is sufficient to track the satellite positions for 100 seconds with an error of only a few feet.* However, implementation of Eqs. (F-4) and (F-5) involves the calculation of sines and cosines, which are costly in computer time. Therefore, it is desirable to find a simpler method of updating the satellite positions, possibly at the expense of less accuracy.

The acceptable error in the estimates of satellite positions may be determined as follows. Recall that $\hat{\underline{p}}(t)$ is determined via Eq. (F-1). The first order errors in $\hat{\underline{p}}(t)$ result from errors in $\hat{\underline{\tau}}(t)$ and errors in $\underline{f}(\underline{p}^*(t), t)$. Errors in the latter result from the fact that, whereas the correct value of $f_i(\underline{p}^*(t), t)$ is $\|s_i(t - \delta_i) - \underline{p}^*(t)\|$, the value used in the computations is $\|\underline{s}_i(t_i - \delta_i) - \underline{p}^*(t)\|$. Writing

*This method of satellite tracking is discussed in Section F.9.

$$\|\hat{\underline{s}}_i(t-\delta_i) - \underline{p}^*(t)\| = \|\underline{s}_i(t-\delta_i) - p^*(t) + \hat{\underline{s}}_i(t-\delta_i) - \underline{s}_i(t-\delta_i)\|$$

$$\cong \|\underline{s}_i(t-\delta_i) - p^*(t)\| + \underline{u}_i'(\hat{\underline{s}}_i(t-\delta_i) - \underline{s}_i(t-\delta_i))$$

where $\underline{u}_i$ is the unit vector pointing from $\underline{p}^*(t)$ to $\underline{s}_i(t-\delta_i)$, it is seen that satellite tracking errors introduce errors in $\hat{\underline{p}}(t)$ through the term

$$\underline{u}_i'(\hat{\underline{s}}_i(t-\delta_i) - \underline{s}_i(t-\delta_i))$$

Errors in $\hat{\tau}_i(t)$ are on the order of 50 nsec. Thus acceptable tracking errors are those where

$$|\underline{u}_i'(\hat{s}_i(t-\delta_i) - \underline{s}_i(t-\delta_i))| < 50 \text{ feet}$$

That is, satellite tracking errors in the direction of $\underline{u}_i$ should be less than 50 feet, while errors perpendicular to $\underline{u}_i$ can be considerably larger.*

One simple method of updating the satellite positions is to numerically solve the differential equations (F-3). A third order numerical solution giving errors less than 10^{-10} per update is

$$\hat{\underline{s}}_i(t-\delta_i+1) = \left(1 - \frac{1}{2}\left(\frac{2\pi}{T}\right)^2 \frac{R^3}{\|\hat{\underline{s}}_i(t-\delta_i)\|^3}\right)\hat{\underline{s}}_i(t-\delta_i)$$

$$+ \left(1 - \frac{1}{6}\left(\frac{2\pi}{T}\right)^2 \frac{R^3}{\|\hat{\underline{s}}_i(t-\delta_i)\|^3}\right)\hat{\underline{v}}_i(t-\delta_i) \qquad \text{(F-6)}$$

$$\hat{\underline{v}}_i(t-\delta_i+1) = \left(\frac{2\pi}{T}\right)^2 \frac{R^3}{\|\underline{s}_i(t-\delta_i)\|^3}\left(\frac{3}{2}\,\frac{\hat{\underline{s}}_i'(t-\delta_i)\,\hat{\underline{v}}_i(t-\delta_i)}{\|\hat{\underline{s}}_i(t-\delta_i)\|^2} - 1\right)\hat{\underline{s}}_i(t-\delta_i)$$

$$+ \left(1 - \frac{1}{2}\left(\frac{2\pi}{T}\right)^2 \frac{R^3}{\|\underline{s}_i(t-\delta_i)\|^3}\right)\hat{\underline{v}}_i(t-\delta_i)$$

*For satellite constellations with a geometric dilution of about 10db, satellite tracking errors should be kept to about 5 to 10 feet.

An error of 10^{-10} at synchronous altitude corresponds to about .02 feet.

However, to express a number accurately to within 10^{-10} requires about 33 bits. Thus, if 30 bit registers were to be used in performing the above calculations, one would expect that, after 100 iterations, roundoffs in the calculations would produce much larger errors than would inaccuracies in Eq. (F-6). Because it is desirable to perform the calculations with registers of 30 bits or less, it is now meaningful to attempt to simplify Eq. (F-6).

If the assumption is made that $\|\underline{s}(t)\|$ changes very little over a 100 second interval, then Eqs. (F-3) can be approximated over the interval $(t_1 - \epsilon, t_1 + \epsilon)$ as

$$\dot{\hat{\underline{s}}}(t) = \hat{\underline{v}}(t)$$

$$\dot{\hat{\underline{v}}}(t) = -\left(\frac{2\pi}{T}\right)^2 \frac{R^3}{\|\underline{s}(t_1)\|^3} \hat{\underline{s}}(t) \qquad \text{(F-7)}$$

These equations are now linear and may be solved exactly:

$$\begin{pmatrix} \hat{s}(t) \\ \hat{v}(t) \end{pmatrix} = \begin{pmatrix} \cos w_o(t - t_1)\underline{I} & \frac{1}{W_o} \sin w_o(t - t_1)\underline{I} \\ -w_o \sin w_o(t - t_1)\underline{I} & \cos w_o(t - t_1)\underline{I} \end{pmatrix} \begin{pmatrix} \hat{\underline{s}}\, t_i \\ \hat{\underline{v}}\, t_i \end{pmatrix}$$

where

$$w_o = \frac{2\pi}{T} \left(\frac{R}{\|\underline{s}(t_1)\|}\right)^{3/2}$$

Now suppose that it is desired to estimate the position of satellite i at times $t_o - \delta_i$, $t_o - \delta_i + 1$, ... $t_o - \delta_i + 100$. A ground based computer calculates the actual satellite position and velocity at time $t_o - \delta_i + 50$ using Eqs. (F-4) and (F-5) and the constant

$$w_o = \frac{2\pi}{T} \left(\frac{R}{\|\underline{s}_i(t_o - \delta_i + 50)\|}\right)^{3/2}$$

It then transmits to the aircraft the constants $\cos w_o$, $\frac{1}{w_o} \sin w_o$, and $-w_o \sin w_o$, as well as the estimated position and velocity at time $t_o - \delta_i$ defined as

$$\hat{\underline{s}}_i (t_o - \delta_i) = \cos (50 w_o) \underline{s}_i (t_o - \delta_i + 50) - \frac{1}{w_o} \sin(50 w_o) \underline{v}_i (t_o - \delta_i + 50)$$

$$\hat{\underline{v}}_i (t_o - \delta_i) = w_o \sin (50 w_o) \underline{s}_i (t_o - \delta_i + 50) + \cos (50 w_o) \underline{v}_i(t_o - \delta_i + 50)$$

The aircraft computer then updates these estimates at one second intervals according to the rule

$$\begin{aligned} \hat{\underline{s}}_i (t - \delta_i + 1) &= \cos w_o \hat{\underline{s}}_i (t - \delta_i) + \frac{1}{w_o} \sin w_o \hat{\underline{v}}_i (t - \delta_i) \\ \hat{\underline{v}}_i (t - \delta_i + 1) &= - w_o \sin w_o \hat{\underline{s}}_i(t - \delta_i) + \cos w_o \hat{\underline{v}}_i (t - \delta_i) \end{aligned} \qquad \text{(F-8)}$$

At time $t_o - \delta_i + 50$ the estimates will be identical to the actual position and velocity, except for errors due to roundoffs in the calculations. At time $t_o - \delta_i + 100$ new constants and estimates of the satellite position and velocity are transmitted to the aircraft from the ground.

It has been verified that, for orbits of eccentricity .4 and less, the error due to the approximations of Eq. (F-8) is less than 5 feet over a 100 second interval, if the tracking is done as described in the preceding paragraph. Thus, if the roundoff errors from 100 iterations introduce no more than 45 feet of error, it is clear that the error in $\hat{\underline{s}}_i$ (t) will be bounded by 50 feet.

To estimate the roundoff error produced by 100 iterations, let each of the three position coordinates and three velocity coordinates per satellite be represented by 30 bits (sign bit plus 29 magnitude bits). For a synchronous orbit of maximum eccentricity .4 the maximum magnitudes of position and velocity can be bounded by

$$\begin{aligned} \|\underline{s}(t)\| &< 2 \times 10^8 \text{ feet} \\ \|v(t)\| &< 2 \times 10^4 \text{ feet/sec} \end{aligned} \qquad \text{(F-9)}$$

Since a number can be represented by 29 magnitude bits with a relative error less than $2^{-30} = 10^{-9}$, the satellite position coordinates can be represented to within .2 feet, and the velocity coordinates, to within 2×10^{-5} feet/sec:

$$\begin{aligned} \Delta s &= .2 \\ \Delta v &= 2 \times 10^{-5} \end{aligned} \qquad \text{(F-10)}$$

From Eq. (F-8) it is seen that the dynamics of each coordinate of $\hat{\underline{s}}_i$ (and $\hat{\underline{v}}_i$) are uncoupled, so that each coordinate can be updated independently of the others. Consider one coordinate and define the 2-vector $\underline{x}(t)$ to have as elements the position and velocity for this coordinate. Then, Eq. (F-8) implies that

$$\underline{x}(t+1) = \Phi\, \underline{x}(t)$$

where $\underline{\Phi}$ is the following 2 by 2 matrix

$$\underline{\Phi} = \begin{pmatrix} \cos w_o & \frac{1}{w_o} \sin w_o \\ -w_o \sin w_o & \cos w_o \end{pmatrix}$$

Due to roundoff and truncation errors the aircraft computer generates a sequence of vectors $\hat{\underline{x}}(t_o)$, $\hat{\underline{x}}(t_o + 1)$, ... $\hat{\underline{x}}(t_o + 1)$, ... $\hat{\underline{x}}(t_o + 100)$ according to the equations

$$\hat{\underline{x}}(t+1) = \hat{\underline{\Phi}}\,\hat{\underline{x}}(t) + \underline{n}(t)$$

$$\hat{\underline{x}}(t_o) = \underline{x}(t_o) + \underline{\epsilon}(t_o) \qquad \text{(F-11)}$$

In the above $\hat{\underline{\Phi}}$ represents an approximation to $\underline{\Phi}$ resulting from representing the elements of $\underline{\Phi}$ with 30 bits; $\underline{\Phi}$ and $\hat{\underline{\Phi}}$ are related by the error matrix $\underline{E}$:

$$\underline{\Phi} = \hat{\underline{\Phi}} + \underline{E} \qquad \text{(F-12)}$$

The vector $\underline{\epsilon}(t_o)$ is the truncation error in the initial condition $\hat{\underline{x}}(t_o)$; $\underline{n}(t)$ is the error resulting from rounding $\hat{\underline{\Phi}}\,\underline{x}(t)$ to 30 bits.

The sizes of the elements of $\underline{E}$, $\underline{\epsilon}(t_o)$, and $\underline{n}(t)$ may be bounded as follows. From Eq. (F-10)

$$|\epsilon_1(t_o)| < .2 \text{ feet}$$

$$|\epsilon_2(t_o)| < 2 \times 10^{-5} \text{ feet/sec} \qquad \text{(F-13)}$$

If the additions involved in computing $\underline{\Phi}\,\underline{x}(t)$ are performed prior to rounding the elements of this vector, then it is clear that

$$|n_1(t)| < .2 \text{ feet}$$

$$|n_2(t)| < 2 \times 10^{-5} \text{ feet/sec} \qquad \text{(F-14)}$$

The elements Φ_{11}, Φ_{12}, and Φ_{22} are all approximately of unit value; thus the roundoff errors e_{11}, e_{12}, satisfy

$$
\begin{aligned}
|e_{11}| &< 10^{-9} \\
|e_{12}| &< 10^{-9} \qquad \text{(F-15)} \\
|e_{22}| &< 10^{-9}
\end{aligned}
$$

The element φ_{21} has an approximate value of $-w_o^2$ which has a maximum absolute value (at the perigee of an orbit of eccentricity .4) of 2.5×10^{-8}. Thus the error e_{21} may be bounded as

$$|e_{21}| < 2.5 \times 10^{-17} \qquad \text{(F-16)}$$

Having bounded these error terms, the error in $x(t_o + 100)$ may be bounded by solving Eq. (F-11):

$$\underline{x}(t_o + 100) = \underline{\hat{\Phi}}^{100} (\underline{x}(t_o) + \underline{\varepsilon}(t_o)) + \sum_{i=0}^{99} \underline{\hat{\Phi}}^{i} \, \underline{m}(t_o + 99 - i)$$

Since the true value of $\underline{x}(t_o + 100)$ is $\underline{\Phi}^{100} \underline{x}(t_o)$, the error in $\hat{\underline{x}}(t_o + 100)$ is

$$\underline{\varepsilon}(t_o + 100) = (\underline{\hat{\Phi}}^{100} - \underline{\Phi}^{100}) \, \underline{x}(t_o) + \underline{\hat{\Phi}}^{100} \underline{\varepsilon}(t_o) + \sum_{i=0}^{99} \underline{\hat{\Phi}}^{i} \, \underline{n}(t_o + 99 - i)$$

Now using Eq. (F-12), and ignoring terms that are second order in the errors, it follows that

$$\underline{\varepsilon}(t_o + 100) = \left(\sum_{i=0}^{99} \underline{\Phi}^{i} \, \underline{E} \, \underline{\Phi}^{99-i} \right) \underline{x}(t_o) + \underline{\hat{\Phi}}^{100} \, \underline{\varepsilon}(t_o)$$

$$+ \sum_{i=0}^{99} \underline{\Phi}^{i} \, \underline{n}(t_o + 99 - i)$$

$\underline{\Phi}^i$ may be approximated with very little error as

$$\underline{\Phi}^{i} = \begin{pmatrix} \cos i w_o & \frac{1}{w_o} \sin i w_o \\ -w_o \sin i w_o & \cos i w_o \end{pmatrix} \cong \begin{pmatrix} 1 & i \\ -w_o^2 i & 1 \end{pmatrix}$$

Thus the positional error due to roundoff at time $t_o + 100$ may be bounded by

$$|\varepsilon_1(t_o + 100)| < \Big(100 |e_{11}| + \frac{100 \cdot 99}{2} |e_{21}| + w_o^2 \frac{100 \cdot 99}{2} |e_{12}| +$$

$$w_o^2 \frac{100 \cdot 99 \cdot 98}{6} \cdot |e_{22}|\Big) \; |x_1(t_o)|$$

$$+ \Big(\frac{100 \cdot 99}{2} |e_{11}| + \frac{100 \cdot 99 \cdot 98}{6} |e_{21}| + 100 |e_{12}| + \frac{100 \cdot 99}{2} |e_{22}|\Big) \; |x_2(t_o)|$$

$$+ |\varepsilon_1(t_o)| + 100 \; |\varepsilon_2(t_o)|$$

$$+ \sum_{i=0}^{99} \Big[|m_1(t_o + 99 - i)| + i \, |m_2(t_o + 99 - i)| \Big]$$

Now using

$$w_o^2 < 2.5 \times 10^{-8}$$

$$|x_1(t_o)| < 2 \times 10^{8}$$

$$|x_2(t_o)| < 2 \times 10^{4}$$

with Eqs. (F-13), (F-14), (F-15), and (F-16) it follows that

$$|\epsilon_1 (t_o + 100)| < 41 \text{ feet}$$

It is clear that this bound is quite conservative since many of the roundoff errors will tend to cancel rather than accumulate. However, the bound of 41 feet is the worst case, and, added to the previous error of 5 feet due to using Eqs. (F-7), it is within the desired maximum of 50 feet.

The computer requirements for updating the satellite positions may be summarized as follows. Each satellite needs six 30 bit registers for position and velocity as well as three 30 bit registers for the matrix elements

$$\varphi_{11} = \varphi_{22} = \cos w_o$$

$$\varphi_{12} = \frac{1}{w_o} \sin w_o$$

$$\varphi_{21} = -w_o \sin w_o$$

used in updating the positions and velocities; this totals to forty-five bit registers for five satellites. The computation requirements of Eq. (F-8) are 12 multiplications and 6 adds per satellite; for five satellites this totals to: 60 multiplications and 30 adds.*

---

*A realization of Eq. (F-7) that is computationally more efficient than Eq. (F-8) is

$$\underline{x}(t+1) = \begin{pmatrix} 0 & 1 \\ -1 & 2 \cos w_o \end{pmatrix} \underline{x}(t)$$

For appropriate initial conditions, $x_1(t)$ tracks one of the coordinates of s(t). However, in spite of the computational efficiency, the roundoff errors due to 100 iterations of the above can be considerably greater than 50 feet. A possible subject of future work is the determination of a realization that is simultaneously efficient and accurate.

F.4 Computing the Distances $\|\hat{\underline{s}}_i (t - \delta_i) - \underline{p}^*(t)\|$

The components of the vector f ($\underline{p}^*$ (t), t) are defined as

$$f_i (\underline{p}^* (t), t) = \|\hat{\underline{s}}_i(t - \delta_i) - \underline{p}^*(t)\|$$
$$= \left[(\hat{\underline{s}}_i (t - \delta_i) - \underline{p}^*(t))' (\underline{s}_i (t - \delta_i) - \underline{p}^*(t)\right]^{1/2}$$

These numbers can be easily computed via a Newton-Raphson iteration to the square root; i.e. for

$$x_{k+1} = \frac{x_k^2 + a}{2 x_k}$$

the sequence $\{x_k\}$ converges to $\sqrt{a}$, for any nonzero initial guess x_o. In fact, if x_k is related to $\sqrt{a}$ as

$$x_k = (1 + \epsilon) \sqrt{a}$$

then it follows that

$$x_{k+1} = (1 + \frac{1}{2} \frac{\epsilon^2}{1 + \epsilon}) \sqrt{a}$$

With respect to the computation of $f_i(\underline{p}^*(t), t)$, there are two cases to consider: that case where the computation of f_i ($\underline{p}^*(t - 1)$, t - 1) has been performed one second in the past, and the case where f_i ($\underline{p}^*(t-1)$, t - 1) has not been computed. The latter case arises at the beginning of a flight and whenever the tracking of a new satellite is initiated. In such cases a reasonable initial guess of f_i ($\underline{p}^*(t)$, t) is

$$26,000 \text{ miles} = 1.37 \times 10^8 \text{ feet}$$

The error in this initial guess may be bounded by considering an orbit of maximum eccentricity .4, in which case

$$-.36 < \epsilon < 1.24$$

For such initial errors, a maximum of five iterations is needed to reduce the error to less than 10^{-9}. The computation requirements are: 3 multiplications and 5 adds to determine $\|\hat{\underline{s}}_i (t - \delta_i) - \underline{p}^* (t)\|^2$, then 5 multiplications, 5 adds, and 5 divides to converge to $\|\hat{\underline{s}}_i (t - \delta_i) - \underline{p}^*(t)\|$. This totals to: 8 multiplications, 10 adds, and 5 divides per satellite.

If $f_i (\underline{p}^*(t - 1), t - 1)$ has been previously computed, then this value may be used as the initial guess. Since the satellite velocity is bounded by 2×10^4 feet/sec, and the aircraft velocity, by 10^3 feet/sec, it follows that the error in this initial guess may be bounded by

$$|\epsilon| < 3.5 \times 10^{-4}$$

For this initial error two iterations are required to reduce the error to below 10^{-9}. Thus the total number of computations in this case for five satellites totals to: 25 multiplications, 35 adds, and 10 divides per satellite.

F.5 Computation of the Vectors $\underline{u}_i$ and the Matrix $\underline{H}\ \underline{F}$

As the vectors $(\hat{\underline{s}}_i (t - \delta_i) - \underline{p}^*(t))$ have been computed previously, the calculation of $\underline{u}_i$ merely involves dividing each component of $(\hat{\underline{s}}_i (t - \delta_i) - \underline{p}^*(t))$ by $\|\underline{s}_i (t - \delta_i) - \underline{p}^*(t)\|$, hence three divides per satellite. Computation of each row of $\underline{H}\ \underline{F}$ requires 3 adds. Since $\underline{H}\ \underline{F}$ has (N - 1) rows, where N is the number of satellites, this phase of the computation has the following requirements for five satellites: 15 divides and 12 adds.

F. 6 Solving for $\hat{\underline{p}}(t)$ in the Rectangular Coordinate System

The most efficient method of solving

$$(\underline{F}'\underline{H}'\underline{H}\underline{F})(\hat{\underline{p}}(t) - \underline{p}^*(t)) = \underline{F}'\underline{H}'(c\underline{H}\hat{\underline{\tau}}(t) + c\underline{H}\underline{\delta} - \underline{H}\underline{f}(\underline{p}^*(t), t))$$

for $\underline{p}(t) - \underline{p}^*(t)$ is to use the Gaussian elimination method. The initial phase of this method involves computing the elements of the array $(\underline{F}'\underline{H}'\underline{H}\underline{F})$ and the elements of the vector $\underline{F}'\underline{H}'(c\underline{H}\underline{\tau}(t) + c\underline{H}\underline{\delta} - \underline{H}\underline{f}(\underline{p}^*(t), t))$. Since $(\underline{F}'\underline{H}'\underline{H}\underline{F})$ is a symmetric 3 by 3 matrix, only six elements need be computed, each by computing the scalar product of two (N - 1)-vectors. For five satellites this requires: 24 multiplications and 18 adds.

The components of the vector $c\underline{H}\underline{\delta}$ are stored as constants in the computer; and the vector $\underline{H}\hat{\underline{\tau}}(t)$ is an input to the computer. Therefore, the computation of each element of the (N-1)-vector $(cH\hat{\tau}(t) + cH\delta - Hf(\underline{p}^*(t), t))$ requires 1 multiplication and 3 adds; this totals to 4 multiplications and 12 additions for five satellites. Multiplication of this (N-1)-vector by the 3 by (N-1) matrix $\underline{F}'\underline{H}'$ requires 3(N-1) multiplications and 3(N-2) adds; for five satellites this is 12 multiplication and 9 adds.

Thus, for five satellites, the initial phase of the Gaussian elimination requires a total of 40 multiplications and 39 adds.

Having performed the intial phase of solving for $\hat{\underline{p}}(t) - \underline{p}^*(t)$, the Gaussian elimination algorithm may now be used. However, some care must be taken to avoid divide overflows while still maintaining accuracy by representing each number with as many bits as possible. For simplicity of notation define

$$\underline{A} = \underline{F}'\underline{H}'\underline{H}\underline{F}$$

$$\underline{b} = \underline{F}'\underline{H}'(c\underline{H}\hat{\underline{\tau}}(t) + c\underline{H}\delta - \underline{H}\underline{f}(\underline{p}^*(t), t))$$

$$\underline{x} = \hat{\underline{p}}(t) - \underline{p}^*(t)$$

Thus, the problem is to find the solution $\underline{x}$ to $\underline{A}\ x = \underline{b}$.

The first step in the Gaussian elimination involves finding the largest diagonal element of $\underline{A}$. If this element is not a_{11}, the rows and columns of $\underline{A}$, $\underline{b}$, and $\underline{x}$ are permuted so that a_{11} becomes the largest diagonal element. Now the array $(\underline{A}:\underline{b})$ is premultiplied by the matrix $\underline{P}_1$:

$$\underline{P}_1 = \begin{pmatrix} 1 & 0 & 0 \\ -\frac{a_{21}}{a_{11}} & 1 & 0 \\ -\frac{a_{31}}{a_{11}} & 0 & 1 \end{pmatrix}$$

to obtain

$$\underline{P}_1\ (\underline{A}:\underline{b}) = \begin{pmatrix} & \underline{a}_1' & b_1 \\ \underline{0} & \underline{\hat{A}} & \underline{\hat{b}} \end{pmatrix}$$

where $\underline{a}_1'$ is the first row of $\underline{A}$. The diagonal elements of $\underline{\hat{A}}$ are searched, and the rows and columns of $\underline{\hat{A}}$, $\underline{a}_1'$, $\underline{\hat{b}}$, and x are permuted so that a_{11} is the larger. $\underline{P}_1\ (\underline{A}:\underline{b})$ is now premultiplied by $\underline{P}_2$:

$$\underline{P}_2 = \begin{pmatrix} 1 & 0 & 0 \\ 0 & 1 & 0 \\ 0 & -\frac{\hat{a}_{21}}{\hat{a}_{11}} & 1 \end{pmatrix}$$

to obtain

$$\underline{P}_2 . \underline{P}_1\ (\underline{A}:\underline{b}) = \begin{pmatrix} & \underline{a}_1' & & b_1 \\ 0 & & \underline{\hat{a}}_1' & \hat{b}_1 \\ & 0 & \tilde{a} & \tilde{b} \end{pmatrix}$$

The solution $\underline{x}$ is now found as

$$x_3 = \frac{\tilde{b}}{\tilde{a}}$$

$$x_2 = \frac{1}{\hat{a}_{11}} (\hat{b}_1 - \hat{a}_{12} x_3)$$

$$x_1 = \frac{1}{a_{11}} (b_1 - a_{12} x_2 - a_{13} x_3)$$

The matrix $\underline{A}$ is symmetric; since $\underline{H}\,\underline{F}$ may be assumed to have rank equal to three, $\underline{A}$ is also positive definite. It thus follows that for $1 \leq i \leq 3$ and $1 \leq j \leq 3$

$$|a_{ij}| \leq \max_k a_{kk} < \mathrm{tr}\,(\underline{A})$$

where tr($\cdot$) is the trace operation. Also,

$$\mathrm{tr}\,(\underline{A}) = \mathrm{tr}\,(\underline{F}'\underline{H}'\underline{H}\,\underline{F}) = \mathrm{tr}\,(\underline{H}\,\underline{F}\,\underline{F}'\underline{H}')$$

$$= \sum_{i=1}^{4} \|\underline{u}_i - \underline{u}_{i+1}\|^2$$

$$= 4 \sum_{i=1}^{4} \sin^2 \left(\frac{\theta_{i,\ i+1}}{2}\right)$$

where $\theta_{i,\ i+1}$ is the angle between the unit vectors $\underline{u}_i$ and $\underline{u}_{i+1}$ (In the above it is assumed that there are five satellites). A conservative bound for each a_{ij} is thus

$$|a_{ij}| < 16$$

From the above inequality, it is clear that all the elements of A may be stored in 30-bit registers with the following format:

sign bit	4 integer bits	25 fraction bits

The error in these numbers is thus bounded by

$$\epsilon_a = 2^{-26} \cong 1.5 \times 10^{-8}$$

The matrix $\hat{\underline{A}}$ is given by

$$\hat{\underline{A}} = \begin{pmatrix} a_{22} - \dfrac{a_{12}^2}{a_{11}} & a_{23} - \dfrac{a_{12}\, a_{13}}{a_{11}} \\ \\ a_{23} - \dfrac{a_{12}\, a_{13}}{a_{11}} & a_{33} - \dfrac{a_{13}^2}{a_{11}} \end{pmatrix}$$

$\hat{\underline{A}}$ can be easily shown to be positive definite. Thus, since a_{22} and a_{33} are both less than a_{11}, all the elements of $\hat{\underline{A}}$ are bounded by a_{11}, and thus by 16. Similarly $\tilde{a}$ is bounded by 16. Therefore the Gaussian elimination produces no left overflows in the elements of $\underline{A}$.

The vector $\underline{x}$ represents the difference between $\underline{p}^*(t)$ and $\hat{\underline{p}}(t)$. The length of $\underline{x}$ thus depends on the error in the prediction $\hat{\underline{p}}^*(t)$ (which, in turn, depends on the errors in the estimates $\hat{\underline{p}}(t - 1)$ and $\hat{\underline{p}}(t - 2)$) and errors in $\hat{\underline{T}}(t)$ and $\underline{s}_i\ (t - \delta_i)$, i = 1, 2, 3, 4, 5. Assuming that there are no gross errors, $\|\underline{x}\|$ may be bounded a priori as

$$\|x\| < 10^3 \text{ feet}$$

From the above bound, and the relation $\underline{A}\,\underline{x} = b$, $\underline{b}$ may be bounded as

$$\|\underline{b}\| < \lambda_{max} \cdot 10^3$$

where λ_{max} is the largest eigenvalue of $\underline{A}$. Since $\underline{A}$ is positive definite,

$$\lambda_{max} < tr\,(\underline{A}) < 16$$

and so a conservative bound for $\|b\|$ is

$$\|\underline{b}\| < 1.6 \times 10^4$$

In the Gaussian elimination the vector $\hat{\underline{b}}$ is given by

$$\hat{\underline{b}} = \begin{pmatrix} b_2 - \dfrac{a_{12}\, b_1}{a_{11}} \\ \\ b_3 - \dfrac{a_{13}\, b_1}{a_{11}} \end{pmatrix}$$

and since $\dfrac{a_{12}}{a_{11}}$ and $\dfrac{a_{13}}{a_{11}}$ are both bounded in absolute value by unity, it follows that

$$|\hat{b}_i| < 3.2 \times 10^4$$

by similar reasoning,

$$|\tilde{b}| < 6.4 \times 10^4$$

Thus, a format for the elements of $\underline{b}$ that assures no left overflows is

sign bit	16 integer bits	13 fraction bits

The errors in these numbers are bounded by

$$\epsilon_b = 2^{-14} \cong 6 \times 10^{-5}$$

An analysis of the error in the solution $\underline{x}$ reveals that the predominating sources are the truncation errors in the elements of $\underline{A}$ and $\underline{b}$; roundoff errors in the computations contribute only slightly. Thus, if $\underline{x}$ is the result of the Gaussian elimination,

$$(\underline{A} + \underline{E})\,\hat{\underline{x}} = \underline{b} + \underline{e}$$

where $\underline{E}$ represent truncation errors in $\underline{A}$, and $\underline{e}$, truncation errors in $\underline{b}$. Writing this as

$$\underline{A}(\underline{I} + \underline{A}^{-1}\underline{E})\,\hat{\underline{x}} = \underline{b} + \underline{e}$$

to first order $\hat{\underline{x}}$ is

$$\begin{aligned}\hat{\underline{x}} &= (\underline{I} + \underline{A}^{-1}\underline{E})^{-1}\underline{A}^{-1}(\underline{b} + \underline{e}) \\ &\cong (\underline{I} - \underline{A}^{-1}\underline{E})\,\underline{A}^{-1}(\underline{b} + \underline{e}) \\ &\cong \underline{A}^{-1}\underline{b} - \underline{A}^{-1}\underline{E}\,\underline{A}^{-1}\underline{b} + \underline{A}^{-1}\underline{\epsilon}\end{aligned}$$

Thus the solution error $\|\underline{x} - \hat{\underline{x}}\|$ may be approximately bounded as

$$\|\underline{x} - \hat{\underline{x}}\| \cong \|\underline{A}^{-1}\,\underline{E}\,\underline{x} + \underline{A}^{-1}\,\underline{e}\|$$

$$\|\underline{x} - \hat{\underline{x}}\| \leq \|\underline{A}^{-1}\,\underline{E}\,\underline{x}\| + \|\underline{A}^{-1}\,\underline{e}\|$$

$$\|\underline{x} - \hat{\underline{x}}\| \leq \frac{1}{\lambda_{min}} \left(3\,\|\underline{x}\|\;\epsilon_a + \sqrt{3}\;\epsilon_b\right)$$

where λ_{min} is the smallest eigenvalue of $\underline{A}$.

The determinant of $\underline{A}$ depends on the satellite configuration; a conservative lower bound is

$$\det(\underline{A}) > 5 \times 10^{-4}$$

The product of the eigenvalues of $\underline{A}$ equals det $(\underline{A})$, and since the sum of the eigenvalues is the trace and thus less than 16, λ_{min} can be bounded as

$$\lambda_{min} > \frac{5 \times 10^{-4}}{8 \cdot 8}$$

$$\lambda_{min} > 8 \times 10^{-6}$$

The error $\|x - \hat{x}\|$ may thus be bounded as

$$\|\underline{x} - \hat{\underline{x}}\| < \frac{3 \times 10^{3} \times 1.5 \times 10^{-8} + 1.7 \times 6 \times 10^{-5}}{8 \times 10^{-6}}$$

$$\|\underline{x} - \hat{\underline{x}}\| < 20 \text{ feet}$$

This is the error resulting from a worst case; in most cases $\|x - \hat{x}\|$ will be only a few feet.

The computational requirements for the Gaussian elimination solution of $\hat{\underline{p}}(t) - \underline{p}^*(t)$ are: 10 multiplications, 6 divides, and 10 adds. Adding $\hat{\underline{p}}(t) - \underline{p}^*(t)$ to $\underline{p}^*(t)$ requires 3 adds. Thus the total computation requirements for determining $\hat{\underline{p}}(t)$ are: 50 multiplications, 52 adds, and 6 divides.

F.7 Conversion of $\hat{\underline{p}}(t)$ to Latitude, Longitude, and Altitude

The final stage in the computation is to convert $\hat{\underline{p}}(t)$ to a position in a rotating spherical coordinate system. The latitude $\hat{\lambda}(t)$, longitude $\hat{\Upsilon}(t)$, and radius $\hat{r}(t)$, are related to $\hat{\underline{p}}(t)$ by

$$\hat{p}_x(t) = \hat{r}(t) \cos \hat{\lambda}(t) \cos \left(\hat{\Upsilon}(t) - \frac{2\pi t}{T} \right)$$

$$\hat{p}_y(t) = -\hat{r}(t) \cos \hat{\lambda}(t) \sin \left(\Upsilon(t) - \frac{2\pi t}{T} \right)$$

$$\hat{p}_z(t) = \hat{r}(t) \sin \hat{\lambda}(t)$$

Thus, $\hat{\lambda}(t)$, $\hat{\Upsilon}(t)$, and $\hat{r}(t)$ are determined by the equations

$$\hat{r}(t) = \sqrt{\hat{p}_x^2(t) + \hat{p}_y^2(t) + \hat{p}_z^2(t)}$$

$$\hat{\lambda}(t) = \sin^{-1} \frac{\hat{p}_z(t)}{\hat{r}(t)}$$

$$\hat{\gamma}(t) = \frac{2\pi t}{T} - \sin^{-1} \left(\frac{\hat{p}_y(t)}{\hat{p}_x^2(t) + \hat{p}_y^2(t)} \right)$$

To express the aircraft position to within 50 feet in terms of $\hat{r}$, $\hat{\lambda}$, and $\hat{\gamma}$, it is sufficient for the accuracy of $\hat{r}$ to be 25 feet, and the accuracies of $\hat{\lambda}$ and $\hat{\gamma}$ to be 4×10^{-3} minutes of arc. Therefore, 30 bits are more than sufficient for each of these quantities. The on-board clock has an accuracy of two parts in 10^6; thus, over a 100 second interval of time, the quantity $\frac{2\pi t}{T}$ can be computed to within 5×10^{-5} minutes of arc. (Recall that the real-time aircraft clock is reset at 100 second intervals). This accuracy is certainly more than adequate.

The square root computation for $\hat{r}(t)$ can be performed via the Newton-Raphson method. Since $\hat{r}(t)$ differs from $\hat{r}(t-1)$ by at most 10^3 feet, or a factor of about 5×10^{-5}, one iteration of the Newton-Raphson method is sufficient to get accuracy of 2.5×10^{-2} feet. Thus $\hat{r}(t)$ may be computed as

$$\hat{r}(t) = \frac{\hat{r}^2(t-1) + \|\hat{p}(t)\|^2}{2\,\hat{r}(t-1)}$$

This computation requires 4 multiplications, 3 adds, and 1 divide.

The value of $\sqrt{\hat{p}_x^2 + \hat{p}_y^2}$ at time t differs from its value at time t-1 by at most 10^3 feet. If it is assumed that the aircraft remains south of 60° North latitude, the smallest that $\sqrt{\hat{p}_x^2(t-1) + \hat{p}_y^2(t-1)}$ can be is 2,000 miles, or about 10^7 feet. Then $\sqrt{\hat{p}_x^2 + \hat{p}_y^2}$ changes by at most a factor of 10^{-4} in one second. Therefore, if $\sqrt{\hat{p}_x^2(t) + \hat{p}_y^2(t)}$ is computed as

$$\sqrt{\hat{p}_x^2(t) + \hat{p}_y^2(t)} = \frac{\left[\sqrt{\hat{p}_x^2(t-1) + \hat{p}_y^2(t)}\right]^2 + \left[\hat{p}_x^2(t) + \hat{p}_y^2(t)\right]}{2\sqrt{\hat{p}_x^2(t-1) + \hat{p}_y^2(t-1)}}$$

then the accuracy of 10^{-1} feet is attained. This computation requires 1 multiplication, 1 add, and 1 divide since $p_x^2(t) + p_y^2(t)$ is computed during the computation of $r(t)$.

The inverse sines in the expressions for $\lambda(t)$ and $\gamma(t)$ could be evaluated via a series. However, the following table look-up method is faster. A table (read-only memory) of 364 entries contains the numbers

$$a_k = \sin^{-1}(k \cdot 2^{-9}), \quad k = 0, 1, 2, \ldots 363$$

Each of these numbers is specified by 22 bits, to give an accuracy of 5×10^{-4} minutes of arc. To compute the inverse sine of x where $0 \leq x \leq \sqrt{2}/2$, let n be the integer part of $x \cdot 2^9$, and let α be the fraction part of $x \cdot 2^9$. Then the inverse since of x, to within 4×10^{-3} minutes, is

$$\sin^{-1}(x) \cong a_n + \alpha \cdot (a_{n+1} - a_n)$$

If $\sqrt{2}/2 < x \leq 1$, one first computes $1 - x^2$ and uses

$$\sin^{-1}(x) = 90^\circ - \sin^{-1}(\ 1 - x^2)$$

The inverse sine of $1 - x^2$ is computed via the avove table look up. Computation of $1 - x^2$ can be done via Newton-Raphson. A maximum of five iterations is required if $\sqrt{2^{2n}(1 - x^2)}$ is found, where $.25 < 2^{2n}(1 - x^2) < 1$, and if $2^{2n}(1 - x^2)$ is used as a starting point. Then $1 - x^2$ is found as

$$1 - x^2 = 2^{-n}\sqrt{2^{2n}(1 - x^2)}$$

Using this table look-up method, $\sin^{-1}(x)$ may be found with only 2 adds and 1 multiplication, if $0 < x < \sqrt{2}/2$. An additional 6 multiplication, 7 adds, and 5 divides are needed if $\sqrt{2}/2 < x < 1$. This averages to 6 adds, 3 divides, and 4 multiplications. Some additional logic is also required to determine the correct branch of the inverse sine.

In summary, calculation of $\hat{r}$ requires 4 multiplications, 3 adds, and 1 divide; to find the altitude one additional add is used. Calculation of $\hat{\lambda}$ requires a divide and an inverse sine; thus 6 adds, 4 multiplications, and 4 divides. Computation of $\hat{\gamma}$ requires 6 multiplications, 8 adds, and 5 divides. The total computation requirements are thus: 14 multiplications, 18 adds, and 10 divides.

F.8 Total Computer Requirements

The total number of airthmetic operations required for each aircraft position estimates is

149 multiplications
41 divisions
150 additions

Each of these operations involves 30-bit registers.

It is estimated that eighty-six 30-bit registers of read-write memory are required. In addition, a read-only memory consisting of three hundred and sixty-four 22-bit registers forms the table for computing inverse sines. If one allows five non-computation instructions (e.g., shifts, stores, loads, etc.) per computational instruction, then the total program length can be conservatively estimated at 2100 instructions.

One can expect that by 1990 the cost of such a computer, designed as a special purpose computer and produced in quantities of 10^5, will be insignificant compared with the costs of the aircraft receiver and display system.

However, the computational load is also well within the capacity of a 1971 minicomputer costing only several thousand dollars. For example, it is estimated that a 16-bit, 4096 word Nova computer with a memory cycle time of 2.6μsec can easily perform the necessary calculations (using double precision arithmetic) in 10 to 20 msec. Thus, if a Nova computer were to be used for the navigation calculations, it would be free for other calculations 98% of the time.

F.9 Improved Satellite Tracking

An aircraft computer designed according to the preceding sections should provide sufficiently accurate estimates of the aircraft position, particularly if a satellite constellation with low geometric dilution is used. However, errors in estimating the satellite positions produce errors in the aircraft position estimate; moreover, these satellite tracking errors are amplified by the geometric dilution. Thus, if the geometric dilution is 10, the possible satellite tracking errors of 46 feet (as determined in Section F.3) could produce aircraft position errors of 460 feet. Such an error could be unacceptable.

Satellite tracking errors can be reduced in a number of ways. If the satellite positions are updated recursively as in Section F.3 then the total error after K_2 iterations can be bounded by

$$.05 K_2 + 2^{-(b - 30)} (.4K_2 + .5) \text{ feet}$$

where b is the number of bits used in the computations. Thus it is seen that if

$$K_2 = 50$$

$$b = 33$$

then the satellite tracking error will be bounded by about five feet. Of course, this implies that correct satellite ephermeris data are received every 50 seconds.

A second method of reducing the satellite tracking errors is to calculate the satellite positions using Eqs. (F-4) and (F-5). These calculations involve computing sines and cosines to 30 - bit accuracy; thus the implementation of these equations could be quite costly in terms of computation time. However, it has been estimated in Section F. 8 that only about 20 msec will be spent each second on the aircraft position computations. Thus there should be ample time for tracking the satellites using Eqs. (F-4) and (F-5). Note that if these computations were performed just before the pulses arrive from the satellites, the aircraft position computations could still be completed 20 msec after the last pulse arrival time.

The accuracy with which the satellites can be tracked using Eqs. (F-4) and (F-5) depends on the accuracy with which time can be measured on the aircraft. From Eq. (F-4) follows that

$$\dot{\varphi}(t) = \frac{2\pi}{T} \quad \frac{1}{1 - e \cos \varphi(t)},$$

and so

$$|\dot{\varphi}(t)| \leq \frac{7.27 \times 10^{-5}}{1 - e} \qquad \text{(F-17)}$$

If the aircraft clock has an rms error of 2 parts in 10^6, the rms timing error at the end of a 100 second interval is .2 msec. Thus, the rms error in $\varphi(t)$ is exactly calculated by Eq. (F-4), is bounded by

$$(\Delta \varphi)_{rms} \leq \frac{1.45 \times 10^{-8}}{1 - e} \quad \text{radians} \tag{F-18}$$

To solve Eq. (F-4), one would probably use the Newton-Raphson technique. That is, the sequence x_n defined by

$$x_{n+1} = \frac{\frac{2\pi (t - t_p)}{T} + e \sin x_n - e\, x_n \cos x_n}{1 - e \cos x_n} \tag{F-19}$$

converges to $\varphi(t)$. If the error in x_n is Δ radians, then the error in x_{n+1} is less than $\frac{\Delta^2}{2}$ radians. If one lets

$$x_o = \varphi(t - 1)$$

then, by Eq. (F-17), the error in x_o is bounded by

$$|\Delta_o| \leq \frac{7.27 \times 10^{-5}}{1 - e}$$

Thus, after only one iteration of Eq. (F-19), the error in x_1, is bounded by

$$|\Delta_1| \leq \frac{2.6 \times 10^{-9}}{(1 - e)^2}$$

Combining the above with Eq. (F-18), it follows that the rms error in the calculated value of $\varphi(t)$ is bounded by

-3-

$$\Delta\varphi_{rms} \leq \frac{1.45 \times 10^{-8}}{1 - e} + \frac{2.6 \times 10^{-9}}{(1 - e)^2} \quad \text{radians}$$

Only the satellite tracking errors in the radial direction introduce errors in the estimated aircraft position. The rms error in the satellite radius is bounded by

$$(\Delta r)_{rms} \leq e\, R\, \Delta\varphi_{rms}$$

where R = 26000 miles = 1.37×10^8 feet. Thus, when the orbit eccentricity is less than or equal to .4, the satellite tracking errors in the radial direction are bounded by

$$(\Delta r)_{rms} \leq 1.8 \text{ feet}$$

Thus, a significant improvement in the accuracy of tracking the satellite can be obtained at the expense of somewhat more time consuming calculations.

To track each satellite using Eqs. (F-4) and (F-5) would require the following computations each second:

Calculation of one sine and one cosine
6 additions
11 multiplications
1 divide

These computational requirements (for tracking five satellites) are about the same as those listed at the end of Section F. 3, with the exception of the sine and cosine calculations.

APPENDIX G

REFLECTION MULTIPATH AND ANTENNA APERTURE SIZE FOR AIR-TO-GROUND SYSTEM

G.1 Introduction

Reflection multipath is an important factor to consider in the design of an air to ground multilateration system. Reflections from the surface of the ground or sea, buildings, water towers, aircraft, and vehicles can all be important, depending upon the site chosen for the ground based antenna. We assume that the antenna sites are chosen so that reflections from buildings, water towers, aircraft and vehicles are not a major problem. This can be done by mounting the antenna on a high tower, well above all buildings, and away from areas where there are low flying aircraft. With this type of siting the only reflections that one needs to consider are reflections from the surface of the ground or the sea. These reflections will dominate the multipath effect on the system.

If the ground is very rough a valid mathematical model of the multipath phenomenon must postulate a large number of individual scatterers. The phase angles of the signals received from the different scatters will not be the same but will vary. This is due to the differences in total path lengths from the aircraft to each of the scatterers to the ground based antenna. Thus, multipath signals received from very rough ground will add incoherently rather than in phase. The resultant interference at the receiving antenna is called "non-specular multipath." (In radar terminology this is called clutter). This interference is similar in effect to background noise at the receiver; however, it increases in proportion to the signal level. In the air-to-ground system environment, non-specular multipath is not expected to present much problem.

Multipath reflections from ground which is locally smooth at the point of reflection can present a considerable interference problem. We shall consider in this Appendix the effect of multipath interference emanating from a ground plane which is perfectly smooth around the point of reflection and which has a reflection coefficient of unity.

The assumption of a smooth, perfectly reflecting ground plane, although not generally valid, is a good approximation as we discuss below. We are primarily concerned with aircraft which have low elevation angles, φ, relative to the ground antenna because the multipath problem is not particularly severe for aircraft at high angles, especially for the type of ground antennas needed to combat multipath for aircraft at low angles. A commonly accepted "rule of thumb" regarding surface roughness is the Raleigh criterion. Applied to the geometry considered here it implies that if the average of the peak to valley variations in the surface, δ, is less than $\lambda/(8 \sin\varphi)$ where λ is the wavelength, the reflected signal will be approximately equal to that from a smooth surface. For $\varphi = 0.5$ degrees considered later, δ must be less than 12.5λ or roughly 10 feet which certainly is true of the ground in many parts of the country. Thus, our assumption of a smooth ground plane is reasonable. Regarding the second assumption, unity reflection coefficient, it has been shown that for elevation angles of less than 0.8 degrees sea water, dry earth, and wet earth all have reflection coefficients greater than 0.8. This is even true when one takes into account the spherical nature of the surface of the Earth, which must really be done at transmission ranges of the order of 200 miles. (This is usually taken into account by a parameter called the divergence factor.) Thus, the assumption of unity reflection coefficient is reasonable.

G.2 Analysis

With the assumptions of a smooth surface, the signal received at the ground antenna can be decomposed into two components: One coming directly from the aircraft and the other, the specular component, reflected from the ground. In the design of the air to ground system two parameters are of primary interest: the amplitude of the reflected signal relative to the direct signal and the time delay of the reflected signal relative to the direct signal.* From geometry the relative time delay can be approximated by

$$t_D = \frac{2h}{c} \sin \varphi$$

where h is the height of the antenna above the ground plane, c is the speed of light and it is assumed that the distance of the aircraft from the antenna is much greater than h. For $\varphi = 0.5$ degrees, even for a 500 foot high antenna tower t_D is only 10^{-2} μsec. Thus with available bandwidths of 10 to 20 MHz, there is no possibility of discriminating against this reflection multipath using sophisticated modulation techniques. Thus the full amplitude of this multipath must be included as a propagation loss in the link calculation as was done in Sections 2 and 4 of this report.

We now determine the amplitude of the reflected signal relative to the direct signal as it appears at the output terminals of the antenna. The results of a computer analysis** to determine the relative amplitude are shown in the curves of Figs. G.1 through G.4. These curves can be interpreted as follows. The hyperbolic-like curves are lines of constant altitude above the surface of the spherical earth obtained using the 4/3 earth approximation. Thus one can relate the elevation angle and range of the aircraft to its altitude. The solid parabolic-like curve is basically

*The relative phase shift of the two signals is a thrid parameter that is not of direct interest here. It can be obtained from the relative delay and the phase angle of the reflection coefficient.

**The results shown in Figs. G.1 through G.4 were obtained by H. Berger of Lincoln Laboratory.

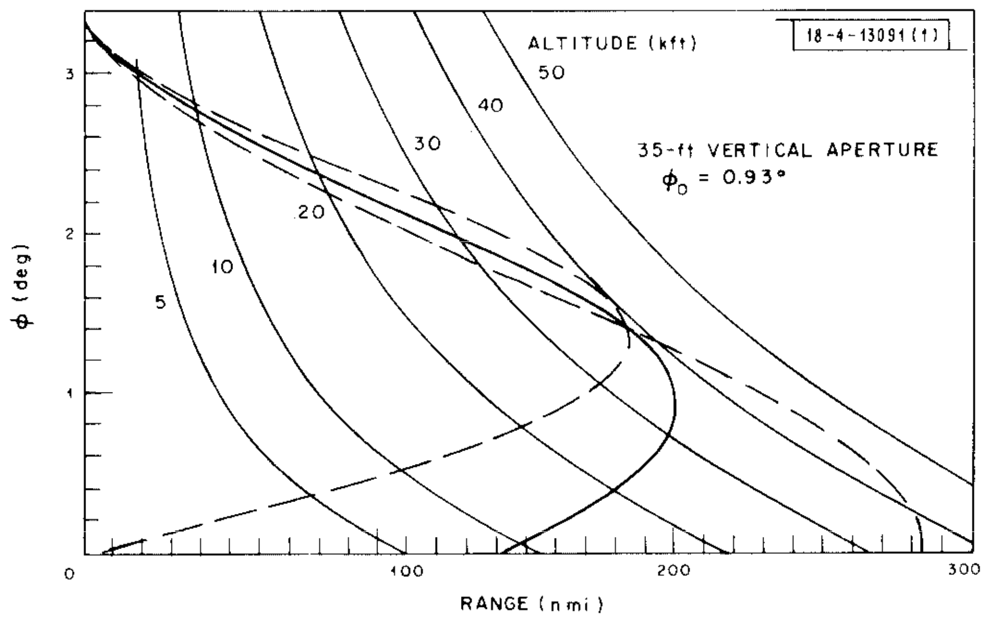

Fig. G.1. Antenna pattern for 35-foot vertical aperture with a perfectly conducting ground plane reflector, elevation angle of 0.93°.

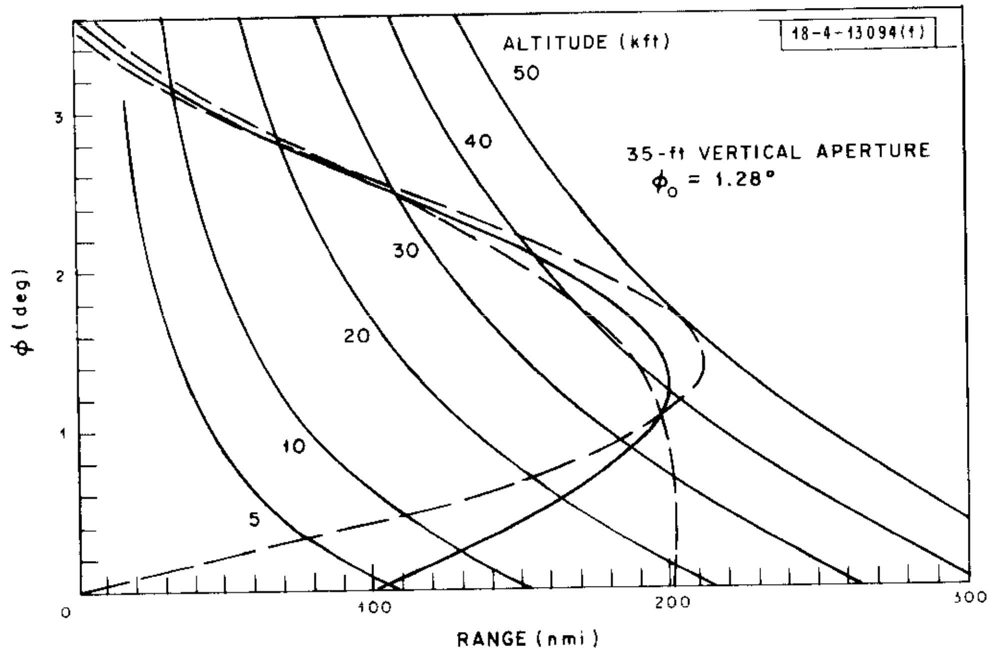

Fig. G.2. Antenna pattern for 35-foot vertical aperture with a perfectly conducting ground plane reflector, elevation angle of 1.28°.

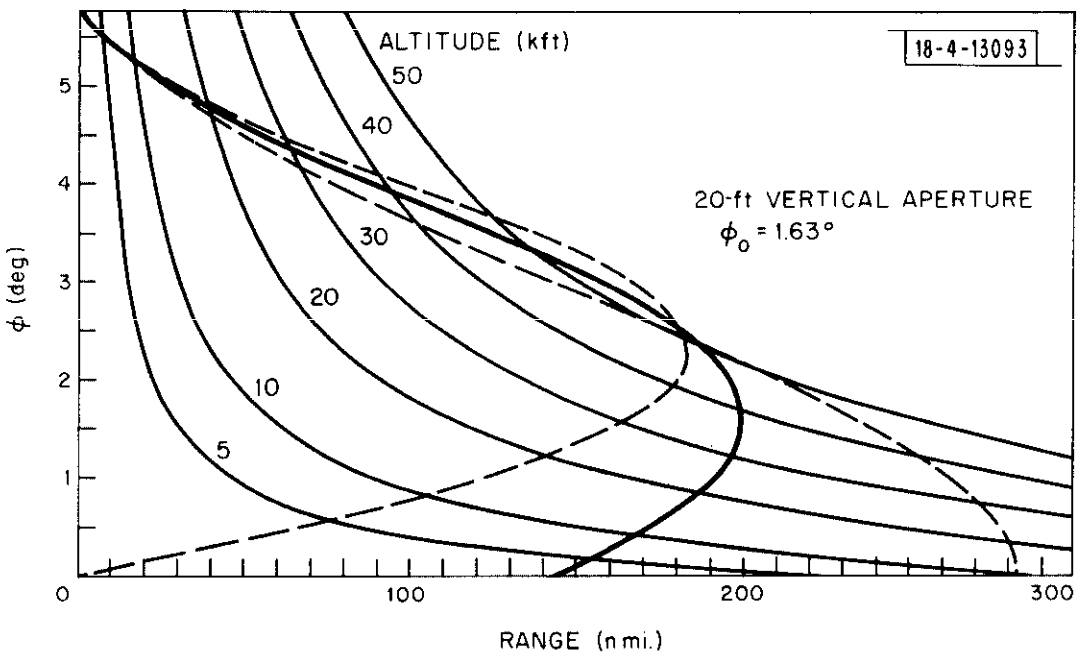

Fig. G.3. Antenna pattern for 20-foot vertical aperture with a perfectly conducting ground plane reflector, elevation angle of 1.63°.

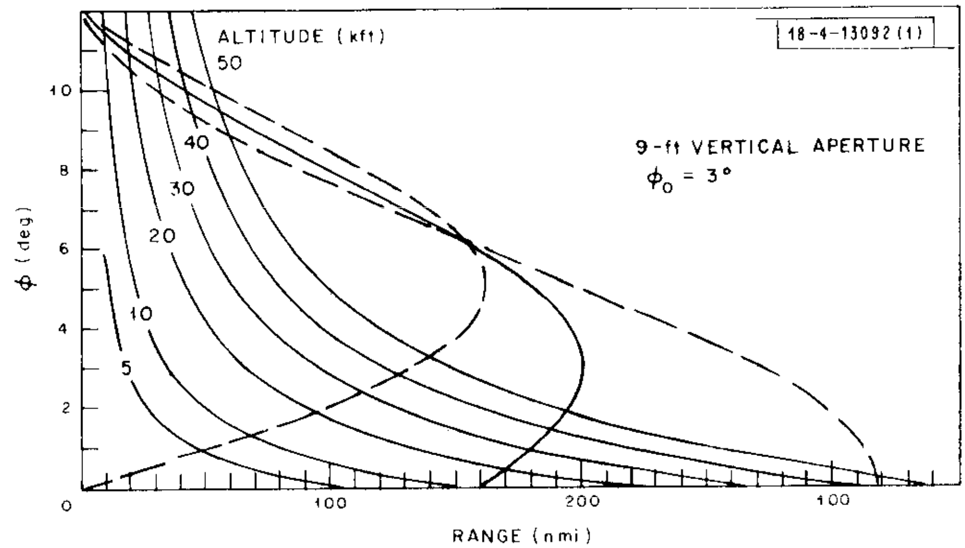

Fig. G.4. Antenna pattern for 9-foot vertical aperture with a perfectly conducting ground plane reflector, elevation angle of 3°.

the pattern of the antenna* which one could measure if the ground plane did not exist.** Because the ground plane exists, the antenna pattern will have maxima and minima. The width of the lobes thus formed will depend upon h, the height of the antenna. The envelope of these lobes is, to first order, independent of h, however. The dashed curves are the envelopes of the maxima and minima.

G.3 Results

Fig. G.1 shows an antenna with a vertical aperature of 35 feet and thus a narrow elevation beamwidth.

As can be seen from Fig. G.1, the following two cases result in the same size signal at the antenna output terminals.

i) An aircraft at 200 miles range and $\varphi = 1^{\circ}$ elevation, i.e. on the peak of the antenna beam, when no ground plane is present.

ii) An aircraft at 100 miles range and $\varphi = 0.5^{\circ}$ elevation when the ground plane is present and h is chosen such that the deepest part of a null occurs at $\varphi = 0.5^{\circ}$.

This implies that if a link calculation is done on the basis of an aircraft at 200 miles range on the peak of the beam, one must include a multipath loss of $6\text{db} = 10 \log_{10} \left(\frac{200}{100}\right)^2$ if one desires to provide surveillance to aircraft at 200 miles range and $\varphi = 0.5^{\circ}$ when they happen to fly into a null.

Fig. G.2 indicates that the result is about the same for $\varphi_o = 1.28^{\circ}$ where φ_o is the angle between the axis of the beam and the ground plane.

Figs. G.3 and G.4 indicate that as the vertical aperture of the antenna is decreased from 35 feet to 20 feet and 9 feet, the multipath loss

---

*The curve can be more precisely described as a line of constant power density.

**It should be noted that the antenna pattern used is not generic or fundamental, but merely representative of a broad class of patterns.

increases from 6 db to 10 db and 16db, respectively. Thus the desirability of employing a large vertical aperture to create a narrow elevation beam-width to keep multipath losses to a reasonable level is quite evident.

APPENDIX H

SIGNAL DISADVANTAGE IN AIR-TO-GROUND MULTILATERATION SYSTEM

In evaluating the performance of air-to-ground multilateration systems an important parameter is the aircraft signal disadvantage. This is the ratio, r, defined by

$$r = \frac{E(P)}{P_{dis}} \tag{H-1}$$

where P_{dis} is the power received from an aircraft which is furthest from the ground station and E(P) is the average (over the ensemble of all transmission distances between aircraft and ground station) power received from an aircraft.

In this appendix we shall evaluate this ratio, r, under the following idealized assumption:

1. The earth is perfectly spherical.
2. The ground based antenna is located on the surface of the earth.
3. The received power decreases as the square of the distance between the aircraft and the ground based antenna.
4. Aircraft are uniformly distributed within a spherical cap of height h above the surface of the earth. The boundaries of this cap are the spherical earth, a concentric sphere with a radius greater than the earth by an amount h and a cone of half angle θ_o with its vertex at the earth's center. For convenience it is assumed that h is normalized so that it is measured in units of the earth's radius.

Figure H.1 illustrates the geometric situation described by assumption 4. The shaded area is a cross section of the geometric solid in which

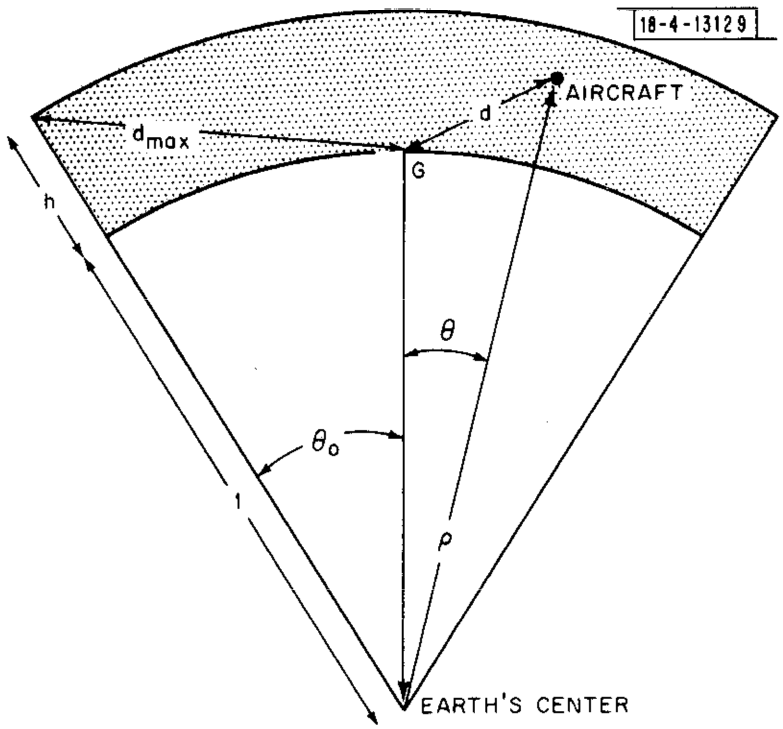

Fig. H.1. Geometry for power disadvantage calculation.

the aircraft are distributed. The cross section is taken perpendicular to the surface of the earth. "d" is the distance of a typical aircraft from the ground station G.* "d_{max}" is the maximum value attainable by d. This corresponds to the transmission range of the most disadvantaged aircraft.

In terms of the geometry of Figure H.1 we have

$$r = \frac{E(P)}{P_{dis}} = d^2_{max} \; E\left(\frac{1}{d^2}\right) \tag{H-2}$$

Utilizing Figure H.1 we have by the law of cosines

$$d^2_{max} = (1+h)^2 + 1 - 2(1+h)\cos\theta_o. \tag{H-3}$$

Since the height of the spherical cap is very small relative to the earth's radius, (i.e. $h \ll 1$), (H-3) yields

$$d^2_{max} \approx 2\,(1-\cos\theta_o) \tag{H-4}$$

Let "V" represent the volume of the airspace illustrated in Figure H.1. V is computed quite simply as

$$V = \int_o^{\theta_o} \int_1^{1+h} 2\pi\rho^2 \sin\theta \, d\rho \, d\theta$$

$$V = \frac{2}{3}\pi \left[(1+h)^3 - 1\right] \left[1 - \cos\theta_o\right] \tag{H-5}$$

Again using the assumption of small h relative to unity (H-5) yields

$$V \approx 2\pi h\,(1-\cos\theta_o). \tag{H-6}$$

*"d" is measured in units of the earth's radius.

Applying (H-4) to (H-6) results in

$$V = \pi h d_{max}^2 \tag{H-7}$$

$E\left(\frac{1}{d^2}\right)$ can be computed using assumption 4.

Specifically,

$$E\left(\frac{1}{d^2}\right) = \int_1^{1+h} \int_0^{\theta_o} \frac{2\pi\rho^2 \sin\theta}{V} \frac{1}{d^2} \, d\theta \, d\rho \tag{H-8}$$

Applying (H-8) to (H-2) results in

$$r = \frac{d_{max}^2}{V} \int_1^{1+h} \int_0^{\theta_o} 2\pi\rho^2 (\sin\theta_o) \frac{1}{d^2} \, d\theta \, d\rho \tag{H-9}$$

By the law of cosines

$$d^2 = \rho^2 + 1 - 2\rho\cos\theta \tag{H-10}$$

Applying (H-10) and (H-7) to (H-9) yields

$$r = \int_1^{1+h} \int_0^{\theta_o} \frac{\rho^2 \sin\theta}{\rho^2 + 1 - \cos\theta} \, d\theta \, d\rho$$

$$r = \frac{1}{h} \int_1^{1+h} \rho \ln\left(\frac{\rho^2 + 1 - 2\rho\cos\theta_o}{(\rho - 1)^2}\right) d\rho \tag{H-11}$$

The assumption of h small relative to unity is again introduced to give the following approximation

$$\rho^2 + 1 - 2\rho \cos \theta_o \approx 2(1 - \cos \theta_o). \tag{H-12}$$

Applying (H-12) to (H-11), integrating and utilizing the small h assumption results in

$$r \approx 2 \left[\ln \left(\frac{d_{max}}{h} \right) + 1 \right] \tag{H-13}$$

which is a desired formula.

For d_{max} = 100 miles and h = 40,000 feet, r = 8.45 db

For d_{max} = 200 miles and h = 40,000 feet, r = 9.3 db

APPENDIX I

GEOMETRIC DILUTION WITH SATELLITE MULTILATERATION SURVEILLANCE SYSTEMS

This Appendix consists of a derivation of expressions for the geometric dilution of satellite multilateration surveillance systems. The analysis also applies to satellite navigation systems. Results are first found for N satellites; these results are then specialized to the case where the minimum number of satellites is used, i.e., where N equals four.

In the satellite multilateration surveillance system known as the air-to-satellite-to-ground system the aircraft emits a signal which is received by N satellites at the times t_1, t_2, ... t_N. If the locations of the aircraft and the N satellites are denoted, respectively, by the N+1 3-vectors $\underline{p}$, $\underline{s}_1$, $\underline{s}_2$, ... $\underline{s}_N$, the following relation holds:

$$\underline{t} = \frac{1}{c}\,\underline{f}\,(\underline{p};\,\underline{s}_1,\,\ldots\,\underline{s}_N) + t_o\,\underline{1} + \underline{\varepsilon}_1$$

In the above, $\underline{t}$ and $\underline{1}$ are N-vectors:

$$\underline{t} = (t_1,\ t_2,\ \ldots\ t_N)'$$

$$\underline{1} = (1,\ 1,\ \ldots\ 1)'$$

(the prime " ' " denotes transposition), c is the speed of light, and $\underline{f}(\cdot\,;\cdot)$ is the following N-vector valued function

$$\underline{f}\,(\underline{p};\,\underline{s}_1,\ldots\underline{s}_N) = \begin{pmatrix} \|\underline{p} - \underline{s}_1\| \\ \|\underline{p} - \underline{s}_2\| \\ \vdots \\ \|\underline{p} - \underline{s}_N\| \end{pmatrix}$$

($\|\underline{x}\|$ is the Euclidean norm of $\underline{x}$). The N-vector $\underline{\epsilon}_1$ accounts for refractions due to the atmosphere, and t_o is the time that the aircraft transmits its signal.

The times of arrival of the signal at the satellites are measured with resultant errors that may be denoted by the N-vector $\underline{\epsilon}_2$. Thus, the vector of estimated times of arrival, $\hat{\underline{t}}$, is just

$$\hat{\underline{t}} = \underline{t} + \underline{\epsilon}_2$$

$$\hat{\underline{t}} = \frac{1}{c}\,\underline{f}\,(\underline{p};\, \underline{s}_1, \ldots \underline{s}_N) + t_o\,\underline{1} + \underline{\epsilon}_1 + \underline{\epsilon}_2$$

Unfortunately, the exact locations of the satellites are not known; rather the position of satellite i is estimated to be $\hat{\underline{s}}_i$. Since the error in this estimated position, $\hat{\underline{s}}_i - \underline{s}_i$, is extremely small compared with $\|\underline{s}_i - \underline{p}\|$, to a very good approximation

$$\|\underline{p} - \underline{s}_i\| = \|\underline{p} - \hat{\underline{s}}_i\| - \underline{u}_i'\,(\hat{\underline{s}}_i - \underline{s}_i)$$

where $\underline{u}_1$ is the unit vector pointing from $\underline{p}$ to $\underline{s}_i$:

$$\underline{u}_i = \frac{1}{\|\underline{s}_i - \underline{p}\|}\,(\underline{s}_i - \underline{p}) \qquad \text{(I-1)}$$

Denoting the vector $\underline{\epsilon}_3$ as

$$\underline{\epsilon}_3 = \begin{pmatrix} \underline{u}_1'\,(\hat{\underline{s}}_1 - \underline{s}_1) \\ \underline{u}_2'\,(\hat{\underline{s}}_2 - \underline{s}_2) \\ \vdots \\ u_N'(\hat{\underline{s}}_N - \underline{s}_N) \end{pmatrix}$$

the relation between $\underline{p}$, $\hat{\underline{t}}$, $\hat{\underline{s}}_1$, ... $\hat{\underline{s}}_N$ is seen to be

$$\hat{\underline{t}} = \frac{1}{c} \underline{f}(\underline{p}; \hat{\underline{s}}_1, \ldots \hat{\underline{s}}_N) + t_o \underline{1} + \underline{\varepsilon}_1 + \underline{\varepsilon}_2 - \frac{1}{c} \underline{\varepsilon}_3$$

From the estimated satellite positions and times of arrival, an estimated aircraft position $\hat{\underline{p}}$ is to be computed. This estimate should be consistent with any known statistics of the quantities t_o, $\underline{\varepsilon}_1$, $\underline{\varepsilon}_2$, and $\underline{\varepsilon}_3$. The model that is used for the aircraft transmission time, t_o, is that of a completely unknown parameter. The vectors $\underline{\varepsilon}_2$ and $\underline{\varepsilon}_3$ can be reasonably modeled as uncorrelated zero mean random vectors, each with uncorrelated components. The vector $\underline{\varepsilon}_1$, which accounts for the refractive effects of the atmosphere, has a deterministic part, $\underline{\varepsilon}_{1d}$, and a random part, $\underline{\varepsilon}_{1r}$, the latter of which may be modeled as a zero mean random vector, uncorrelated from $\underline{\varepsilon}_2$ and $\underline{\varepsilon}_3$, with uncorrelated components. Thus, according to this model,

$$\hat{\underline{t}} = \frac{1}{c} \underline{f}(\underline{p}; \hat{\underline{s}}_1, \ldots \hat{\underline{s}}_N) + t_o \underline{1} + \underline{\varepsilon}_{1d} + \underline{\varepsilon} \tag{I-2}$$

where $\underline{\varepsilon} = \underline{\varepsilon}_{1r} + \underline{\varepsilon}_2 - \frac{1}{c} \underline{\varepsilon}_3$ is a zero mean random vector with the covariance matrix

$$\underline{P}_\varepsilon = E\left[\underline{\varepsilon}\ \underline{\varepsilon}'\right] = \sigma^2 \underline{I} \tag{I-3}$$

Since t_o is assumed to be completely unknown, it must be removed from Eq. (I-2). This is accomplished by operating on Eq. (I-2) with any (N-1) by N matrix $\underline{H}$ satisfying

$$\begin{aligned} \underline{H}\,\underline{1} &= \underline{0} \\ \text{rank}\,(\underline{H}) &= N - 1 \end{aligned} \tag{I-4}$$

to obtain the vector $\hat{\underline{d}}$:

$$\underline{\hat{d}} = \underline{H}\,\underline{\hat{t}} = \frac{1}{c}\,\underline{H}\,\underline{f}(p;\,\underline{\hat{s}}_1, \ldots \underline{\hat{s}}_N) + \underline{H}\,\underline{\epsilon}_{1d} + \underline{H}\,\underline{\epsilon} \qquad \text{(I-5)}$$

For the special case where $\underline{H}$ is given by

$$\underline{H} = \begin{pmatrix} 1 & -1 & 0 & 0 & \ldots & 0 & 0 \\ 0 & 1 & -1 & 0 & \ldots & 0 & 0 \\ \vdots & & & & & & \\ 0 & 0 & 0 & 0 & \ldots & 1 & -1 \end{pmatrix}$$

the vector $\underline{\hat{d}}$ has as components estimated time differences. It is easily seen that the amount of information that $\underline{\hat{d}}$, as defined in Eq. (I-5), contains about the aircraft position, $\underline{p}$, is independent of the choice of $\underline{H}$, provided that Eqs. (I-4) are satisfied.

An expression for the estimated aircraft position, $\underline{\hat{p}}$, may now be derived by first linearizing Eq. (I-5) about a point $\underline{p}^*$. The vector $\underline{p}^*$ could be the last estimated aircraft position, a predicted aircraft position computed from several previous estimated positions, or just a good guess of the aircraft position. Thus, Eq. (I-5) can be approximated as

$$\underline{\hat{d}} = \frac{1}{c}\,\underline{H}\,\underline{f}\,(\underline{p}^*;\,\underline{\hat{s}}_1, \ldots \underline{\hat{s}}_N) + \frac{1}{c}\,\underline{H}\,\underline{F}(\underline{p} - \underline{p}^*) + \underline{H}\,\underline{\epsilon}_{1d} + \underline{H}\,\underline{\epsilon} \qquad \text{(I-6)}$$

where $\underline{F}$ is the matrix of partial deviatives of f $(\underline{p}^*;\,\underline{\hat{s}}_1, \ldots \underline{\hat{s}}_N)$ with respect to the components of $\underline{p}^*$. It is easily seen that (assuming the error in $\underline{s}_i$ is small)

$$\underline{F} = -\begin{pmatrix} \underline{u}_1' \\ \underline{u}_2' \\ \vdots \\ \underline{u}_N' \end{pmatrix}$$

where the unit vectors $\underline{u}_i$ are given by Eq. (I-1).

Defining the vector $\underline{\alpha}$ as

$$\underline{\alpha} = \frac{1}{c} \underline{H} \underline{f} (\underline{p}^*; \underline{s}_1, \ldots \underline{s}_N) + \underline{H} \underline{\epsilon}_{1d} \quad \text{(I-7)}$$

(a known quantity), Eq. (I-6) becomes

$$\hat{\underline{d}} = \underline{\alpha} + \frac{1}{c} \underline{H} \underline{F} (\underline{p} - \underline{p}^*) + \underline{H} \underline{\epsilon}$$

If the aircraft position were modeled as a random vector, then knowledge of the mean and covariance matrix of $\underline{p}$ and the cross covariance matrix of $\underline{p}$ and $\underline{\epsilon}$ would be sufficient to determine the minimum-mean-square-error estimator of $\underline{p}$. However, it is simpler to assume that $\underline{p}$ is a nonrandom, albeit unknown, quantity. With this assumption, since the components of $\underline{\epsilon}$ are assumed to be uncorrelated and to have equal variances (Eq. (I-3)), a reasonable estimate of $\underline{p}$ is the least-squares estimate. That is, the estimate of $\underline{p}$, $\hat{\underline{p}}$, is defined to be that vector for which the quantity $\|\hat{\underline{\epsilon}}\|^2$ is minimized, subject to the constraint that

$$\underline{H} \hat{\underline{\epsilon}} = \hat{\underline{d}} - \underline{\alpha} - \frac{1}{c} \underline{H} \underline{F} (\hat{\underline{p}} - \underline{p}^*) \quad \text{(I-8)}$$

The interpretation of this approach is that of finding the aircraft position $\hat{\underline{p}}$ which is consistent with the smallest measurement error $\underline{\epsilon}$. (It is also the maximum likelihood estimate if $\underline{\epsilon}$ is assumed to be Gaussian.)

The vector $\hat{\underline{\epsilon}}$ of minimum norm which satisfies Eq. (I-8) is easily found to be

$$\hat{\underline{\epsilon}} = \underline{H}' (\underline{H} \underline{H}')^{-1} (\hat{\underline{d}} - \underline{\alpha} - \frac{1}{c} \underline{H} \underline{F} (\hat{\underline{p}} - \underline{p}^*))$$

and the squared norm of $\hat{\underline{\epsilon}}$ is

$$\|\hat{\underline{\epsilon}}\|^2 = (\hat{\underline{d}} - \underline{\alpha} - \frac{1}{c}\underline{H}\,\underline{F}\,(\hat{\underline{p}} - \underline{p}^*))'\,(\underline{H}\,\underline{H}')^{-1}(\hat{\underline{d}} - \underline{\alpha} - \frac{1}{c}\underline{H}\,\underline{F}\,(\hat{\underline{p}} - \underline{p}^*))$$

Finally, that vector $\hat{\underline{p}}$ which minimizes the above is just

$$\hat{\underline{p}} = c\,(\underline{F}'\underline{H}'\,(\underline{H}\,\underline{H}')^{-1}\,\underline{H}\,\underline{F})^{-1}\,\underline{F}'\,\underline{H}'\,(\underline{H}\underline{H}')^{-1}(\hat{\underline{d}} - \underline{\alpha} + \frac{1}{c}\underline{H}\,\underline{F}\,\underline{p}^*)$$

or

$$\hat{\underline{p}} = \underline{p}^* + \underline{K}\,(\hat{\underline{d}} - \underline{\alpha}) \qquad \text{(I-9)}$$

where

$$\underline{K} = c\,(\underline{F}'\underline{H}'\,(\underline{H}\,\underline{H}')^{-1}\underline{H}\,\underline{F})^{-1}\underline{F}'\underline{H}'\,(\underline{H}\,\underline{H}')^{-1} \qquad \text{(I-10)}$$

Equations (I-7), (I-9) and (I-10) define the estimate $\hat{\underline{p}}$. The error in this estimate,

$$\underline{\delta} = \hat{\underline{p}} - \underline{p}$$

is just the following linear transformation on $\underline{\epsilon}$:

$$\underline{\delta} = \underline{K}\,\underline{H}\,\underline{\epsilon}$$

Consequently, the covariance matrix of the position error is

$$\underline{P}_{\delta} = \underline{K}\,\underline{H}\,\underline{P}_{\epsilon}\,\underline{H}'\,\underline{K}' \qquad \text{(I-11)}$$

and from Eqs. (I-3) and (I-10),

$$\underline{P}_{\delta} = (\sigma c)^2 (\underline{F}' \underline{H}' (\underline{H}\underline{H}')^{-1}\underline{H}\underline{F})^{-1}$$

The mean squared position error is now just

$$E[\|\underline{\delta}\|^2] = (\sigma c)^2 \text{ tr } [(\underline{F}' \underline{H}' (\underline{H}\underline{H}')^{-1} \underline{H}\underline{F})^{-1}] \qquad \text{(I-12)}$$

where "tr" is the trace operation.

The geometric dilution, k, of the satellite constellation is defined as the ratio of the rms position error to the rms error in each of the components of the measurement $\hat{\underline{t}}$ (see Eq. (I-2)):

$$k = \frac{1}{\sigma} \|\underline{\delta}\|_{rms}$$

From Eq. (I-12) it is clear that

$$k = c \sqrt{\text{tr } [(\underline{F}'\underline{H}' (\underline{H}\underline{H}')^{-1}\underline{H}\underline{F})^{-1}]} \qquad \text{(I-13)}$$

The definition of geometric dilution, as given above, depends on the model that was used for the random vector $\underline{\epsilon}$. In several cases, e.g. a satellite-to-air navigation system, it is not reasonable to model the components of $\underline{\epsilon}$ as being uncorrelated and having equal variances. In such cases the geometric dilution can be used to bound the value of $\|\underline{\delta}\|_{rms}$. That is, from Eq. (I-11),

$$E[\|\underline{\delta}\|^2] = \text{tr}[\underline{K}\,\underline{H}\,\underline{P}_{\epsilon}\,\underline{H}'\underline{K}']$$

$$= \text{tr}[\underline{P}_{\epsilon}\,\underline{H}'\underline{K}'\underline{K}\,\underline{H}]$$

Now, by the Schwarz' inequality,

$$E\left[\|\underline{\delta}\|^2\right] \leq \sqrt{\mathrm{tr}\ (\underline{P}_\epsilon^2)\ \mathrm{tr}\ ((\underline{H}'\underline{K}'\underline{K}\ \underline{H})^2)}$$

Since $\underline{P}_\epsilon$ and $\underline{H}'\underline{K}'\underline{K}\ \underline{H}$ are both positive semidefinite, it follows that

$$\mathrm{tr}\ (\underline{P}_\epsilon^2) \leq [\mathrm{tr}\ (\underline{P}_\epsilon)]^2$$

$$\mathrm{tr}\ ((\underline{H}'\underline{K}'\ \underline{K}\underline{H})^2) \leq [\mathrm{tr}\ (\underline{H}'\underline{K}'\ \underline{K}\underline{H})]^2$$

and consequently

$$E\left[\|\underline{\delta}\|\right]^2 \leq \mathrm{tr}\ (\underline{P}_\epsilon)\ \mathrm{tr}\ (\underline{H}'\underline{K}'\underline{K}\ \underline{H})$$

But,

$$\mathrm{tr}\ (\underline{P}_\epsilon) = E\left[\|\underline{\epsilon}\|\right]$$

and from Eqs. (I-10) and (I-13)

$$\begin{aligned} \mathrm{tr}\ (\underline{H}'\underline{K}'\underline{K}\underline{H}) &= \mathrm{tr}\ (\underline{K}\ \underline{H}\ \underline{H}'\underline{K}') \\ &= \mathrm{tr}\left[c^2\ (\underline{F}'\underline{H}'\ (\underline{H}\ \underline{H}')^{-1}\underline{H}\underline{F})^{-1}\right] \\ &= k^2 \end{aligned}$$

Therefore, it follows that

$$\|\underline{\delta}\|_{rms} \leq k\ \|\underline{\epsilon}\|_{rms} \qquad \text{(I-14)}$$

It should be noted that this bound uses the rms value of the entire vector ϵ, not just the rms value of one component.

Finally, the bound in Eq. (I-14) can be improved slightly by noting that, since $\underline{\delta} = \underline{K}\,\underline{H}\,\underline{\epsilon}$, that portion of $\underline{\epsilon}$ which lies in the null space of $\underline{H}$ contributes nothing to $\underline{\delta}$. Since the null space of $\underline{H}$ is spanned (see Eqs. (I-4)) by the vector $\underline{1}$, it follows that the portion of $\underline{\epsilon}$ that is orthogonal to this null space is

$$\underline{\epsilon} - \left(\frac{\underline{1}'\,\underline{\epsilon}}{\underline{1}'\,\underline{1}}\right)\underline{1} = \left(\underline{I} - \frac{1}{N}\,\underline{1}\,\underline{1}'\right)\underline{\epsilon}$$

Therefore, an improvement on Eq. (I-14) is the following bound:

$$\|\underline{\hat{\delta}}\|_{rms} < k\left\|\left(\underline{I} - \frac{1}{N}\,\underline{1}\,\underline{1}'\right)\underline{\epsilon}\right\|_{rms} \qquad \text{(I-15)}$$

The expression for the geometric dilution in Eq. (I-13) can be simplified somewhat by assuming a particular matrix $\underline{H}$; note that k, as given by Eq. (I-13) is invariant with respect to all $\underline{H}$ satisfying Eqs. (I-4). Letting

$$\underline{H} = \begin{pmatrix} 1 & 0 & 0 & \dots & 0 & -1 \\ 0 & 1 & 0 & \dots & 0 & -1 \\ \vdots & & & & & \\ 0 & 0 & 0 & \dots & 1 & -1 \end{pmatrix} \qquad \text{(I-16)}$$

it is a simple exercise to show that

$$k = c\sqrt{\mathrm{tr}\left[\left(\sum_{i=1}^{N} \underline{u}_i\,\underline{u}_i' - \frac{1}{N}\left(\sum_{i=1}^{N}\underline{u}_i\right)\left(\sum_{i=1}^{N}\underline{u}_i\right)'\right)^{-1}\right]}$$

where $\underline{u}_i$ is the unit vector defined in Eq. (I-1). The numerical values of k for several satellite constellations have been computed and may be found at the end of Appendix D.

Of considerable importance are those cases where the geometric dilution becomes very large; this can occur with a poorly designed satellite constellation. From Eq. (I-13) it is clear that a necessary and sufficient condition for the geometric dilution to be finite is that

$$\text{rank}\ (\underline{H}\,\underline{F}) = 3$$

where $\underline{H}$ is any (N-1) by N matrix satisfying Eqs. (I-4). For example, using the $\underline{H}$ of Eq. (I-16), the criterion for a finite geometric dilution is that the (N-1) 3- vectors $\underline{u}_1 - \underline{u}_N$, $\underline{u}_2 - \underline{u}_N$, ... $\underline{u}_{N-1} - \underline{u}_N$ span three dimensional space.

From the last remark it is clear that the minimum number of satellites needed to estimate the aircraft position is four. When four satellites are used, the matrix $\underline{H}\,\underline{F}$ in Eq. (I-13) is 3 by 3, and thus Eq. (I-13) can be simplified somewhat. In fact, the geometric dilution k can be expressed in terms of the various dot and cross products of the unit vectors $\underline{u}_i$. However, little intuition can be obtained from this expression.

In both surveillance and navigation systems, due to the aircraft antenna pattern, those satellites which may be used in estimating the aircraft position must lie in a conical region of space. Given this restriction, it is important to be able to design a satellite constellation with an acceptable geometric dilution. A rule of thumb that may be used to obtain a good geometric dilution is to position the satellites so that the unit vectors $\underline{u}_i$ are distributed evenly throughout the allowable conical region. At least one satellite should be nearly overhead; and the rest should be close to the minimum allowed angle of elevation, with an even distribution of angles of azimuth. Whenever possible, bunching of the unit vectors $\underline{u}_i$ should be avoided.

Of course, a satellite constellation with a good geometric dilution at one aircraft location may have a poor geometric dilution at another location.

If four satellites are used and positioned within a cone of half-angle ϕ so that one unit vector is coincident with the conical axis and the remaining three are spaced 120° apart on the conical surface (all the unit vectors radiate from the conical vertex), then the geometric dilution can be shown to be

$$k = c\sqrt{\frac{8}{3\,(1 - \cos\phi)^2\,(1 + \cos\phi)}} \qquad \text{(I-17)}$$

It appears that the above satellite positioning gives the smallest geometric dilution subject to the constraints that only four satellites are used and that they all lie in a conical region of half-angle ϕ. Thus Eq. (I-17) is a lower bound on k subject to these constraints. Figure I-1 is a plot of Eq. (I-17); the value $k = 4.27$ at the angle $\phi = 45^{\circ}$ is of particular interest, as in the air-to-satellite-to-ground system the satellites must be in a cone of half-angle 45°.

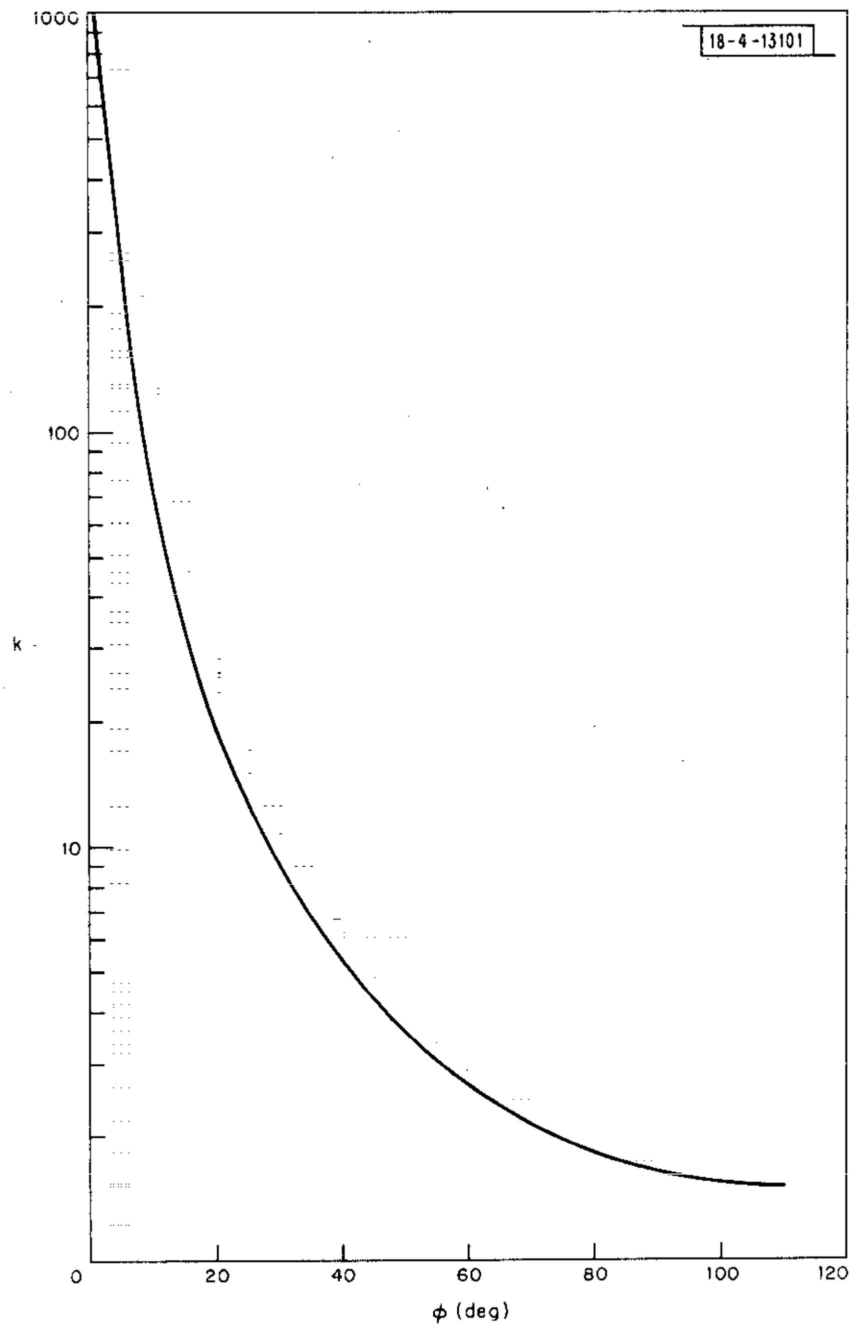

Fig. I. 1. A lower bound to the geometric dilution factor, k, with four satellites within a cone of half angle ϕ.